Molecular Mechanism of Peroxisome Division

Tong Guo

A Thesis

in

The Department

of

Biology

Presented in Partial Fulfillment of the Requirements

for the Degree of Doctor of Philosophy at

Concordia University

Montreal, Quebec, Canada

June 2006

Your file Votre référence
ISBN: 978-0-494-23829-5
Our file Notre référence
ISBN: 978-0-494-23829-5

ABSTRACT

Molecular Mechanism of Peroxisome Division

Tong Guo, Ph.D.

Concordia University, 2006

The peroxisome is an organelle known for its essential role in lipid metabolism and hydrogen peroxide detoxification. In the yeast *Yarrowia lipolytica*, six subforms of peroxisomes, termed P1 to P6, are organized into a multistep peroxisome assembly pathway. The pathway operates by conversion of the subforms in a temporally ordered manner from P1 to P6. The pathway leads to the formation of mature peroxisomes, P6, carrying the complete set of matrix and membrane proteins. The stepwise import of distinct subsets of matrix proteins into immature peroxisomal vesicles P1 to P5 provides them with an increasing fraction of the matrix proteins present in mature peroxisomes P6. This increase in the total mass of matrix proteins above a critical level causes the redistribution of a peroxisomal protein, acyl-CoA oxidase (Aox), from the matrix to the membrane. A significant redistribution of Aox occurs only in mature peroxisomes. Inside mature peroxisomes, the membrane-bound pool of Aox interacts with Pex16p. Pex16p is a membrane-associated protein that negatively regulates the membrane bending, scission and fission events required for the division of immature peroxisomal vesicles, thereby preventing their excessive proliferation. In the inner (lumenal) membrane leaflet of these

vesicles, Pex16p binds lysophosphosphatidic acid (LPA). The binding of Pex16p to LPA prevents the formation of phosphatidic acid (PA) and diacylglycerol (DAG), the two cone-shaped membrane lipids known for their ability to promote the destabilization of the membrane bilayer and to induce strong membrane bending. Only inside mature peroxisomes Pex16p interacts with Aox. This interaction between Aox and Pex16p greatly decreases the affinity between Pex16p and LPA, thereby allowing LPA to enter a two-step biosynthetic pathway leading to the formation of PA and DAG. The resulting accumulation of PA and DAG in the inner (lumenal) leaflet of the membrane of mature peroxisomes and the subsequent transbilayer movement of DAG and the glycerophospholipid phosphatidylserine destabilize and curve the membrane. A complex between the peroxins Pex10p and Pex19p, the dynamin-like GTPase Vps1p, and several actin cytoskeletal proteins is then assembled on the peroxisomal surface. This protein team promotes membrane scission and fission, thereby executing the terminal steps of peroxisome division.

Acknowledgements

I am grateful to my supervisor, Dr. Vladimir Titorenko, for his guidance and support during the years I spent in his laboratory. I would like to thank the members of my committee, Dr. Patrick Gulick and Dr. Adrian Tsang, for their valuable suggestions during the course of my graduate research and studies.

Many thanks to all of my current and former lab-mates Tatiana Boukh-Viner, Simon Bourque, Alex Goldberg, Christopher Gregg, Pavlo Kyryakov, Oleh Petriv, Zeinab Aziz, David Cyr, Andrew Naimi, Florentina Negoita, Aloysius Oluoha, Eric Scazzosi, Alex Alexandrian, Farhana Banu, Adrian Buensuceso, Aman Brar, Andre Cerracchio, Eileen Colella, Christopher Dieni, Ozlem Doygun, Colin Goldfinch, Sandra Haile, Karen Hung Yeung San, Robert Kyskan, Lydia Makoroka, Svetlana Milijevic, Janine Morcos, Mehdi Noei, Reza Noei, Nishant Ramlal, Cristina Sison, Jonathan Solomon, Lisiana Vigliotti and Vivianne Wong for their friendship and support.

I am grateful to my husband, Changhe Yu, for his great patience and invaluable support.

Table of Contents

List of Figures

List of Abbreviations

Aox, acyl-CoA oxidase; APX, ascorbate peroxidase; ARF1, ADP-ribosylation factor1; COPI, coat protein complex I; BFA, brefeldin A; COPII, coat protein complex II; DAG, diacylglycerol; DSP, dithio-*bis*-(succinimidylpropionate); ECR, ergosterol- and

ceramide-rich; ER, endoplasmic reticulum; ERPIC, ER-peroxisome intermediate compartment; F_i, fluorescence for intact peroxisomes; F_{ol}, fluorescence for osmotically lysed peroxisomes; GPI, glycosylphosphatidylinositol; MCFA, medium-chain fatty acids; GTP-bp, GTP-binding and hydrolyzing proteins; ICL, isocitrate lyase; LPA, lysophosphosphatidic acid; LPAAT, LPA acyltransferase; Mfe2, multifunctional enzyme type 2 or 2-enoyl-CoA hydratase/d-3-hydroxyacyl-CoA dehydrogenase; MLS, malate synthase; OG, n-octyl-β-D-glucopyranoside; P1 to P5, immature peroxisomal vesicles P1 to P5; P6, mature peroxisomes P6; PA, phosphatidic acid; PAP, PA phosphatase; PBDs, peroxisome biogenesis disorders; PC, phosphatidylcholine; pER, peroxisomal ER; PI(4)P-bp, phosphatidylinositol-4-phosphate-binding proteins; $PI(4,5)P_2$-bp, phosphatidylinositol-4,5-bisphosphate-binding proteins; PLA, peroxisomal liposomes type A; PLB, peroxisomal liposomes type B; PLC, peroxisomal liposomes type C; PLD, peroxisomal liposomes type D; PMPs, peroxisomal membrane proteins; pMVBs, peroxisomal multivesicular bodies; PNS, postnuclear supernatant; PPT, pre-peroxisomal template; PPV1, pre-peroxisomal vesicles 1; PPV2, pre-peroxisomal vesicles 2; PS, phosphatidylserine; PTS1, peroxisomal targeting signal type 1; TBSV, tomato bushy stunt virus; tER, transitional ER; THI, thiolase; 20KgP, 20,000 x *g* pellet; 20KgS, 20,000 x *g* supernatant; 200KgP, 200,000 x *g* pellet; 200KgS, 200,000 x *g* supernatant.

1 Introduction

1.1 Peroxisome function and pathology

Peroxisomes are organelles found in most eukaryotic cells [1-3]. They contain at least one hydrogen-peroxide-producing oxidase and a catalase to decompose the hydrogen peroxide [1]. Peroxisomes are spherical in transmission electron micrographs, ranging in diameter from 0.1 μm to 1.0 μm [2]. These organelles are delimited by a single lipid bilayer and contain a fine granular matrix and occasionally a paracrystalline core [3]. Peroxisomes do not contain DNA [2, 3]. Accordingly, all peroxisomal proteins are encoded by nuclear genes [1–3]. Peroxisomes do not have an independent protein synthesis machinery [2, 3]. Most of the known peroxisomal proteins are synthesized on free polysomes in the cytosol [1–3], whereas two peroxisomal membrane proteins (PMPs) are produced on ribosomes attached to the rough endoplasmic reticulum (ER) [4, 5].

Peroxisomes show remarkable morphological and metabolic plasticity, as their number, size, morphology, protein composition and biochemical functions vary depending on the organism, cell type and/or environmental milieu [6-8]. These organelles compartmentalize metabolic pathways for the degradation and biosynthesis of various compounds, mostly lipids [2]. Degradative metabolic pathways include the α- and β-oxidation of fatty acids, purine and amino acid catabolism, and the degradation of prostaglandin and polyamines [6-8]. Biosynthetic metabolic pathways housed in peroxisomes lead to the formation of ether phospholipids (plasmalogens), cholesterol, bile acids and polyunsaturated fatty acids [6-8].

Peroxisomes are indispensable for normal human development and physiology, as shown by the severity and lethality of numerous peroxisomal disorders [9-12]. These disorders can be divided into two groups, peroxisomal single enzyme disorders [7, 8, 13] and peroxisome biogenesis disorders (PBDs) [9-11, 14]. The PBDs affect multiple peroxisomal metabolic pathways, as PBD patients fail to assemble functionally intact peroxisomes [9-14]. The PBDs are due to autosomal recessive mutations in any of twelve *PEX* genes encoding proteins called peroxins [15, 16]. A prominent feature of the Zellweger spectrum of the PBDs is a global developmental delay caused by the incomplete migration and differentiation of neuroblasts during psychomotor development, defects in the development of central white matter, and post-developmental enhanced apoptosis of neurons [17]. Another distinct form of PBD, rhizomelic chondrodysplasia punctata type 1, is characterized by abnormal psychomotor development and mental retardation [15].

Because the PBDs exhibit global developmental delay and lead to severe and progressive neurological deficits [13, 17-19], a great deal of attention has been paid to the molecular mechanisms regulating peroxisome biogenesis [12, 14, 20, 21]. Assembly, division and inheritance of peroxisomes are regulated by at least 32 proteins called peroxins [14, 16, 20-26] that are encoded by the *PEX* genes. In addition to its well known roles in lipid metabolism and hydrogen peroxide detoxification, the peroxisome can function both as an intracellular signaling compartment and as an organizing platform that orchestrates certain developmental decisions from inside the cell [27-42]. Much

progress has recently been made in defining various strategies and molecular mechanisms for the integration of peroxisomes into the processes of development, differentiation and morphogenesis in evolutionarily distant organisms [43]. This knowledge provides greater insight into the mechanisms responsible for the global developmental delay and severe neurological dysfunction characteristic of the PBDs [34, 43].

1.2 Peroxisome biogenesis

1.2.1 Peroxisome biogenesis as it was presented in cell-biology textbooks

The prevailing paradigm of peroxisome biogenesis was that peroxisomes, as organelles outside the secretory and endocytic pathways of dynamic vesicular flow [44], constitute an autonomous, static and homogenous organellar compartment [45] and that peroxisome assembly does not involve intercompartmental vesicular trafficking and membrane fusion [46]. In the "growth and division" model for peroxisome biogenesis [1], structurally and functionally identical pre-existing peroxisomes were proposed to enlarge progressively by the posttranslational import of peroxisomal membrane and matrix proteins in bulk and to then undergo division to form new peroxisomes (Figure 1.1). In this model, the ER was seen only as a source of lipids for the growth of the membrane of pre-existing peroxisomes [3]. On the other hand, the ER was not considered as an endomembrane template for the formation of peroxisomal vesicles carrying a distinct set of proteins [1, 3].

1.2.2 A revision of the peroxisome biogenesis paradigm

An important conceptual advance in our understanding of the basic principles of

cellular organization is that the peroxisome is derived from the ER [47-54]. A growing body of evidence also supports the view that peroxisomes, similar to the secretory endomembrane system of vesicular flow, constitute a multi-compartmental endomembrane system in which individual compartments undergo a stepwise, time-ordered conversion into mature, metabolically active peroxisomes [55-58]. All of these findings contradict the common textbook rendition of the peroxisome as a semi-autonomous, static and homogenous subcellular compartment, whose assembly, as an organelle outside the secretory and endocytic pathways of vesicular flow, does not involve inter-compartmental vesicular trafficking [59].

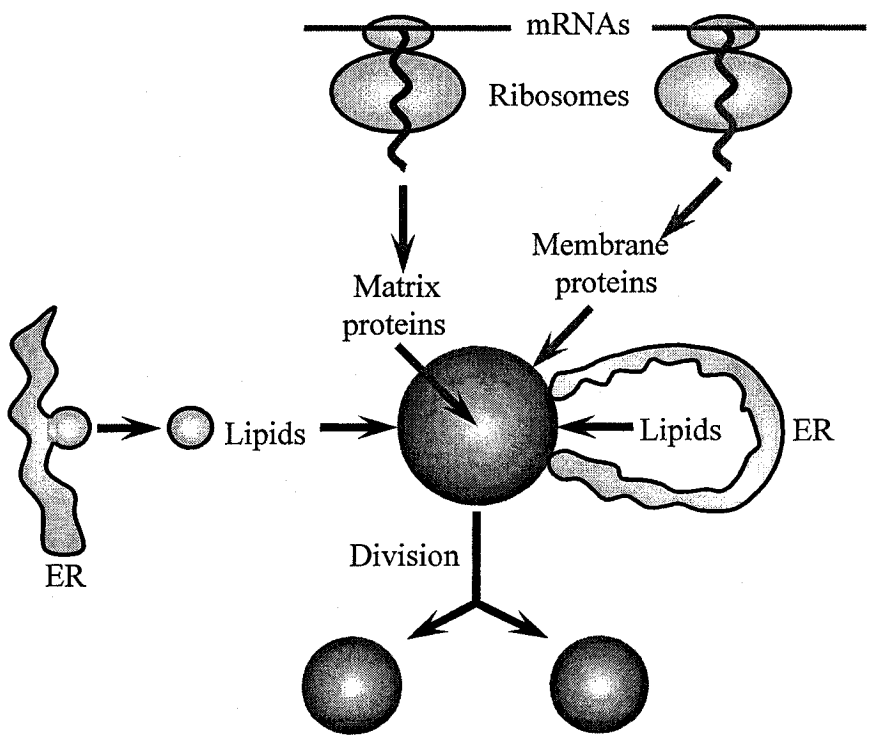

Figure 1.1. The "growth and division" model for peroxisome biogenesis.

1.2.3 Targeting of peroxisomal membrane proteins to the ER and their sorting within the ER

The origin of peroxisomes has long been matter of debate and partially underscoring this controversy has been the mode by which peroxisome-destined proteins are synthesized and targeted within the cell. For instance, a major tenet of the previous "ER-vesiculation" model for peroxisome biogenesis was that all of the soluble and membrane-bound protein constituents of the peroxisome were synthesized co-translationally on the ER [60]. These nascent proteins were proposed to be then sequestered into an expanding vesicle that would eventually bud from the ER to produce a mature, functional peroxisome [60]. However, subsequent observations suggested that peroxisomal proteins were not synthesized on the ER, but rather on free polyribosomes in the cytosol. These and other data led to the "growth and division" model for peroxisome biogenesis wherein peroxisomes, like mitochondria and chloroplasts, were considered to increase in size by the post-translational import of their protein constituents and proliferate only through the division of pre-existing peroxisomes [1, 3, 59]. Notably, the ER in the "growth and division" model was deemed only to be a source of membrane lipids for the enlargement of pre-existing peroxisomes [3, 59].

While for most of the past two decades the "growth and division" model has been generally considered the paradigm for peroxisome biogenesis, the recent monitoring of the sorting of various PMPs in evolutionarily diverse organisms has revealed that for at least a subset of these PMPs, referred to as group I PMPs [34], the initial sorting site is the ER rather than the peroxisome membrane. Sorting of group I PMPs to and within

the ER also appears to be mediated by several different mechanisms. For instance in mammalian cells, the group I PMP Pex16p is inserted co-translationally into ER membranes and seems to be localized throughout the entire ER prior to its sorting to peroxisomes [5]. In the yeast *Saccharomyces cerevisiae*, *Yarrowia lipolytica* and *Hansenula polymorpha*, group I PMPs Pex2p, Pex3p and Pex16p are also initially targeted to the "general" ER [48, 50, 53]. However, unlike mammalian Pex16p, the ER targeting and insertion of these essential components of peroxisome assembly in *S. cerevisiae* does not require the Sec61p-dependent machinery for co- and post-translational import of secretory proteins [61]. Furthermore, unlike mammalian Pex16p that remains in the "general" ER prior to its sorting to peroxisomes [5], at least one of the group I PMPs in *S. cerevisiae*, namely Pex3p, is directed from the "general" ER to a distinct subdomain of the ER [50]. This ER subdomain is referred to as the pre-peroxisomal template [34] and considered to be the site where pre-peroxisomal carriers are formed. That is, after being segregated into the pre-peroxisomal template, Pex3p serves as a docking factor for Pex19p, a predominantly cytosolic protein [50]. The Pex3p-dependent recruitment of Pex19p from the cytosol to the outer face of the pre-peroxisomal template in *S. cerevisiae* is mandatory for the budding of small pre-peroxisomal vesicles [50]. These ER-derived carriers of Pex2p, Pex3p, Pex16p and Pex19p lack secretory cargo proteins [27].

In contrast to yeast Pex2p, Pex3p and Pex16p and mammalian Pex16p, other group I PMPs, such as ascorbate peroxidase (APX) in plant cells [49] and Pex13p in mouse

dendritic cells [57], can only be detected in a distinct portion of the ER, suggesting that they are targeted from the cytosol directly to a pre-existing subdomain of the ER membrane. The terms peroxisomal ER (pER) and the lamellar ER extension were coined for this ER found in plants and mice, respectively [62, 63]. At least one notable difference between these two ER subdomains is that pER is considered to be a portion of rough ER membrane [64], whereas the lamellar ER extension is a specialized domain in smooth ER membrane [57]. In plant cells, the cytosol-to-pER targeting of APX occurs post-translationally and requires ATP as well as least three components of the Hsp70 chaperone machinery [49]. Taken together, the above findings suggest that, by segregating a distinct set of membrane proteins and lipids into specialized ER subdomains, plant and mouse dendritic cells have evolved a platform for the targeting of group I PMPs from the cytosol to the ER membrane [65]. It has been proposed that the existence of such a platform in the ER membrane could increase the efficiency of the ER-dependent, multi-step process of peroxisome assembly in these cells [65].

What structural features of group I PMPs are crucial for their sorting to the ER or to the peroxisomal membrane via either "general" ER or an ER subdomain remain to be determined. At present it seems that the targeting of these PMPs from the cytosol to the ER membrane and their subsequent exit from the ER are mediated by two partially overlapping sets of sorting signals. One set of signals targets group I PMPs either co- or post-translationally to the "general" ER or an ER subdomain, whereas the other set of signals act from within the ER lumen to sort these PMPs to the peroxisome [5, 66-68].

1.2.4 Exit of PMPs from the ER via pre-peroxisomal carriers

Although all group I PMPs exit the ER via distinct pre-peroxisomal carriers that do not enter the classical secretory pathway of vesicular flow [48, 57], the morphology of these carriers in at least yeast and mammalian cells appears to differ. In *S. cerevisiae*, *Y. lipolytica* and *H. polymorpha*, the ER-derived pre-peroxisomal carriers are small vesicles [48, 50, 53]. In contrast, the pre-peroxisomal carriers in mouse dendritic cells arise through direct *en block* protrusion of the specialized ER subdomain, the lamellar ER extension [57]. After reaching a considerable size, the lamellar extension detaches from the ER, giving rise to pleomorphic tubular-saccular carriers of group I PMPs. This detachment of pre-peroxisomal tubular-saccular carriers from the ER does not require coat protein complexes I and II (COPI and COPII, respectively) that function in the formation of ER-derived carriers for secretory proteins [57]. It is noteworthy that, akin to ER-derived pre-peroxisomal carriers in yeast cells, all known types of transport carriers for secretory proteins are small vesicles in these cells [69]. On the contrary, just like the pre-peroxisomal carriers in mammalian cells, at least a subset of ER-to-Golgi carriers for many secretory proteins in these cells are pleomorphic tubular-saccular structures that are formed through direct *en block* protrusion of specialized domains in the ER membrane [70]. This fundamental difference in the morphology of ER-derived transport carriers is likely due to the difference in the spatial organization of transitional ER (tER), a specialized ER subdomain at which proteins are packaged into membrane-enclosed carriers. In the traditionally used model yeast organism, *S. cerevisiae*, the entire ER acts as tER facilitating the budding of COPII-coated vesicles [71]. In contrast, the tER of

mammalian cells is organized into discrete ER export sites [72]. Therefore, it has been suggested that, by segregating a distinct set of membrane proteins and lipids into a specialized ER subdomain for the cytosol-to-ER targeting of group I PMPs, higher eukaryotic organisms have not only separated these domains from the sites for the ER targeting of secretory proteins, but have also developed a platform for the sculpturing of these peroxisomal ER subdomains into pleomorphic tubular-saccular carriers of PMPs [65].

Presently, no solid data exists for the nature of the pre-peroxisomal carriers in plant cells, although, similar to mammals, the tER in these cells is restricted to discrete sites in the ER membrane [73], suggesting that the organization of the pER subdomain as well as the formation of pre-peroxisomal carriers in plants is similar to that in mammals.

1.2.5 Spatio-temporal organization of the peroxisomal endomembrane system

Recent findings have provided strong evidence that, analogous to some organelles of the secretory endomembrane system, peroxisomes constitute a dynamic organelle population consisting of many structurally distinct compartments that differ in their import competency for various proteins [65]. Moreover, it appears that the individual compartments of this peroxisomal endomembrane system undergo a multi-step conversion to mature peroxisomes in a time-ordered manner [65].

Two multi-step pathways for peroxisome assembly and maturation have been described [65]. In the yeast *Y. lipolytica*, a limited subset of group I PMPs, including Pex2p and Pex16p, is initially post-translationally targeted to the ER (Figure 1.2) [27, 48, 74]. These PMPs are then *N*-glycosylated in the ER lumen [48] and directed to a distinct subdomain of the ER, the pre-peroxisomal template (PPT) [20, 34]. Budding of the PPT

leads to the formation of two populations of pre-peroxisomal vesicles (PPV1 and PPV2) that contain Pex2p and Pex16p [27, 48, 74]. PPV1 and PPV2 are distinct from secretory vesicles (SV). The budding of SV from another specialized domain of the ER initiates the export of proteins to the external medium and the delivery of proteins for plasma-membrane and cell-wall synthesis via the Golgi apparatus [27, 28, 74].

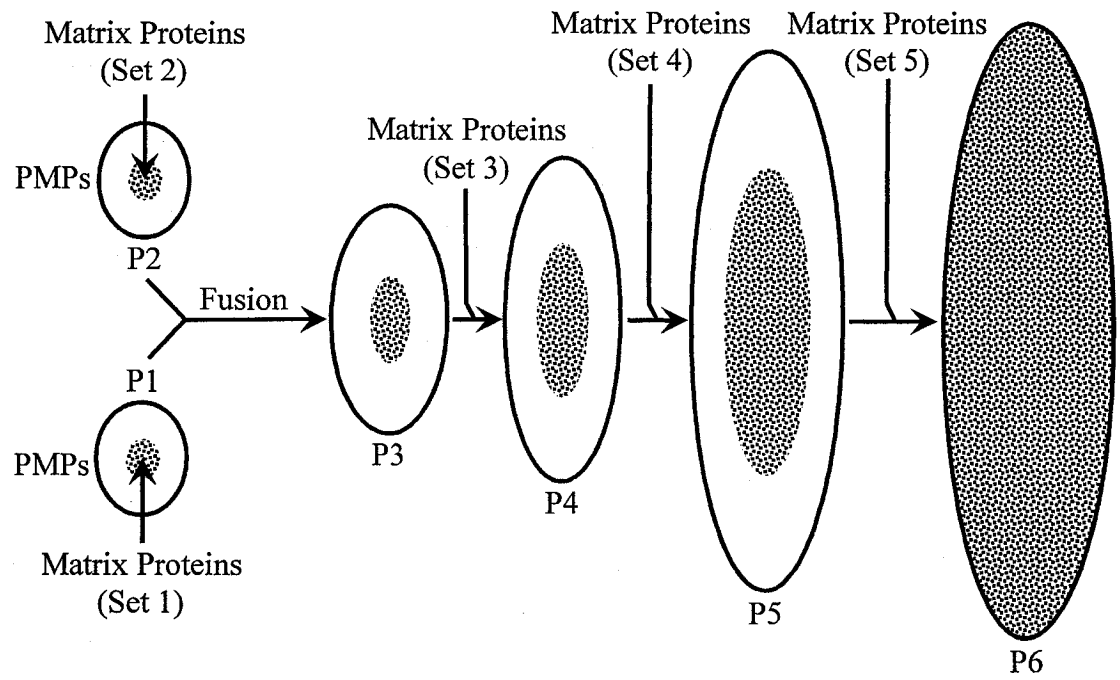

Figure 1.2. A model for the multistep peroxisome assembly pathway acting in the yeast *Yarrowia lipolytica.*

The post-translational sorting of two partially overlapping sets of group II PMPs converts PPV1 and PPV2 to the early peroxisomal precursors P1 and P2 [20, 34, 55]. P1 and P2 are the earliest intermediates in a multistep pathway that leads to the formation of mature peroxisomes, P6, carrying the complete set of matrix and membrane proteins

(Figure 1.2) [20, 27, 34, 48, 55, 74, 75]. P1 and P2 contain most of PMPs associated with mature peroxisomes, but carry only a few matrix proteins [55, 75]. P1 and P2 undergo fusion to generate larger and more dense vesicles, P3 [55, 56]. Conversion of P3 to mature peroxisomes P6 proceeds through several consecutive steps. At each of these steps, the uptake of lipids and the selective import of a limited subset of matrix proteins result in the formation of a peroxisomal subform that is larger and more dense than its precursor [55, 75]. Intermediates of the peroxisome assembly pathway differ in their import competency for various matrix proteins (Figure 1.2) [20, 34, 55, 65]. In fact, the small pre-peroxisomal vesicles P1 and P2, which are the earliest intermediates in the peroxisome assembly pathway, are import-competent for the peroxisomal matrix protein malate synthase, whereas the other peroxisomal subforms are not [55]. Malate synthase is targeted to the matrix of P1 and P2 by a peroxisomal targeting signal type 1 (PTS1) [55]. Moreover, P2 vesicles import two other matrix proteins, the PTS3-targeted acyl-CoA oxidase and the PTS2-sorted thiolase, directly from the cytosol, while the other five peroxisomal subforms do not [55]. Furthermore, only P3 vesicles can import a 62-kDa protein carrying a PTS1, while P4 vesicles show selective import for the PTS1-sorted matrix protein isocitrate lyase [55]. Altogether, these findings provided evidence that import machineries specific for different peroxisomal matrix proteins undergo a temporally ordered assembly in distinct vesicular intermediates along the peroxisome maturation pathway [20, 34, 55, 65].

The plasticity of these import machineries is further underscored by the observation that the efficiency with which they recognize non-overlapping targeting

signals present on some of their protein substrates varies under different metabolic conditions. In fact, peroxisomal subforms present in cells of the yeast *Saccharomyces cerevisiae* growing under conditions that induce peroxisome proliferation differ from basal, non-proliferated subforms with respect to the targeting sequence motifs that are used to direct the same PMP to these different subforms of peroxisomes [76]. In this yeast, two PMPs, Pmp47p and Pex8p, contain non-overlapping peroxisomal targeting signals. *S. cerevisiae* cells grown in medium with glucose as the sole carbon source contain only a very limited number of small peroxisomes, called "basal" (*i.e.*, non-proliferated) peroxisomes. In contrast, growth of *S. cerevisiae* in medium containing oleic acid as the only available carbon source induces peroxisome proliferation, thereby dramatically increasing the size and number of the so called "proliferated" peroxisomes [76]. Wang et al. provided evidence that while one region of Pmp47p (TMD4R) efficiently targets this PMP to "basal" peroxisomes, it is inefficient for its targeting to "proliferated" peroxisomes [76]. On the contrary, another region of Pmp47p (TMD2R), which does not overlap with TMD4R, efficiently targets Pmp47p to "proliferated" peroxisomes but poorly to "basal" peroxisomes [76]. Furthermore, the carboxyl-terminal PTS1 within Pex8p dramatically increases the efficiency of this PMP's targeting to "basal" peroxisomes, but has no effect on Pex8p targeting to "proliferated" peroxisomes. It is noteworthy that the "basal" and "proliferated" peroxisomes differ from each other with respect to the spectra and relative abundance of their PMP constituents [77]. Some of these variable PMPs are components of the targeting and assembly machineries specific for many other PMPs [3, 12, 14, 20, 21, 34]. Taken together, the above findings

in *S. cerevisiae* suggested that the efficacy of peroxisomal targeting signals located within at least some of the PMPs is greatly influenced by the composition of protein machineries for their targeting to and their assembly in the peroxisomal membrane [65, 76]. These findings also suggested that different peroxisomal populations vary with respect to the composition and functional properties of the sorting machineries specific for their PMPs [65].

A quite different scenario orchestrates a multi-step process of peroxisome assembly and maturation in mouse dendritic cells. Herein, the extrusion of the lamellar ER extensions is culminated by the detachment of pleomorphic tubular-saccular carriers of Pex13p from the ER [57]. Only after their separation from the ER, these pre-peroxisomal carriers are able to recruit to their membranes the ATP-binding cassette transporter protein PMP70 and, perhaps, the membrane components of the import machinery for peroxisomal matrix proteins [63]. This latter step of the peroxisome maturation pathway also results in the formation of the so-called "peroxisomal reticulum". Only the peroxisomal reticulum is capable of importing at least two peroxisomal matrix proteins, namely thiolase and catalase, directly from the cytosol [57]. Notably, these two peroxisomal matrix proteins do not fill the entire peroxisomal reticulum. Instead, they are sorted exclusively into mature globular peroxisomes that, during the final step in the peroxisome maturation pathway in mouse cells, bud from the peroxisomal reticulum [57, 63]. It remains to be established whether other peroxisomal matrix proteins, similar to thiolase and catalase, are imported into the domain of the peroxisomal reticulum that

gives rise to mature globular peroxisomes or, alternatively, these other matrix proteins in mouse cells are sorted to globular (mature) peroxisomes only after their budding from the peroxisomal reticulum [65].

In both models for the multi-step assembly and maturation of peroxisomes, the targeting of PMPs to the membrane of the early intermediates in a pathway precedes, and is mandatory for, the import of soluble peroxisomal proteins into the matrix of later intermediates. Because this strategy for peroxisome biogenesis has been conserved in the course of evolution, it has been suggested that it provides an important advantage for the efficient, stepwise assembly of mature, metabolically active peroxisomes. It remains to be established whether, similar to a stepwise assembly of import machineries specific for different peroxisomal matrix proteins in yeast cells [20, 34], the import machineries for such proteins in mammalian cells can undergo a temporally ordered assembly in distinct intermediates along the peroxisome maturation pathway [65].

It is also unclear at the moment whether the peroxisome maturation pathway acting in mammalian cells, akin to the pathway that functions in yeast cells [20, 34], includes fusion of any early pathway intermediates. It has been proposed that such fusion of early pathway intermediates in yeast results in the formation of an ER-peroxisome intermediate compartment (ERPIC) [65]. Such a compartment could: 1) provide a template for the formation of downstream intermediates in the peroxisome assembly and maturation pathway; and 2) function in the sorting of PMPs from those escaped ER resident proteins that are retrieved by retrograde vesicular transport between the ERPIC and the ER. Both of these tentative functions of the ERPIC share similarity with the functions that have

been proposed for the ER-Golgi intermediate compartment, also known as vesicular tubular clusters, which may regulate a bi-directional traffic of membrane-enclosed carriers through the classical secretory pathway [69]. Importantly, the resident proteins of the post-ER compartments in both the peroxisomal endomembrane system and the classical secretory system return back to the ER in response to the treatment of yeast cells with brefeldin A (BFA), an inhibitor of COPI coat formation [78]. Hence, it has been suggested that, similar to its role in the secretory endomembrane system, yeast COPI can function in the retrieval of those ER resident proteins that had entered the peroxisomal endomembrane system by mistake [65]. This is in contrast to COPI in cultured human fibroblasts, in which peroxisome-to-ER retrograde protein transport, if any, does not depend on COPI [79, 80]. These findings further support the notion that yeast and higher eukaryotic organisms may use different strategies for the ER-dependent formation and maintenance of their peroxisomal endomembrane systems [65].

1.2.6 Peroxisome-to-ER retrograde protein transport

While it is not yet known whether, in plants, a multi-step pathway for peroxisome assembly and maturation exits that is either similar or distinct from that in yeast and/or mammals, recent findings suggest that peroxisomes in plants cells can form large pleomorphic structures reminiscent of the mammalian "peroxisomal reticulum" [81] and are engaged in ER-destined retrograde vesicular flow. Evidence for this latter conclusion comes from observations that when the tomato bushy stunt virus (TBSV) replication protein p33 is expressed on its own in plant cells, it is sorted initially from the cytosol to peroxisomes and then, via peroxisome-derived vesicles and together with resident PMPs,

to pER [82]. Remarkably, several aspects of the peroxisome-to-pER sorting of p33- and resident PMPs-laden vesicles are similar to the Golgi-to-ER retrograde vesicular transport. For instance, both these processes depend on the ADP-ribosylation factor1 (ARF1), which promotes the formation of COPI-coated vesicles [69, 82]. In addition, the targeting signal of p33 that mediates the sorting of peroxisomal-derived vesicles to pER resembles an arginine-based motif responsible for vesicle-mediated retrieval of escaped ER membrane proteins from the Golgi [82]. This motif functions as the recognition site for COPI and other specialized cytosolic proteins required for the Golgi-to-ER retrograde vesicular transport [83]. Importantly, COPI and the cytosol-to-peroxisome and peroxisome-to-pER sorting events for p33 are essential for the functioning of the TBSV RNA replication complex [82, 84]. This complex assembles in the peroxisomal multivesicular bodies (pMVBs) that are formed due to the TBSV-induced extensive inward vesiculations of the peroxisomal membrane [85, 86]. Therefore, it has been suggested that the p33-promoted peroxisome-to-pER retrograde transport of vesicles delivers to the pER "early peroxins" that could then stimulate the formation of membrane-enclosed carriers of PMPs [81, 82]. It has been also proposed that this, in turn, causes the dramatic increase in the peroxisome surface area, thereby initiating a pMVB biogenetic step of the virus life cycle [81, 82].

Although the mechanism of the pER-dependent pMVB biogenesis remains to be established, the identification of a reverse protein sorting pathway between plant peroxisomes and ER has provided a valuable tool for studying the peroxisome-to-ER retrograde protein transport [81, 82]. It remains to be established whether such ARF1-

and COPI-dependent retrograde route of protein trafficking can only be induced in TBSV-infected plant cells, as an essential phase of the p33-driven TBSV life cycle, or can also function in uninfected plants, or in other higher eukaryotic organisms, as a mechanism for the retrieval of escaped ER resident proteins [81, 82].

1.3 Peroxisome division

1.3.1 Organelle growth and division during the cell cycle

In order to be accurately partitioned during cell division and inherited by the daughter cells, organelles must double in size and divide during the cell cycle [87-90]. How organelles divide is one of the key questions of cell biology. The division of mitochondria and chloroplasts, the organelles of endosymbiotic origin that are bound by two membranes and contain DNA, is uncoupled from cell division and requires the FtsZ-like and/or dynamin-related GTPases [88, 91-93]. In contrast, the division of the Golgi apparatus, an organelle of the secretory pathway that is surrounded by a single membrane and lacks DNA, is coupled to the cell division cycle and is served by a division machinery that is unique for this non-endosymbiotic organelle [87, 94-96]. Similar to Golgi and in contrast to endosymbiotic organelles, peroxisomes derive from the endoplasmic reticulum [20, 27, 34, 48-54, 57, 63, 65, 74, 97, 98], are bound by a single membrane and do not contain DNA. On the other hand, akin to mitochondria and chloroplasts and contrary to Golgi, peroxisomes require dynamin-related GTPases for their division that is uncoupled from cell division [90, 99-104]. Although the mechanisms by which mitochondria, chloroplasts and Golgi divide are well defined [87, 88, 91, 92-

96], the molecular mechanism for the integration of multiple components of the peroxisome division machinery remains to be established [90, 103, 104]. Importantly, it seems that different organisms have developed different ways to divide their mitochondria, chloroplasts and Golgi [87, 88, 92, 93, 105-108].

1.3.2 Coordination of compartment assembly and division in the peroxisomal endomembrane system

In addition to their proposed role in the peroxisome-to-ER retrograde protein transport in virus-infected plant cells [81, 82; see above], both ARF1 and COPI can induce the proliferation of the peroxisomal endomembrane system in other evolutionarily diverse organisms by promoting the membrane scission and fission events required for peroxisome division. In fact, yeast mutants impaired in ARF1 and COPI, as well as mammalian cells deficient in COPI assembly, accumulate a reduced number of elongated tubular peroxisomes, consistent with impairment in peroxisome vesiculation [109, 110]. Incubation of highly purified rat liver peroxisomes with cytosol results in specific binding of both ARF1 and COPI to the peroxisomal membrane, further supporting the notion that their recruitment from the cytosol in living cells is an initial event in the proliferation of the peroxisomal endomembrane system [111]. Moreover, similar to ARF1, the subtype 3 of yeast ARF also controls peroxisome division *in vivo*, although, in contrast to ARF1, in a negative fashion [110]. Taken together, these findings suggest that the peroxisomal endomembrane system and the classical secretory system of vesicular flow are served by a similar set of core protein components required for their communication with the ER and for their proliferation. The proliferation of the individual compartments of the

peroxisomal endomembrane system is also driven by a peroxisome-specific protein machinery, which includes a distinct set of the PMPs and the dynamin-related proteins DLP1/DRP3A/Vps1p recruited from the cytosol to the peroxisomal surface by their receptor Fis1p [90, 103, 104]. It remains to be established how the interplay of all these protein components governs such proliferation under different metabolic conditions in a given cell type or tissue.

Importantly, peroxisome biogenesis appears to occur by way of a collaborative effort between two equally important pathways. The first pathway operates through the ER-dependent formation and maturation of the individual compartments of the peroxisomal endomembrane system, whereas the second pathway involves the precisely controlled division of these peroxisomal compartments [65]. Growing evidence supports the view that cells have evolved at least two strategies for the coordination of compartment assembly and division in the peroxisomal endomembrane system. In the first strategy, the multi-step growth and maturation of the ER-derived pre-peroxisomal carriers occurs before the completely assembled, mature peroxisomes undergo division [20, 34, 65]. In the second strategy, a significant increase in the number of pre-peroxisomal carriers, either by their massive formation from the ER [54, 65] or by the proliferation of a few pre-existing carriers [20, 34, 65, 77], precedes the growth of these early peroxisomal precursors by membrane and matrix protein import and their conversion to mature, functional organelles containing a complete complement of peroxisomal proteins. It has been suggested [65] that determining the relative contribution of these different mechanisms in the formation of peroxisomes in any given

organism should now be more feasible through the use of live-cell, photo/pulse-chase labeling methods similar to that reported recently for a study of peroxisome biogenesis in mammalian cells [54].

Regardless of the strategy(s) that evolutionarily distant organisms employ for coordinating the assembly and division of individual compartments of the peroxisomal endomembrane system, the tubulation, constriction and scission of these compartments is regulated, depending on cellular and/or environmental conditions of a particular cell type, either by signals emanating from within these compartments or by extraperoxisomal signals that are generated inside the cell in response to certain extracellular stimuli [65, 90, 103, 104]. These intracellular signals include a distinct group of transcriptional factors that induce the transcription of genes encoding several proteins of the Pex11p family [90, 103]. The peroxisome membrane-bound Pex11p-type proteins then directly promote the proliferation of peroxisomal endomembrane compartments or activate peroxisome division indirectly, by recruiting the dynamin-related proteins from the cytosol [90, 103, 104]. Members of the Pex11p family function as positive regulators of peroxisome division, but are not required for peroxisomal protein import [112]. Pex11p is unlikely to regulate peroxisome division during the cell cycle [113], as yeast cells lacking Pex11p do not lose peroxisomes when grown in the absence of extracellular stimuli for peroxisome division [112, 114]. In the yeast *S. cerevisiae*, Pex11p faces the inner surface of the peroxisomal membrane. It seems to be a monomer in immature, dividing peroxisomes but a dimer in mature peroxisomes [113]. One possibility is that the monomeric form of Pex11p could directly activate the division of immature peroxisomes

by promoting membrane fission from inside the organelle [113]. The import of the bulk of matrix proteins into immature peroxisomes, which leads to their maturation, could cause specific changes in the metabolic environment within the organelles, thereby promoting the formation of inactive Pex11p dimers and inhibiting further peroxisome division [113]. An alternative model for the involvement of Pex11p in peroxisome division was inspired by the recent observation that, in *S. cerevisiae*, this peroxin is required for the intraperoxisomal β-oxidation of medium-chain fatty acids (MCFA) and might function in the transport of either MCFAs or of cofactors (ATP or coenzyme A) that are essential for their β-oxidation in the organelle [115]. Therefore, an open question with respect to the function of Pex11p in peroxisome division is whether it acts directly, activating membrane bending, scission and fission in immature peroxisomes, or indirectly, as part of a cascade of events that might lead to the formation of (a) signaling molecule(s) that modulate the rate of peroxisome division [113-115]. The mechanism by which Pex11 mediates peroxisome division seems to vary in different organisms. In contrast to its yeast [112, 114] and trypanosome [116] counterparts, the α-subform of mammalian Pex11p faces the cytosol [109] and contains a carboxyl-terminal dilysine motif, which was shown to ARF1 and COPI from the cytosol [109]. The recruitment of ARF1 and COPI by Pex11p was proposed to initiate fission and/or budding of peroxisomes followed by their scission [109]. Further experiments are necessary to clarify whether or not the observed binding of ARF1 and COPI by mammalian Pex11p is required for Pex11p function in peroxisome division.

Metabolic processes taking place in peroxisomes are important for their division

[115, 117, 118]. PMP47 is involved in the intraperoxisomal β-oxidation of MCFAs and, at the same time, is required for peroxisome division [119]. Furthermore, loss of the enzymatic activity of acyl-CoA oxidase (Aox) [115, 117, 120], fatty acyl-CoA synthetase [115], and/or another peroxisomal β-oxidation enzyme, multifunctional enzyme type 2 or 2-enoyl-CoA hydratase/d-3-hydroxyacyl-CoA dehydrogenase (Mfe2) [117, 121], but not the absence of these proteins [117, 121], causes pronounced changes in peroxisome size and/or number. This so-called metabolic control of peroxisome abundance [117] probably targets primarily the levels of other peroxisomal β-oxidation enzymes that are markedly increased by the loss of Aox [120] or Mfe2 [121] enzymatic activity. The resultant overproduction of abundant matrix proteins leads to a change in peroxisome size [115, 117, 121] and/or number [120, 121]. Notably, whereas some defects in intraperoxisomal β-oxidation cause a significant decrease in peroxisome abundance, others lead to an increase in the abundance of these organelles. The molecular basis for the metabolic control of peroxisome division remains to be established.

A specific subset of peroxins might coordinate the growth and division of peroxisomes indirectly, by modulating the concentration and/or stoichiometry of subcomplexes of components that are essential for membrane assembly, matrix protein import and organelle division and by regulating the abundance of immature peroxisomal precursors. In the yeast *Hansenula polymorpha*, overproduction of the peroxin Pex3p prevents the formation of mature peroxisomes and leads to the accumulation of small peroxisomal vesicles that are deficient in the import of matrix proteins [122]. Therefore, the excessive proliferation of immature peroxisomal vesicles might notably decrease the

concentration of vesicle-associated complexes required for the import of matrix proteins, thereby abrogating the formation of mature peroxisomes [122]. In the yeast *Y. lipolytica*, the peroxin Pex16p functions to prevent excessive division of immature peroxisomal precursors, which are competent for the import of only a limited subset of matrix proteins [55]. This allows for the efficient, stepwise assembly of mature peroxisomes followed by their division [55, 123]. In contrast to its yeast counterpart [123], human Pex16p is required at a very early step of peroxisomal membrane assembly [124]. Because the mechanism by which another peroxin, Pex11p, regulates peroxisome division might also vary in yeasts and mammals, it is conceivable that organisms with different timings of events of peroxisome growth and division might adopt different strategies for the coordination of these processes.

1.4 Lipids and lipid domains of the peroxisomal membrane

1.4.1 Exit of pre-peroxisomal carriers from the ER is the initial step of lipid sorting to the peroxisomal membrane

The dynamic flow of membrane-enclosed carriers through the ER-derived peroxisomal endomembrane system is initiated by the sorting of a limited subset of group I PMPs to the ER [65]. In yeasts, these group I PMPs then move laterally from the "general ER" to a distinct domain of the ER, thereby creating a template for the budding of small pre-peroxisomal vesicles [50, 65]. The term pre-peroxisomal template was coined for this specialized domain of the ER membrane [34]. The vesicular pre-peroxisomal carriers that bud from the pre-peroxisomal template carry group I PMPs but

lack secretory and ER resident membrane proteins [27]. In addition to group I PMPs, the membrane of these ER-derived carriers incorporates a portion of lipids that are synthesized in the ER membrane. Thus, the initial step of lipid sorting to the peroxisomal membrane occurs during exit of pre-peroxisomal carriers from the ER.

What could be the mechanism for the observed lateral segregation of group I PMPs from secretory and ER resident membrane proteins within the ER membrane? What role could individual lipid species and lipid domains of the ER membrane play in this process? Recently, it has been suggested that ergosterol- and ceramide-rich (ECR) domains in the ER membrane of yeast can function as sorting platforms for segregating ER resident proteins, at least two groups of secretory and plasma membrane proteins, and group I PMPs from each other [65]. This hypothesis is based on the following observations. First, glycosylphosphatidylinositol (GPI)-anchored proteins in the yeast *S. cerevisiae* exit the ER in vesicles that are distinct from those that carry many other secretory and plasma membrane proteins that are not anchored to GPI [125]. Analysis of specific requirements for the packaging of GPI-anchored proteins into ER-derived vesicles suggested that their partitioning into ceramide-rich lipid raft domains, which are clustered in distinct regions of the ER, is responsible for their lateral segregation from non-GPI-anchored secretory and plasma membrane proteins [125-131]. In yeasts, these detergent-resistant membrane domains are formed in the ER [132]. Second, the membrane of the ER-derived pre-peroxisomal vesicles in the yeast *Y. lipolytica* has unusual ECR domains that resist solubilization by cold nonionic detergents and are similar to detergent-resistant lipid raft domains found in the membrane of *S. cerevisiae*

ER [133]. Based on the above findings, it has been recently proposed that the ECR domains in the membrane of *Y. lipolytica* ER serve as a sorting station for segregating group I PMPs from secretory and ER resident membrane proteins [65]. It is feasible that the availability of an yeast-based *in vitro* assay for the budding of distinct populations of vesicles from the donor ER membrane [125-130] could help to unravel the mechanism by which these lipid domains govern the sorting of membrane lipids and proteins within the ER membrane, thereby promoting their selective packaging into pre-peroxisomal and secretory vesicles.

1.4.2 Dynamic lipid domains in the membranes of immature peroxisomal vesicles are essential for the initial step of their multistep conversion to mature peroxisomes

In the yeast *Y. lipolytica*, the population of peroxisomes in a cell consists of six distinct vesicular subforms that have been purified and characterized [55]. The six peroxisomal subforms are related through the ordered conversion of one subform to another, being organized into a multistep peroxisome assembly pathway (Figure 1.2) [20, 34, 55]. The pathway leads to the formation of mature peroxisomes, P6, carrying the complete set of matrix and membrane proteins and membrane lipids. The pathway operates by conversion of five immature peroxisomal vesicles, termed P1 to P5, to mature peroxisomes in a temporally ordered manner from P1 to P6 [20, 34, 55]. The earliest intermediates in the pathway, the ER-derived immature peroxisomal vesicles P1 and P2, contain most of PMPs associated with mature peroxisomes but carry only a few matrix proteins [20, 34, 55]. An initial step in the multistep peroxisome assembly pathway involves the fusion of P1 and P2 to yield larger vesicles, P3 [55, 56]. Fusion

between P1 and P2 has been reconstituted *in vitro* [55, 56]. It is driven by ATP hydrolysis, requires cytosolic proteins and depends on the peroxins Pex1p and Pex6p [55, 56], two AAA ATPases essential for peroxisome biogenesis [3, 12, 14, 20]. Fusion of P1 and P2 is a multistep process that includes priming, docking and fusion events [56].

Recent findings of Boukh-Viner et al. provided evidence that membrane bilayers of both P1 and P2 exist in two lipid phases [133]. A detergent-soluble phase is enriched in glycerophospholipids but has only minute amounts of ergosterol and ceramide. The other phase resists solubilization by cold nonionic detergents and is highly enriched in ergosterol and ceramide. The term ergosterol- and ceramide-rich (ECR) domains was coined for this distinct phase of the peroxisomal membrane bilayer [133]. ECR domains in the membranes of P1 and P2 vesicles contain only minor portions of various glycerophospholipids. Similar to the well characterized lipid raft domains in the plasma membrane [134], ECR domains of unprimed P1 and P2 represent a substantial fraction of their membrane bilayers, with about half of membrane lipids and proteins being associated with these membrane domains [133]. Furthermore, both ECR domains in the membranes of P1 and P2 and lipid raft domains in the plasma membrane are extremely dynamic. When P1 and P2 vesicles are stimulated for priming and docking, numerous protein constituents of ECR domains rapidly move from these domains to an ergosterol- and ceramide-poor portion of the membrane [133]. Similarly, lipid raft proteins in the plasma membrane are extremely mobile and undergo rapid lateral diffusion in the membrane bilayer [135]. On the other hand, some key properties of ECR domains in the peroxisomal membrane bilayer clearly distinguish them from lipid raft domains in the

plasma membrane [133]. First, ceramide is the only sphingolipid component of ECR domains. The sphingosine base of this sphingolipid lacks a polar head group [136]. In contrast, sphingolipids of lipid rafts in the plasma membrane have large polar head groups attached to their sphingosine base [136]. Therefore, ceramide in model membrane bilayers forms detergent-insoluble lipid domains that are significantly more stable than those formed in the presence of plasma membrane sphingolipids [137]. Second, ceramide, which spontaneously flips across the membrane bilayer with a half-time of ~ 10 min [136], in ECR domains of the membranes of P1 and P2 is distributed symmetrically between the two leaflets of the bilayers [133]. This is in contrast to asymmetric distribution of sphingolipids, the abundant constituents of lipid rafts, across the lipid bilayer of the plasma membrane. Because, in contrast to ceramide, sphingolipids are unable to move across the bilayer [136], they are restricted to lipid raft domains in the outer leaflet of the plasma membrane [138, 139]. It has been suggested that the symmetric distribution of ceramide across the peroxisomal membrane and its ability to flip between the two leaflets of the bilayer can promote the coordination of events that occur in the cytosolic and lumenal leaflets of ECR domains.

ECR domains in the membranes of P1 and P2 are dynamic assemblies of a distinct set of lipids and proteins, including Pex1p, Pex6p, GTP-binding and hydrolyzing proteins (GTP-bp), and proteins that specifically bind to phosphatidylinositol-4-phosphate [PI(4)P] and phosphatidylinositol-4,5-bisphosphate [PI(4,5)P_2] (PI(4)P-bp and PI(4,5)P_2-bp, respectively) [133]. Recently, Boukh-Viner et al. provided evidence that these membrane domains function as an organizing platform for the fusion of P1 and P2 by

orchestrating the spatial and temporal reorganization of a protein team that only transiently resides in ECR domains and controls peroxisome fusion [133]. Based on these findings, Boukh-Viner et al. suggested the following model for the multistep remodeling of the peroxisome fusion machinery in the membrane bilayers of P1 and P2 (Figure 1.3) [133]. In unprimed P1 and P2, all identified essential components of this machinery, including Pex1p, Pex6p, GTP-bp, PI(4)P-bp and PI(4,5)P_2-bp, are attached to the cytosolic face of ECR domains. The lateral movement of P1-bound Pex1p and P2-associated Pex6p from ECR domains to an ergosterol- and ceramide-poor portion of the membrane initiates priming of both fusion partners. This essential event in the process of activating P1 and P2 for their subsequent docking includes at least three consecutive steps. The initial ergosterol-dependent step is followed by a PI(4)P-requiring step, which precedes a step that needs PI(4,5)P_2. After being segregated from ECR domains, both P1-bound Pex1p and P2-associated Pex6p are released to the cytosol. Such release of both AAA ATPases from ergosterol- and ceramide-poor portions of the membranes of both fusion partners is mandatory for their priming. The release of these AAA ATPases to the cytosol occurs in two steps. The first step depends on cytosolic proteins, whereas the next step is promoted by ATP hydrolysis. Primed peroxisomal vesicles then undergo docking. Docking of primed P1 and P2 is a multistep process. It begins with the lateral movement of PI(4,5)P_2-bp in the membranes of P1 and P2 from ECR domains to ergosterol- and ceramide-poor portions of their membranes. This lateral movement of PI(4,5)P_2-bp occurs in three consecutive steps. The first step depends on ergosterol in the membrane bilayers of both fusion partners. The second step needs Pex1p that resides in ECR

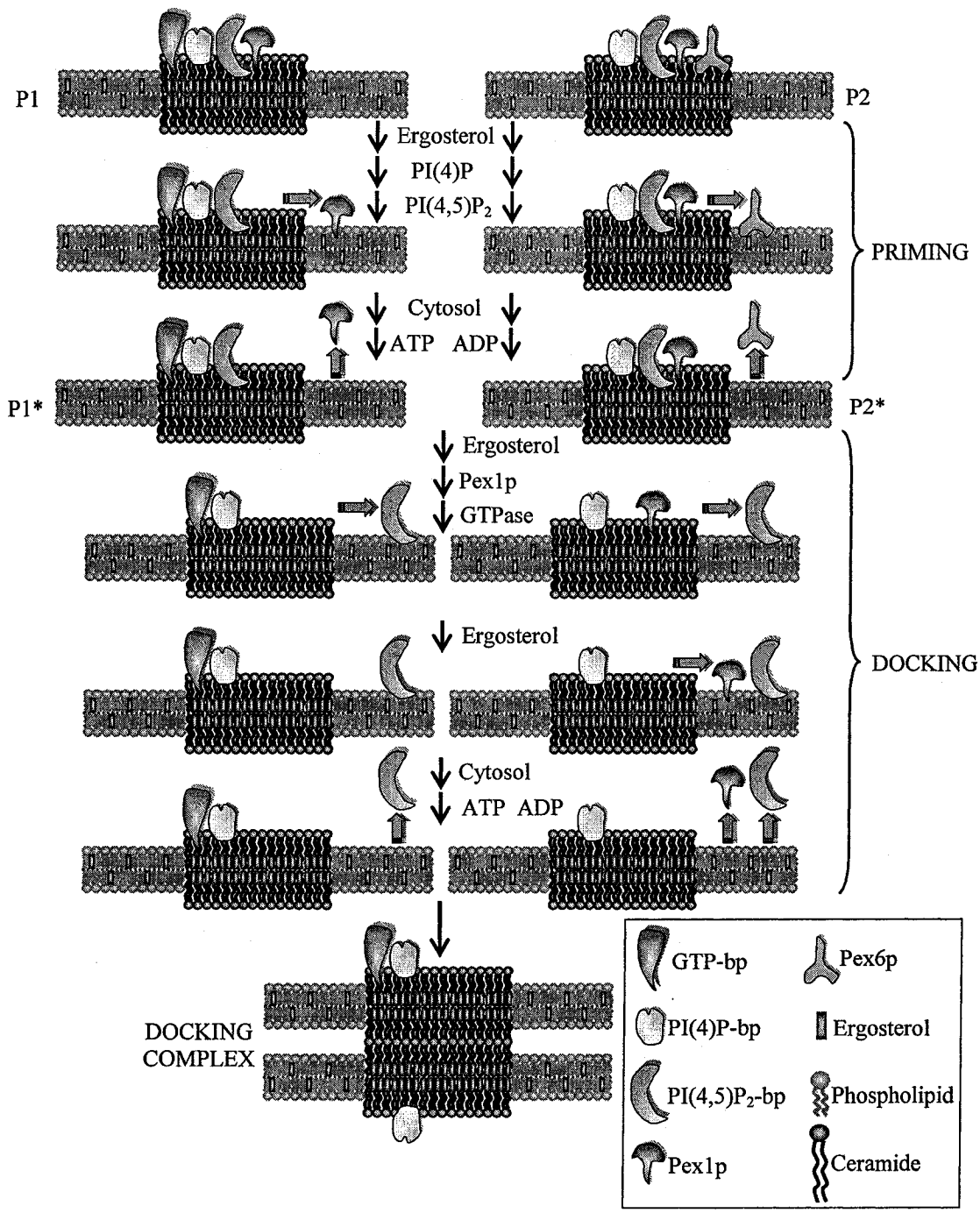

Figure 1.3. A model for the dynamics of temporal and spatial reorganization of the multicomponent peroxisome fusion machinery in the yeast *Y. lipolytica*. See text for details.

domains of P2 vesicles. The third step requires GTP hydrolysis by GTPase(s), perhaps by GTP-bp in ECR domains of P1 vesicles. The docking-specific sliding of PI(4,5)P_2-bp in the membranes of P1 and P2 is followed by the ergosterol-dependent lateral movement of P2-bound Pex1p from ECR domains to ergosterol- and ceramide-poor domains. After their relocation to ergosterol- and ceramide-poor portions of the membranes of both fusion partners, P1-associated PI(4,5)P_2-bp and P2-bound PI(4,5)P_2-bp and Pex1p are released to the cytosol. Such release of PI(4,5)P_2-bp and Pex1p begins with a cytosol-dependent step, which is followed by a step that needs ATP hydrolysis. It remains to be established how the described remodeling of the peroxisome fusion machineries in the membranes of both fusion partners changes the physical properties and topology of lipid bilayers in which these machineries operate, thereby triggering peroxisome docking. By the end of the docking process, PI(4)P-bp and GTP-bp remain in ECR domains of the membrane bilayers of P1 and P2 vesicles. The GTP-bp, together with calmodulin and protein machineries that maintain the gradients of Ca^{2+} and H^+ across the peroxisomal membrane, is mandatory for the fusion of docked P1 and P2 (our unpublished data).

1.4.3 Lipid transfer from the donor membranes of lipid bodies and ER expands the acceptor membranes of maturing peroxisomes

Peroxisomes in yeasts, plants and mammals lack enzymes required for the biosynthesis of their own membrane lipids [140-142]. Thus, any enlargement of peroxisomes that have been already detached from the ER template requires the transfer of lipids to their expanding membranes from the donor membranes of other organelles. What are these donor membranes? Lipid bodies, the ER-derived dynamic organelles

consisting of a core of neutral lipids that are surrounded by a monolayer of glycerophospholipids and associated proteins [143], serve as the major source of membrane lipids for the expansion of peroxisomal membrane in germinated cotton oilseeds [141]. The postgerminative growth of these seeds results in dramatic enlargement of glyoxysomes, a distinct form of peroxisomes that is required for the conversion of storage oil into carbohydrates. Under these conditions, lipid bodies provide the expanding glyoxysome membranes with the bulk of neutral lipids, mostly triacylglycerols, and glycerophospholipids [141]. The transfer of triacylglycerols and glycerophospholipids from the donor membranes of lipid bodies to the acceptor membranes of glyoxysomes requires membrane proteins embedded into the glycerophospholipid monolayer surrounding lipid bodies [141]. The identity of these membrane proteins remains to be established. Importantly, although the ER membrane is the primary cellular location of glycerophospholipid-synthesizing enzymes and functions as the major site of glycerophospholipid biosynthesis [136, 144], it does not serve as a donor membrane for the sorting of this class of lipids to the expanding glyoxysome membrane in germinated oilseeds [141]. It is presently unclear whether lipid bodies can function as a donor of lipids for the rapidly expanding peroxisomal membranes in mammalian or yeast cells. Noteworthy, microperoxisomes in mammalian adipocytes are closely associated with lipid bodies [145]. In addition, it has been shown that distinct peroxisomal structures accumulating in some conditional peroxisome biogenesis mutants of the yeast *Y. lipolytica* wrap around the surface of lipid bodies only if peroxisome biogenesis in these mutants has been induced due to their exposure to exogenous oleic

acid [146]. It remains to be seen whether the observed proximity of lipid bodies and distinct peroxisomal structures in mammals and yeasts can provide a way of transferring membrane lipids from the glycerophospholipid monolayer surrounding lipid bodies to the peroxisomal membrane bilayer.

In the yeast *Y. lipolytica*, the expansion of the membranes of ER-derived immature peroxisomal vesicles is mandatory for their stepwise conversion to mature peroxisomes P6, which carry the complete set of membrane lipids [20, 34, 55]. The bulk of glycerophospholipids in this yeast is transferred from the donor membrane of a specialized sub-compartment of the ER to the closely apposed acceptor membranes of the immature peroxisomal vesicles P3 and P4 [55, 75]. P3 and P4 are the early intermediates of the multistep pathway of peroxisome assembly operating in *Y. lipolytica* [20, 34, 55]. It seems that the peroxisome-bound peroxin Pex2p is required for the transfer of phosphatidylcholine, a major glycerophospholipid of the peroxisomal membrane [142, 147], from the donor membrane of this specialized sub-compartment of the ER to the acceptor membranes of P3 and P4. In fact, the *pex2Δ* knock-out mutation significantly decreases the glycerophospholipid levels of membranes from P3 and P4 and simultaneously increases the level of membrane glycerophospholipids in the P3- and P4-associated sub-compartment of the ER [75]. This ER sub-compartment can be distinguished from the free form of the ER by buoyant density, the level of membrane glycerophospholipids, and protein spectrum [75]. Taken together, these findings suggest that the Pex2p-dependent transfer of glycerophospholipids from the P3- and P4-associated ER sub-compartment to the acceptor membranes of P3 and P4 provides these

membranes with the bulk quantities of this lipid species and is essential for the conversion of P4 to the more mature peroxisomal vesicle, P5. The mechanism responsible for such ER-to-peroxisomal membrane transfer of glycerophospholipids remains to be established. It is conceivable that this transfer occurs at narrow cytosolic gaps called membrane contact sites [148], at which the ER and peroxisomal membranes come into close apposition. Recently, several working models for the role of ER-associated lipid-transfer proteins in the establishment and functioning of such membrane contact sites in yeast and mammalian cells have been proposed [148-152]. These models should serve as a useful starting point for examining such events during the multistep process of peroxisome assembly in *Y. lipolytica.*

1.4.4 Do membrane lipids regulate peroxisome division?

Scission of the peroxisomal membrane is mandatory for peroxisome division. Like any event of membrane scission [136, 153-156], scission of the peroxisomal membrane must be preceded by the destabilization of the membrane bilayer leading to membrane bending (Figure 1.4). Bending and scission of mitochondrial, chloroplast and Golgi membranes in yeasts, plants and mammals are energetically unfavorable processes that require several teams of proteins [156-168] and a distinct set of membrane lipids, including phosphoinositides [154, 159, 160, 169, 170], phosphatidic acid (PA) [136, 155, 158, 163, 171] and diacylglycerol (DAG) [136, 155, 158, 170]. PA induces negative monolayer curvature in the cytosolic leaflet of a membrane bilayer in the constricted neck (Figure 1.4) [136, 155, 159, 168]. The term "negative curvature" is used for defining the regions of a membrane bilayer that curve away from the cytosol, whereas the term "positive

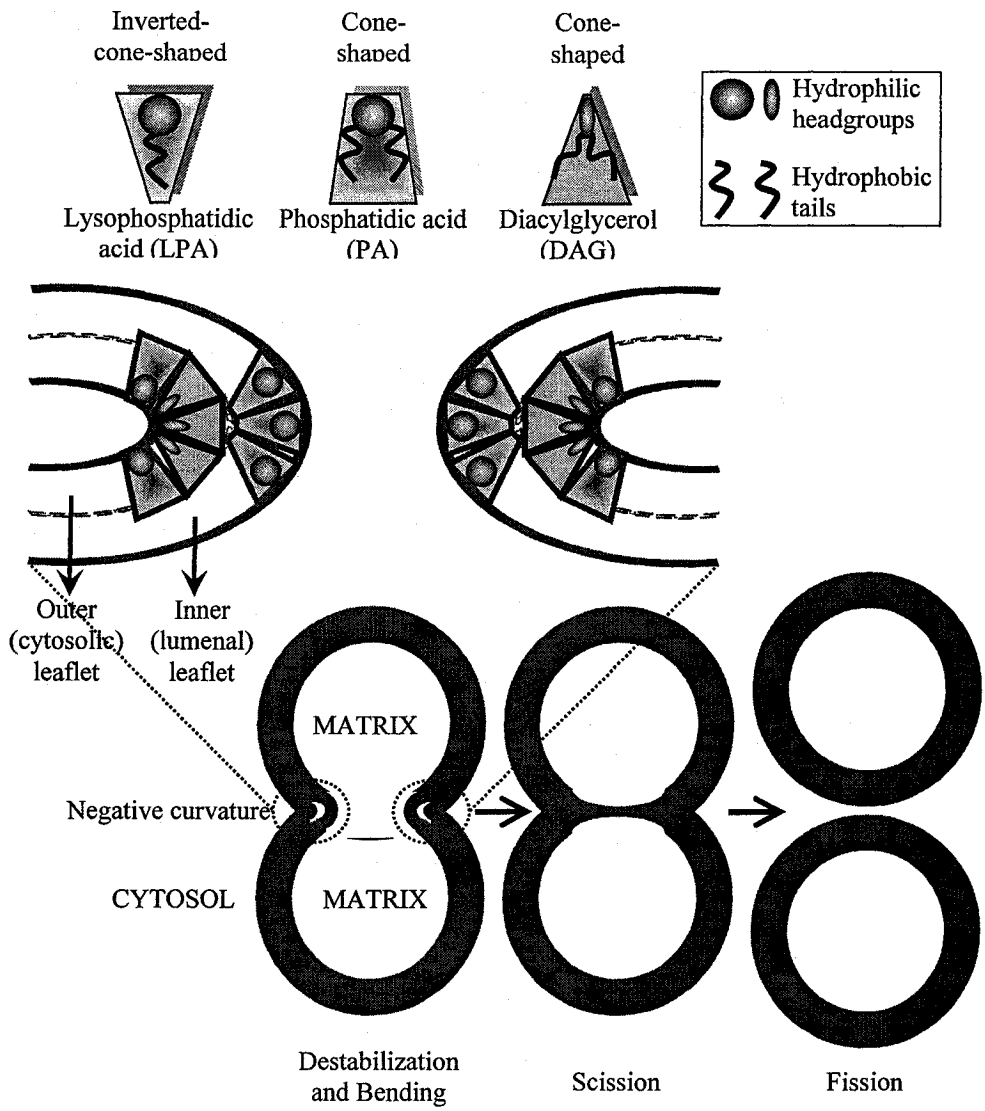

Figure 1.4. The molecular shape of membrane lipids plays an important role in generating membrane curvature.

curvature" indicates membrane areas that curve in the direction of the cytosol [136, 155, 156, 168]. PA has a shape of cone as the cross-section area of its hydrophilic headgroup is smaller than that of their two hydrophobic tails (Figure 1.4) [136, 154-156, 168]. Therefore, PA induces negative monolayer curvature in the outer (cytosolic) leaflet of a membrane bilayer in the constricted neck of a dividing organelle (Figure 1.4) [136, 153-

156, 159, 168]. DAG, which has even more conical shape [155, 159, 168, 172] and is capable of very rapid transbilayer movement and lateral partitioning [136, 148, 168, 172-174], is a particularly potent inducer of negative monolayer curvature and membrane bending (Figure 1.4) [154, 155, 168, 172-174]. In contrast, lysophosphosphatidic acid (LPA) has a shape of inverted cone as the cross-section area of its hydrophilic headgroup considerably exceeds that of its single hydrophobic tail (Figure 1.4) [136, 154-156, 168]. Therefore, this inverted-cone-shaped lipid favors positive monolayer curvature [135, 153-156, 159, 168]. The molecular shape of LPA makes it ideally suited for fitting in the inner (lumenal) leaflet of a membrane bilayer in the constricted neck of a dividing organelle (Figure 1.4) [154, 155, 168, 172-174]. The molecular shape of lipids is not the only determinant of membrane curvature. Several groups of curvature-generating and curvature-sensing proteins [156, 168] team up with membrane lipids in modulating the local curvature of organellar membranes. A major challenge now is to define the mechanism by which individual lipid species and lipid domains initiate the highly dynamic changes in the topology of the membrane bilayer in dividing peroxisomes, thereby generating negative membrane curvature and promoting destabilization, bending, scission and fission of the bilayer.

1.5 Thesis outline and contributions of colleagues

Chapter 2 describes findings providing evidence that, at the last step of assembly of mature peroxisomes from immature intermediates, a significant portion of the Aox complex inside the peroxisome relocates from the matrix to the membrane. This

relocation of Aox from the matrix to the membrane leads to the formation of a supramolecular complex containing two molecules of Aox and two molecules of the membrane-bound peroxin Pex16p. The relocation of Aox from the matrix to the membrane and its attachment to the inner (lumenal) face of this membrane requires two out of five Aox subunits, namely Aox4p and Aox5p, and Pex16p. Chapter 3 outlines evidence that scission of the membrane of mature peroxisomes, which results in their division, can occur only if all the Pex16p inside mature peroxisomes is titrated by its interaction with Aox complex that has relocated from the matrix to the membrane. These data show that Pex16p negatively regulates scission of the peroxisomal membrane required for peroxisome division. My observation that lack of Pex16p in *pex16KO* cells results in the excessive proliferation of immature peroxisomal vesicles further support this conclusion. The mechanism of the relocation of Aox from the matrix to the membrane of mature peroxisomes is described in Chapter 4. In particular, my findings provide evidence that the observed relocation of Aox complex from the matrix to the membrane of mature peroxisomes is due to an increase in the total mass of matrix proteins above a critical level, and that overloading mature peroxisomes with matrix proteins is a major factor in the relocation of Aox. The characteristic changes in the composition of peroxisomal membrane lipids and in their transbilayer distribution, which take place during peroxisome maturation, are described in Chapter 5. This chapter defines the mechanisms by which the Aox-Pex16p intracellular signaling cascade regulates the composition and properties of the membrane lipid bilayer in mature peroxisomes. Chapter 6 describes findings implying that the characteristic changes in the composition

and transbilayer distribution of peroxisomal membrane lipids promote the recruitment of Vps1p from the cytosol to the surface of the mature peroxisome. This recruitment of Vps1p to the peroxisomal membrane results in the formation of a multiprotein complex that includes proteins regulating actin cytoskeleton dynamics, as described in Chapter 7. This chapter includes a model that describes, in molecular terms, how the Pex16p- and Aox-dependent intraperoxisomal signaling cascade drives the division of mature peroxisomes by promoting the stepwise remodeling of lipid and protein composition of the peroxisomal membrane.

The findings presented in Chapters 2 to 4 have been published in *The Journal of Cell Biology* [Guo, T., Kit, Y.Y., Nicaud, J.-M., Le Dall, M.-T., Sears, S.K., Vali, H., Chan, H., Rachubinski, R.A. and Titorenko, V.I. Peroxisome division is regulated by a signal from inside the peroxisome. *J. Cell Biol.* (2003) 162:1255-1266] and reproduced here with the permission of the journal. I carried out more than 80% of all of the work described in this publication and prepared the first draft of the manuscript. Dr. V. Titorenko provided intellectual leadership of this project and edited the manuscript.

The data described in Chapters 5 to 7 are presented in the manuscript of a paper that has been recently submitted to *Molecular Cell*. I carried out and supervised more than 80% of all of the work described in this manuscript and prepared its first draft. Dr. V. Titorenko provided intellectual leadership of this project and edited the manuscript.

All abbreviations, citations, and the numbering of figures and tables that have been used in the published paper and in the submitted manuscript have been changed to the format of this thesis.

2 The Aox complex relocates from the matrix to the membrane inside mature peroxisomes

2.1 Abstract

The monitoring of the intraperoxisomal distribution of several abundant peroxisomal matrix proteins unexpectedly revealed that one of these normally soluble lumenal proteins, namely a heteropentameric protein complex of acyl-CoA oxidase (Aox), changes its localization inside the peroxisome during the last step of its maturation. Specifically, at the last step of assembly of mature peroxisomes from immature intermediates, a significant portion of Aox inside the peroxisome relocates from the matrix to the membrane. The relocation of the Aox complex from the matrix to the matrix face of the membrane of mature peroxisomes requires two Aox subunits, Aox4p and Aox5p, but not the three other subunits of the complex. The relocation of Aox from the matrix to the membrane at the last step of the assembly of mature peroxisomes results in the formation of a supramolecular protein complex. This complex contains two molecules of Aox complex and two molecules of the peroxin Pex16p, which is anchored to the inner (lumenal) face of the peroxisomal membrane.

2.2 Introduction

In the yeast *Yarrowia lipolytica*, five isoforms of acyl-CoA oxidase (Aox), designated Aox1p to Aox5p, constitute a 443-kD heteropentameric complex containing one polypeptide chain of each isoform within the peroxisomal matrix [175]. Assembly of the Aox complex in the cytosol precedes its import into the peroxisome. Peroxisomal targeting of the Aox complex requires the peroxin Pex5p, a component of the matrix

protein targeting machinery [175]. In contrast, peroxisomal import of the Aox complex does not involve the cytosolic chaperone Pex20p, which mediates the oligomerization and import of the peroxisomal matrix protein thiolase [175]. The subunits Aox2p and Aox3p play a pivotal role in the formation of the Aox complex in the cytosol. These two subunits can substitute for one another in promoting assembly of the complex. *In vitro*, the Aox2p and Aox3p subunits retard disassembly of the Aox complex and increase the efficiency of its reassembly [175]. Neither of these two Aox subunits is required for acquisition of the cofactor FAD by three other components of the complex. There is evidence that the Aox2p- and Aox3p-assisted assembly of the Aox complex in the cytosol is a prerequisite for its import into peroxisomes, so that none of the individual components of the Aox complex can penetrate the peroxisomal matrix as a monomer [175].

2.3 Materials and methods

The *Y. lipolytica* wild-type strain *P01d* (*MatA ura3-302 leu2-270 xpr2-302*) [176], the mutant strains *aox5KO* (*MatA ura3-302 leu2-270 xpr2-3 aox5::URA3*) [175], *pex16KO* (*MatA ura3-302 leu2-270 xpr2-3 pex16::LEU2*) and *pex16-TH* (*MatA ura3-302::PEX16TH-URA3 leu2-270 xpr2-3 pex16-1*) [123], and the single *AOX* gene knock-out strains *aox1KO* (*MatA ura3-302 leu2-270 xpr2-3 aox1::URA3*), *aox2KO* (*MatA ura3-302 leu2-270 xpr2-3 aox2::URA3*), *aox3KO* (*MatA ura3-302 leu2-270 xpr2-3 aox3::URA3*), *aox4KO* (*MatA ura3-302 leu2-270 xpr2-3 aox4::URA3*) [176] were used. Yeast strains were initially grown in YPD (1% yeast extract, 2% peptone, 2% glucose) medium to an OD_{600} of ~1.5 and then shifted to YPBO (0.3% yeast extract, 0.5% peptone, 0.5% K_2HPO_4, 0.5% KH_2PO_4, 1% Brij-35, 1% [wt/ vol] oleic acid) medium to

proliferate peroxisomes.

Rabbit polyclonal antibodies to the Aox1p, -3p and –5p subunits of the Aox complex [175], Pex2p [177], Pex5p [178], Pex16p [123], isocitrate lyase (ICL) [48], thiolase (THI) [178] and malate synthase (MLS) [48] have been described.

The initial step in the subcellular fractionation of YPBO-grown cells included the differential centrifugation of lysed and homogenized spheroplasts at 1,000 x *g* for 8 min at 4°C in a rotor (model JS13.1; Beckman Instrs., Inc., Palo Alto, CA) to yield a postnuclear supernatant (PNS) fraction. The PNS fraction was further subjected to differential centrifugation at 20,000 x *g* for 30 min at 4°C in a model JS13.1 rotor (Beckman Instrs.) to yield pellet (20KgP) and supernatant (20KgS) fractions. The 20KgS fraction was further subfractionated by differential centrifugation at 200,000 x *g* for 1 h at 4°C in a model TLA120.2 rotor (Beckman Instrs., Inc.) to yield pellet (200KgP) and supernatant (200KgS) fractions.

To purify mature peroxisomes P6, the 20 KgP was further fractionated by flotation on a three-step sucrose gradient. Specifically, the 20 KgP was resuspended in 400 µl of 60% (wt/wt) sucrose in buffer H (5 mM MES, pH 5.5, 1 mM KCl, 0.5 mM EDTA, 0.1% [vol/vol] ethanol), overlaid with 2.3 ml of 50% (wt/wt) sucrose and 2.3 ml of 20% (wt/wt) sucrose (both in buffer H), and subjected to centrifugation in a model SW50.1 rotor (Beckman Instrs.) at 200,000 x *g* for 18 h at 4°C. Gradients were fractionated from the bottom, and 18 fractions of ~270 µl each were collected. To further purify mature peroxisomes P6, 4 vol of 0.5 M sucrose in buffer H were added to the peak peroxisomal fraction 4 recovered after isopycnic centrifugation on a discontinuous

sucrose gradient. Peroxisomes were sedimented through a 150-µl cushion of 2 M sucrose in buffer H by centrifugation at 200,000 x *g* for 20 min at 4°C in a TLA120.2 rotor. The resultant pellet was resuspended in buffer H containing 1 M sorbitol and was subjected to further centrifugation on a linear 20-60% (wt/wt) sucrose gradient (in buffer H) at 197,000 x *g* for 18 h at 4°C in a model SW41Ti rotor (Beckman Instrs., Inc.). Peak peroxisomal fraction 5 equilibrating at a density of 1.21 g/cm^3 was recovered, and purified mature peroxisomes were pelleted at 200,000 x *g* for 20 min at 4°C in a TLA120.2 rotor, as described above. Pelleted peroxisomes were resuspended in 400 µl of 60% (wt/wt) sucrose in buffer H and subjected to flotation on a three-step sucrose gradient as described above. Peak peroxisomal fraction 4 was recovered and used for biochemical analyses. Peroxisomes isolated by this multistep method were greater than 97% pure, as judged by the presence of marker proteins of other organelles.

To purify immature peroxisomes P1 to P5, a 200,000-*g* pellet fraction (200KgP) was subjected to centrifugation on a discontinuous sucrose (18, 25, 30, 35, 40, and 53%, wt/wt) gradient at 120,000 x *g* for 18 h at 4°C in a Beckman SW28 rotor. 36 fractions of 1 ml each were collected. Fractions containing different subforms of immature peroxisomes were recovered, and 4 vol of 0.5 M sucrose in buffer H (5 mM MES, pH 5.5, 1 mM KCl, 0.5 mM EDTA, 0.1% ethanol, and a mixture of protease inhibitors) were added. Immature peroxisomes were pelleted onto a 150-µl cushion of 2 M sucrose in buffer H by centrifugation at 200,000 x *g* for 20 min at 4°C in a Beckman TLA120.2 rotor. Individual pellets of different subforms of immature peroxisomes were resuspended

in 3 ml of 50% (wt/wt) sucrose in buffer H.

For purification of immature peroxisomes P1 and P2, pellets of P1 and P2 resuspended in 50% (wt/wt) sucrose in buffer H were overlaid with 30, 28, 26, 24, 22, and 10% sucrose (all wt/wt in buffer H). After centrifugation at 120,000 x *g* for 18 h at 4°C in a SW28 rotor, 18 fractions of 2 ml each were collected. P1 and P2 were pelleted, resuspended and subjected to a second flotation on the same multistep sucrose gradient. Gradients were fractionated into 2-ml fractions as above, and P1 and P2 were recovered and pelleted.

For purification of immature peroxisomes P3 and P4, pellets of P3 and P4 resuspended in 50% (wt/wt) sucrose in buffer H were overlaid with 38%, 35%, 33% and 20% sucrose (all wt/wt in buffer H). After centrifugation at 120,000 x *g* for 18 h at 4°C in a SW28 rotor, 18 fractions of 2 ml each were collected. P3 and P4 were pelleted, resuspended in 3 ml of 50% (wt/wt) sucrose in buffer HE (20 mM MES, pH 5.5, 20 mM EDTA, 0.1% ethanol), overlaid with 39, 37, 35, 33, and 20% sucrose (all wt/wt in buffer HE), and subjected to centrifugation as above. Gradients were fractionated into 2-ml fractions, and P3 and P4 were recovered and pelleted. After resuspension in 3 ml of 50% (wt/wt) sucrose in buffer H, P3 and P4 were again subjected to flotation on the second multistep sucrose gradient described above. Gradients were fractionated into 2-ml fractions, and P3 and P4 were recovered and pelleted.

Covalent coupling of affinity-purified antibodies to protein A-Sepharose for

immunoaffinity chromatography was performed as described previously [175]. For immunoaffinity chromatography under native conditions, peroxisomal matrix proteins recovered in the supernatant fraction after centrifugation of osmotically lysed peroxisomes and peroxisomal liposomes were diluted with an equal volume of 50 mM Tris-HCl, pH 7.5, buffer containing 300 mM NaCl, 1% (v/v) Triton X-100 and protease inhibitor cocktail. The pellets of PMPs recovered after centrifugation of osmotically lysed peroxisomes and peroxisomal liposomes were resuspended in 25 mM Tris-HCl, pH 7.5, buffer containing 150 mM NaCl, 0.5% (v/v) Triton X-100 and protease inhibitor cocktail. Samples were cleared of any nonspecifically binding proteins by incubation for 20 min at 4°C with protein A-Sepharose washed five times with 10 mM Tris-HCl, pH 7.5. The cleared samples were then subjected to immunoaffinity chromatography. Bound proteins were washed five times with 25 mM Tris-HCl, pH 7.5, 150 mM NaCl, 0.5% (v/v) Triton X-100, and eluted with 100 mM glycine, pH 2.8. Proteins were precipitated by addition of trichloroacetic acid to 10%, washed in ice-cold 80% (v/v) acetone, and then subjected to SDS-PAGE followed by immunoblotting. For immunoaffinity chromatography under denaturing conditions, PMPs purified by immunoaffinity chromatography under native conditions and proteins recovered in the 200KgS (cytosolic), 200KgP and 20KgP subcellular fractions were diluted with an equal volume of 4% SDS, and samples were warmed at 65°C for 10 min. Samples were then allowed to cool to room temperature, and 4 volumes of 62.5 mM Tris-HCl, pH 7.5, buffer containing 190 mM NaCl, 1.25% (v/v) Triton X-100, and 6 mM EDTA were added. Samples were cleared of any nonspecifically binding proteins by incubation for 20 min at 4°C with protein A-

Sepharose washed five times with 10 mM Tris-HCl, pH 7.5. The cleared samples were then subjected to immunoaffinity chromatography. Bound proteins were washed five times with 50 mM Tris-HCl, pH 7.5, 150 mM NaCl, 1% (v/v) Triton X-100, and eluted with 2% SDS at 95°C for 5 min. Eluted proteins were subjected to a second immunoprecipitation (recapture) step, resolved by SDS-PAGE, and analyzed by immunoblotting.

For flotation gradient analysis, the pellet of PMPs recovered after centrifugation of osmotically lysed P6 peroxisomes was resuspended in 100 µl of buffer M (10 mM MES-KOH, pH 5.5, 1 mM KCl, 0.5 mM EDTA, 0.1% (v/v) ethanol and protease inhibitor cocktail), transferred to the bottom of a 5-ml ultraclear centrifuge tube (Beckman) and supplemented with 5 volumes of 65% (w/w) sucrose in buffer M in order to adjust the sucrose concentration of the sample to 54% (w/w). The sample was then overlaid with 1.1 ml of 45% sucrose, 1.1 ml of 30% sucrose, 1.1 ml 10% sucrose (all w/w in buffer M) and lastly with 1.1 ml of buffer M alone. After centrifugation at 200,000 × *g* for 18 h at 4°C in a SW50.1 rotor (Beckman), 18 fractions of 275 µl each were collected. SDS-PAGE and immunoblotting were performed according to established procedures [48]. Peroxisomal matrix proteins recovered in the supernatant fraction after centrifugation of osmotically lysed P6 peroxisomes were incubated for 2 h at 75°C. Under these conditions, all matrix proteins formed insoluble aggregates, as judged by light scattering at 320 nm and as confirmed by SDS-PAGE followed by Coomassie staining. Aggregates of peroxisomal matrix proteins were pelleted by centrifugation at 20,000 x *g* for 30 min at

4°C and resuspended in 100 µl of buffer M. This material was subjected to flotation on a multi-step sucrose gradient as described above.

2.4 Results

2.4.1 The Aox complex is equally distributed between the matrix and the membrane of mature peroxisomes

Aox is present as a 443-kD heteropentameric complex composed of one polypeptide chain of each of its five subunits, Aox1p to Aox5p, in the matrix of mature peroxisomes P6 [175]. After centrifugation of osmotically lysed mature peroxisomes, this matrix form of Aox was recovered in the supernatant fraction (Figure 2.1 A). In addition, about half of the peroxisome-bound pool of each Aox subunit could be pelleted during centrifugation (Figure 2.1 A). The observed recovery of Aox subunits in the pelletable fraction was not due to the greater resistance of mature peroxisomes to osmotic lysis. In fact, none of the three other most abundant peroxisomal matrix proteins tested, namely isocitrate lyase (ICL), thiolase (THI) and malate synthase (MLS), could be pelleted during centrifugation of osmotically lysed mature peroxisomes (Figure 2.1 B). The pelletable form of each Aox subunit could float out of the most dense sucrose during centrifugation to equilibrium in a sucrose density gradient (Figure 2.2 A). In contrast, temperature-induced aggregates of peroxisomal matrix proteins remained at the bottom of the gradient (Figure 2.2 B). Accordingly, all pelletable Aox subunits in mature peroxisomes were present as membrane-associated forms rather than as aggregates. Furthermore, protease protection experiments revealed that all five Aox subunits were degraded by trypsin only when the membrane of mature peroxisomes was disrupted by Triton X-100, whereas the peripheral

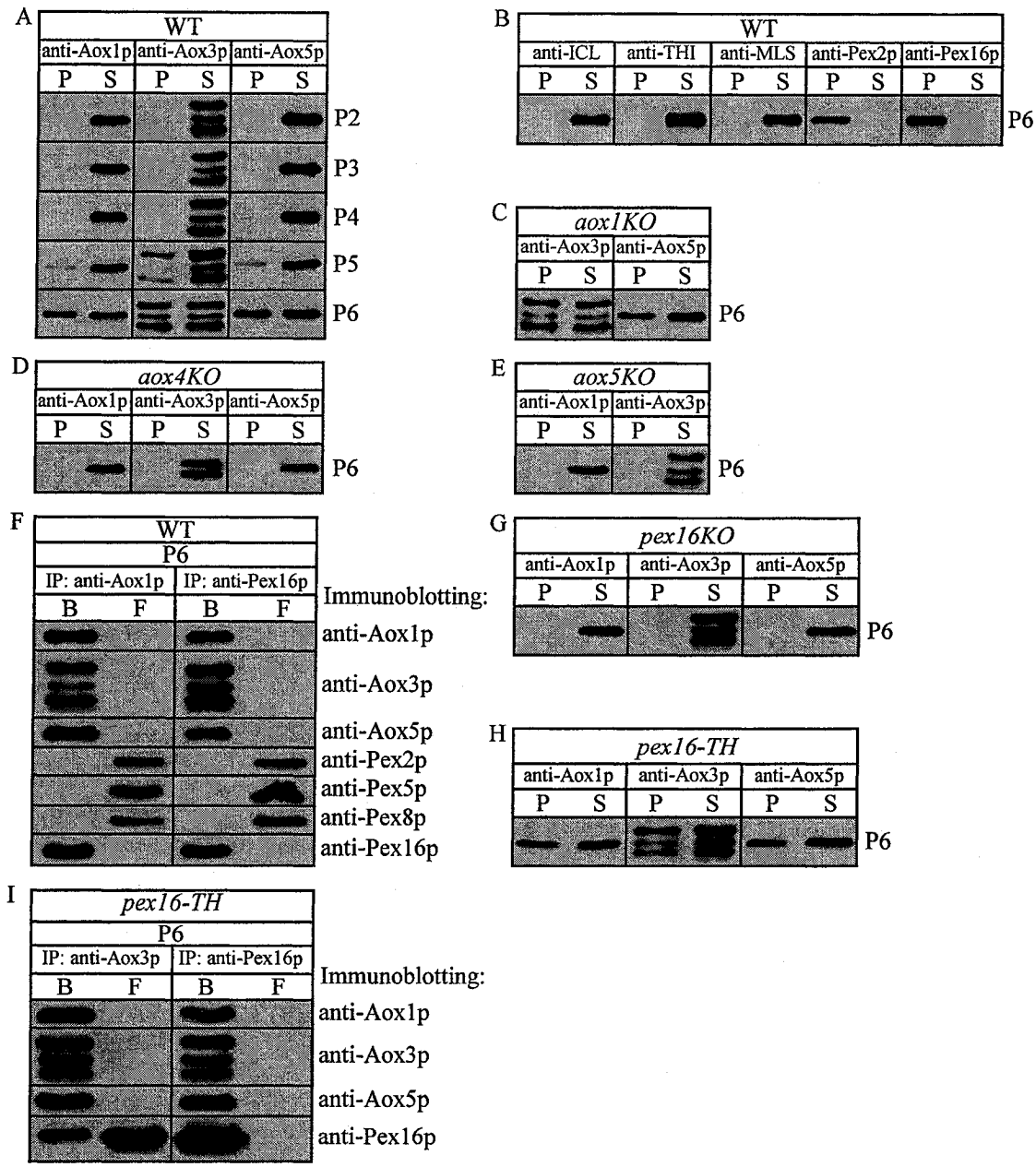

Figure 2.1. Relocation of the heteropentameric Aox complex from the matrix to the membrane occurs in mature peroxisomes P6, requires its Aox4p and Aox5p subunits, and results in its binding to Pex16p. (A, C–E, G, H) The distribution of Aox subunits between the matrix and the membrane of different peroxisomal subforms purified from wild-type (A) and *aox1KO* (C), *aox4KO* (D), *aox5KO* (E), *pex16KO* (G), and *pex16-TH* (H) mutant cells. After osmotic lysis, peroxisomes were subjected to centrifugation to yield supernatant (*S*, matrix proteins) and pellet (*P*, membrane proteins) fractions. Recovered proteins were resolved by SDS-PAGE and immunoblotted with antibodies to the Aox1p, -3p and –5p subunits of the Aox complex. Antibodies raised against Aox1p and Aox5p recognize specifically these subunits. Antibodies raised against Aox3p recognize subunits Aox4p, -2p, and –3p (top, middle, and bottom bands, respectively). (B) The distribution of the peroxisomal matrix proteins isocitrate lyase (ICL), thiolase (THI) and malate synthase (MLS) and of the peroxisomal membrane proteins Pex2p and Pex16p

between the supernatant (*S*, matrix proteins) and pellet (*P*, membrane proteins) fractions recovered after centrifugation of osmotically lysed P6 peroxisomes. Recovered proteins were immunoblotted with the indicated antibodies. (F and I) Membrane proteins of P6 peroxisomes from wild-type (F) and *pex16-TH* mutant (I) cells were subjected to immunoaffinity chromatography under native conditions using anti-Aox1p or anti-Aox3p or anti-Pex16p antibodies covalently coupled to protein A-Sepharose. Proteins bound to the column (*B*) and unbound proteins recovered in the flow-through (*F*) were immunoblotted with the indicated antibodies. *IP*, immunoprecipitation.

membrane proteins Pex1p and Pex6p on the cytosolic surface of peroxisomes [55] were sensitive to trypsin digestion even in the absence of the detergent (Figure 2.2 C). Therefore, all Aox subunits were present as membrane-enclosed forms. Extraction of the membrane-associated Aox subunits with various solubilizing agents showed that they fractionated as peripheral membrane proteins that were solubilized completely by either 1 M NaCl or 0.1 M Na_2CO_3, pH 11.0 (Figure 2. 2 D). Thus, in mature peroxisomes of wild-type cells, Aox was equally distributed between the matrix and the matrix face of the membrane. In contrast, none of Aox subunits in immature peroxisomes P2 to P4, and only a minor portion of each subunit in immature peroxisomes P5, were membrane-bound (Figure 2.1 A). Immature peroxisomes P1 lack Aox [55]. Immunoaffinity chromatography of membrane proteins from mature peroxisomes of the wild-type strain showed that all five Aox subunits coimmunoprecipitated under native conditions with anti-Aox1p antibodies (Figure 2.1 F). Therefore, like the Aox complex in the peroxisomal matrix, the complex at the matrix face of the peroxisomal membrane in mature peroxisomes of wild-type cells includes all five Aox subunits. Taken together, these results strongly suggest that at the last step of assembly of mature peroxisomes from immature intermediates, a significant portion of the Aox complex inside the peroxisome relocates from the matrix to the membrane.

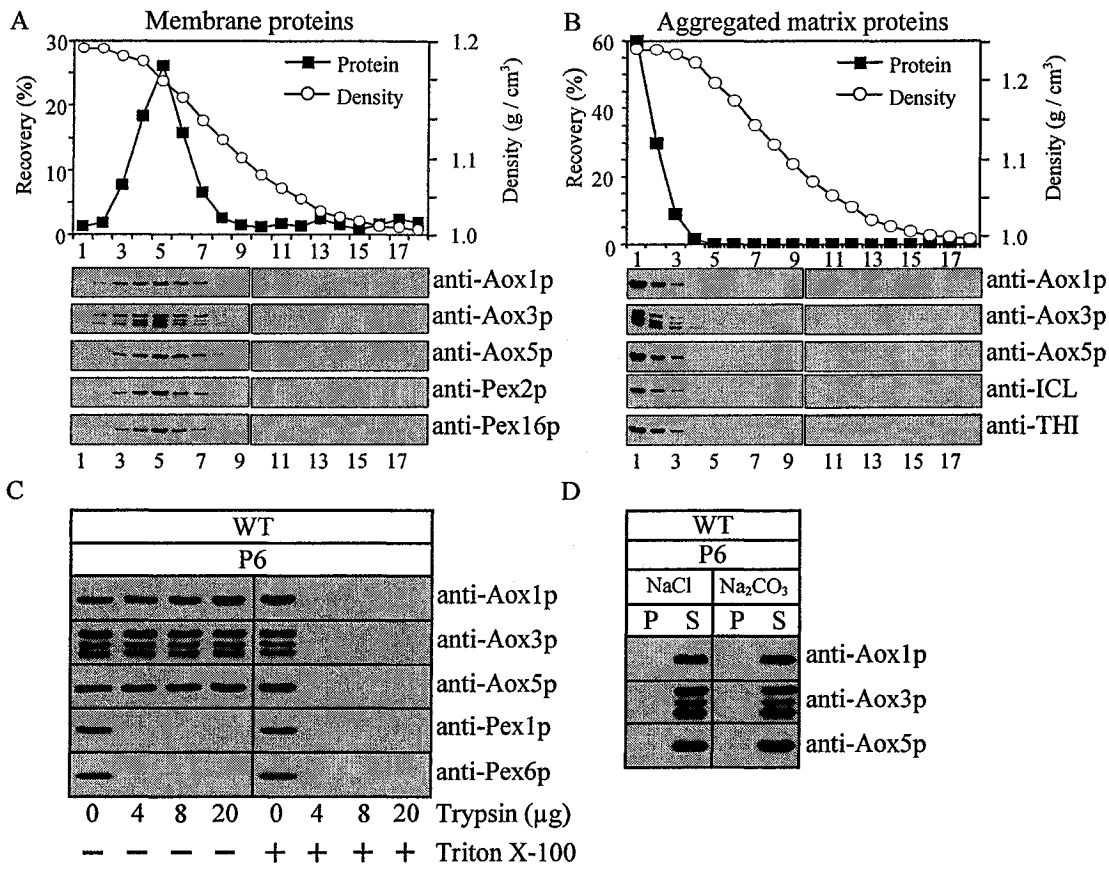

Figure 2.2. Inside mature peroxisomes of wild-type cells, all membrane-bound Aox subunits are attached to the matrix face of the membrane. (A and B) Membrane proteins (A) and heat-aggregated matrix proteins (B) of P6 peroxisomes were subjected to flotation on a multi-step sucrose gradient. Sucrose density (g/cm^3) and percent recovery of loaded protein in gradient fractions are presented. Gradient fractions were immunoblotted with the indicated antibodies. (C) Protease protection analysis. P6 peroxisomes were treated with the indicated amounts of trypsin in the absence (-) or presence (+) of 1.0% (v/v) Triton X-100 for 30 min on ice. Samples were subjected to SDS-PAGE and immunoblotting with the indicated antibodies. (D) Membrane proteins of P6 peroxisomes were treated with either 1 M NaCl or 0.1 M Na_2CO_3, pH 11.0. After incubation on ice for 30 min, samples were separated into supernatant (*S*) and pellet (*P*) fractions by centrifugation and then immunoblotted with anti-Aox1p, -3p and –5p antibodies.

The relocation of the Aox complex from the matrix to the matrix face of the membrane of mature peroxisomes requires two Aox subunits, Aox4p and Aox5p, but not the three other subunits of the complex. Indeed, none of the Aox subunits was associated

with the peroxisomal membrane in the mutant strains *aox4KO* and *aox5KO* deleted individually for the *AOX4* and *AOX5* genes, respectively (Figures 2.1 D and 2.1 E). In contrast, lack of Aox1p (Figure 2.1 C) did not impair the redistribution of other Aox subunits from the matrix to the membrane of mature peroxisomes. In the mature peroxisomes of *aox1KO*, *aox2KO* and *aox3KO* cells, all remaining Aox subunits form a complex both in the matrix [55] and at the matrix face of the membrane (Figure 2.3).

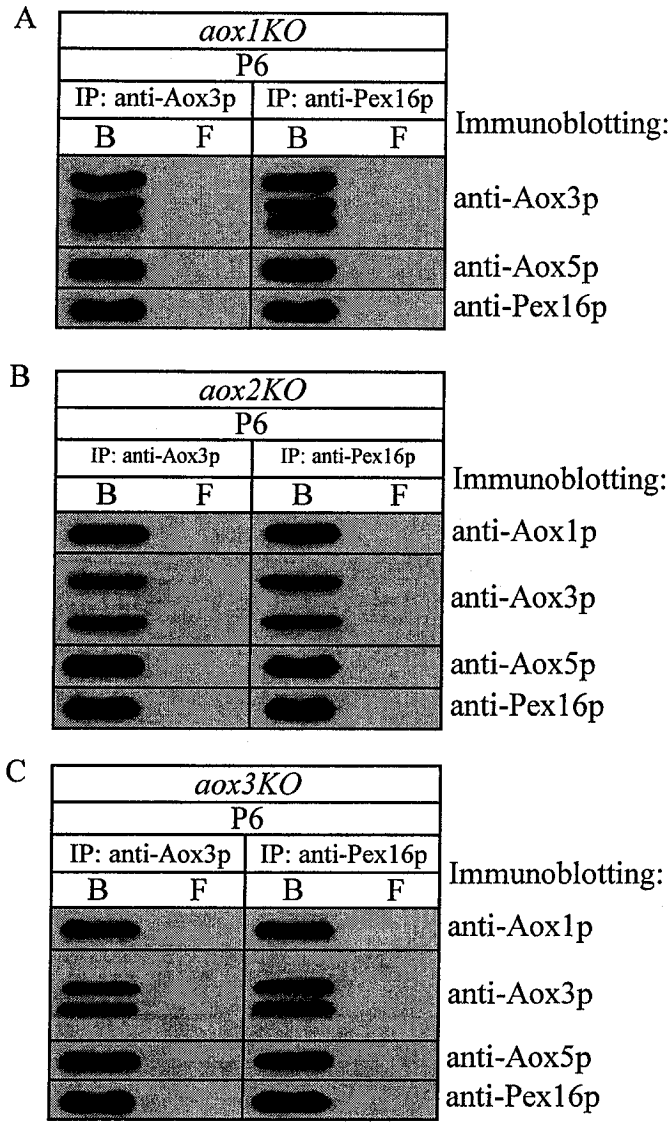

Figure 2.3. All remaining Aox subunits form a membrane-attached complex that interacts with Pex16p inside mature peroxisomes of mutant cells lacking Aox1p or Aox2p or Aox3p. Membrane proteins of P6

peroxisomes from *aox1KO* (A), *aox2KO* (B) and *aox3KO* (C) mutant cells were subjected to immunoaffinity chromatography under native conditions using either anti-Aox3p or anti-Pex16p antibodies covalently coupled to protein A-Sepharose. Proteins bound to the column (*B*) and unbound proteins recovered in the flow-through (*F*) were immunoblotted with the indicated antibodies.

2.4.2 The membrane-bound Aox complex interacts with the peripheral membrane peroxin Pex16p inside mature peroxisomes

The membrane-associated Aox complex of mature peroxisomes of wild-type cells coimmunoprecipitated under native conditions with the peroxin Pex16p (Figure 2.1 F), which is attached to the matrix face of the peroxisomal membrane [123]. Neither Aox nor Pex16p was recovered in the flow-through when native immunoprecipitation was done with anti-Aox1p or anti-Pex16p antibodies (Figure 2.1 F). Thus, the membrane-bound pools of both Aox and Pex16p in mature peroxisomes of wild-type cells were present only as components of a complex, and none of these proteins could be found in its free form. No other peroxisomal membrane peroxin tested, including Pex2p [177], Pex5p [178] and Pex8p [179], interacted with the membrane-bound Aox or Pex16p (Figure 2.1 F).

The different Aox subunits and Pex16p are present in equimolar amounts in their membrane-associated complex, as judged by quantitation of their stoichiometry in *L*-[^{35}S]methionine-labeled complex immunoprecipitated from mature peroxisomes of wild-type cells (Figure 2.4, panels A and C). No other radiolabeled membrane protein coimmunoprecipitated with the components of the Aox-Pex16p complex under native conditions (Figure 2.4 B). Whereas the molecular weight of the Aox complex recovered from the matrix of mature peroxisomes was ~443 kD (Figure 2.5 A) [175], the molecular weight of the Aox-Pex16p complex attached to the matrix face of the peroxisomal

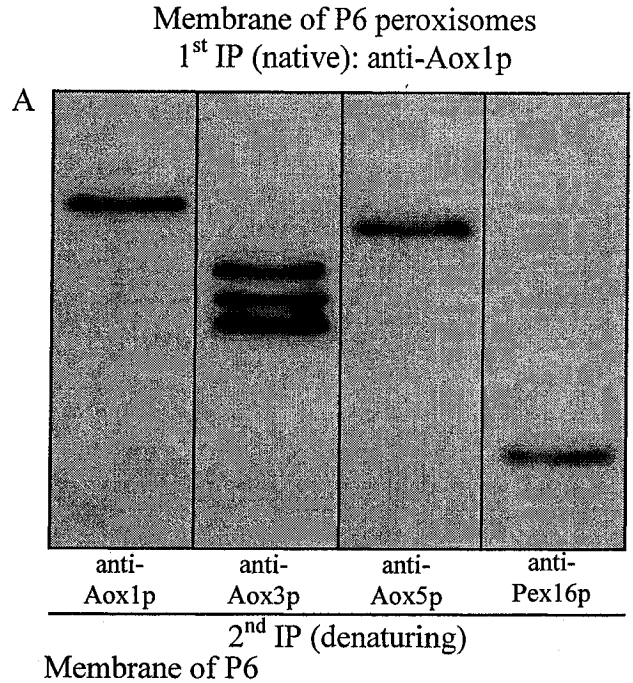

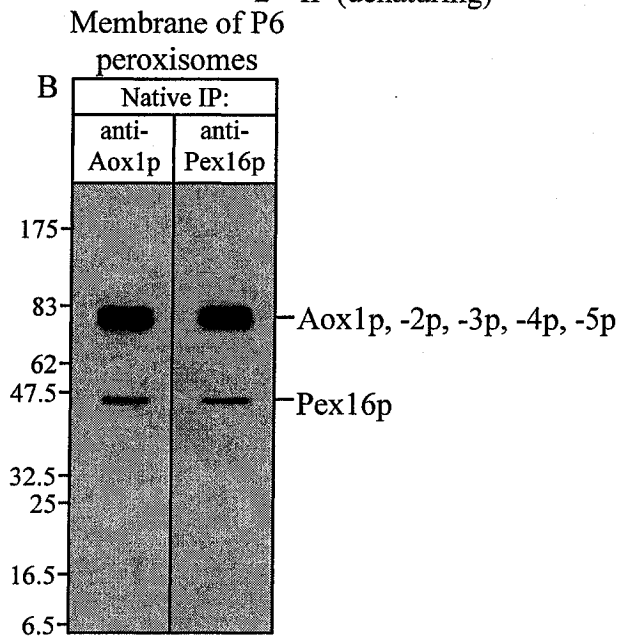

C

Molar ratio of Aox subunits and Pex16p in their membrane-associated complex					
Aox1p	Aox2p	Aox3p	Aox4p	Aox5p	Pex16p
1.0	1.10 ± 0.09	1.05 ± 0.11	0.94 ± 0.07	0.96 ± 0.03	0.92 ± 0.06

Figure 2.4. All five Aox subunits and Pex16p are present in equimolar amounts in their membrane-associated complex inside mature peroxisomes. (A) P6 peroxisomes were purified from wild-type cells pulse-labeled with L-[^{35}S]methionine for 2 min and chased with unlabeled L-methionine for 30 min. Membrane proteins recovered after centrifugation of osmotically lysed peroxisomes were subjected to immunoaffinity chromatography under native conditions using anti-Aox1p antibodies covalently coupled to

protein A-Sepharose. Immunoprecipitated proteins eluted with 100 mM glycine, pH 2.8, were subjected to a second immunoprecipitation under denaturing conditions with anti-Aox1p, anti-Aox3p, anti-Aox5p, or anti-Pex16p antibodies covalently coupled to protein A-Sepharose. Immunoprecipitated proteins were resolved by SDS-PAGE and subjected to fluorography. (B) Pulse-labeled and chased membrane proteins were subjected to a first immunoprecipitation under native conditions, as described in the legend to (A). Proteins immunoprecipitated with either anti-Aox1p or anti-Pex16p antibodies were resolved by SDS-PAGE and visualized by fluorography. The positions of Aox subunits and Pex16p are indicated. (C) To quantify the stoichiometry of the membrane-associated Aox-Pex16p complex, the densities of the signals for Aox1p to Aox5p and Pex16p (A) were divided by 15, 13, 16, 19, 17 and 10, the number of methionine residues in Aox1p, Aox-2p, Aox-3p, Aox-4p, Aox-5p, and Pex16p, respectively.

membrane in wild-type cells was ~900 kD (Figure 2.5 B). From these observations and a consideration of the molecular weights of each Aox subunit (~80 kD) and Pex16p (~45 kD), I conclude that relocation of a significant portion of the Aox complex from the matrix to the membrane at the last step of the assembly of mature peroxisomes leads to the formation of a supramolecular complex containing two molecules of Aox complex and two molecules of Pex16p. Relocation of Aox complex to the matrix face of the peroxisomal membrane requires two Aox subunits, namely Aox4p and Aox5p, and Pex16p. In fact, no membrane-bound form of the Aox complex was detected in mature peroxisomes recovered from mutant cells lacking any of these three proteins (Figure 2.1, panels D, E and G).

2.5 Discussion

Data presented in Figure 2.1 provide evidence that the Aox complex is equally distributed between the matrix and the matrix face of the membrane in mature peroxisomes only. In contrast, none of Aox subunits in immature peroxisomes P2 to P4, and only a minor portion of each subunit in immature peroxisomes P5, are membrane-associated. My findings reported in Figure 2.1 imply that the observed recovery of Aox subunits in the pelletable fraction was not due to the greater resistance of mature peroxisomes to osmotic

lysis. Furthermore, data presented in Figure 2.2 clearly show that all pelletable Aox subunits in osmotically lysed mature peroxisomes are present as membrane-associated forms rather than as aggregates. My data also imply that, like the Aox complex in the peroxisomal matrix, the complex at the matrix face of the peroxisomal membrane in mature peroxisomes of wild-type cells includes all five Aox subunits (Figure 2.1). Data provided in Figure 2.1 also strongly suggest that the relocation of the Aox complex from the matrix to the matrix face of the membrane of mature peroxisomes requires two Aox subunits, Aox4p and Aox5p, but not the three other subunits of the complex. My findings imply that the membrane-bound pool of Aox in mature peroxisomes binds to the membrane-bound peroxin Pex16p attached to the inner (lumenal) face of the peroxisomal membrane (Figures 2.1, 2.3 and 2.4). Importantly, the membrane-bound pools of both Aox and Pex16p in mature peroxisomes of wild-type cells are present only as components of a complex, and none of these proteins can be found in its free form (Figure 2.1).

2.6 Conclusions

Taken together, my findings strongly suggest that, at the last step of assembly of mature peroxisomes from immature intermediates, a significant portion of the Aox complex inside the peroxisome relocates from the matrix to the membrane. The observed relocation of a significant portion of Aox from the matrix to the membrane inside mature peroxisomes leads to the formation of a supramolecular complex containing two molecules of Aox complex and two molecules of the peripheral membrane peroxin

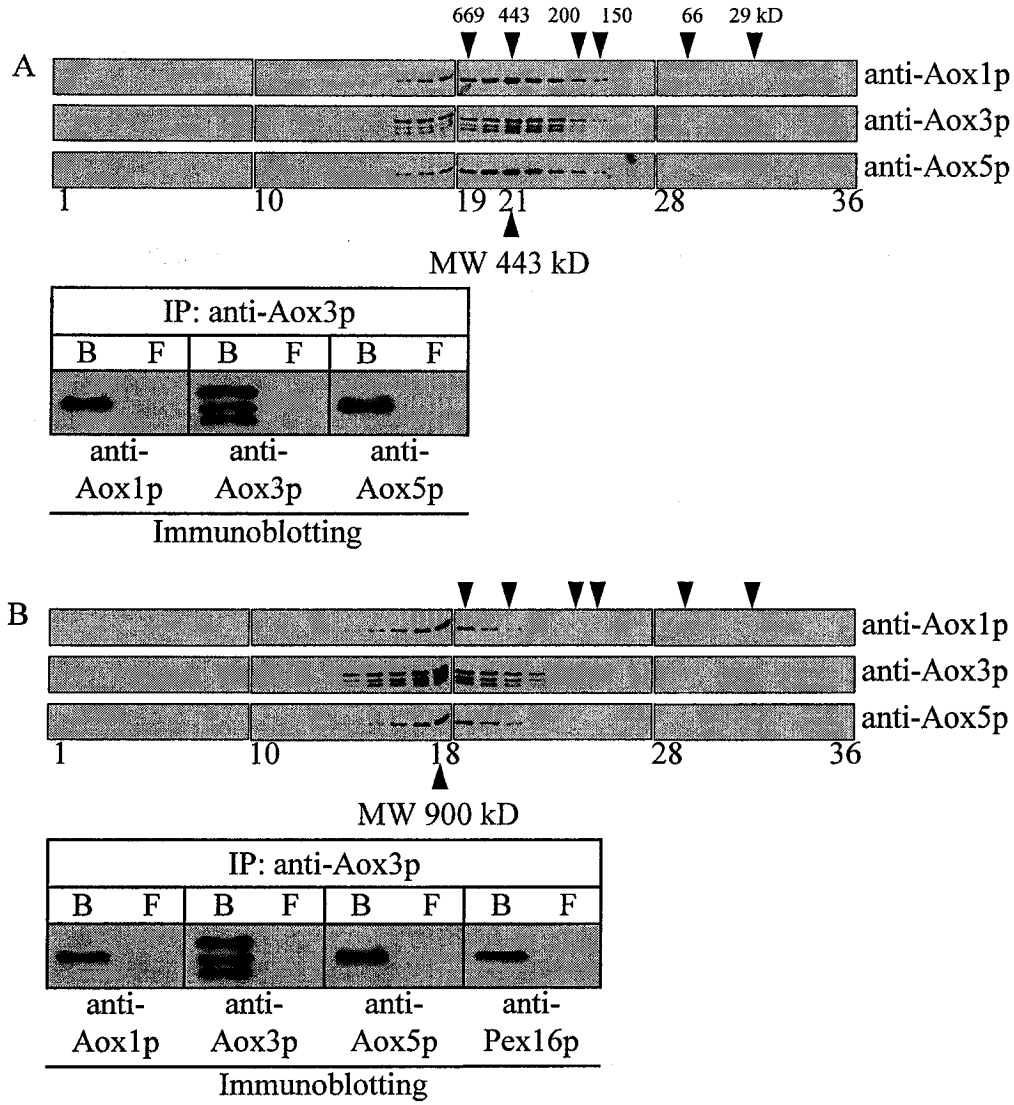

Figure 2.5. Relocation of a 443-kD Aox complex from the matrix to the membrane results in the formation of a 900-kD complex containing Aox and Pex16p. Matrix (A) and membrane (B) proteins recovered from mature peroxisomes of the wild-type strain were fractionated by centrifugation on a glycerol gradient. Equal volumes of each fraction were analyzed by immunoblotting with anti-Aox1p, -Aox3p and –Aox5p antibodies. Arrowheads indicate peak fractions for molecular weight standards. Arrows indicate peak fractions 21 (A) and 18 (B) for the matrix and membrane-bound forms of Aox complex, respectively. These peak fractions were subjected to immunoaffinity chromatography under native conditions using anti-Aox3p antibodies covalently coupled to protein A-Sepharose. Proteins bound to the column (*B*) and unbound proteins recovered in the flow-through (*F*) were immunoblotted with the indicated antibodies.

Pex16p exposed towards the matrix of the peroxisome. The relocation of Aox to the matrix face of the peroxisomal membrane and its attachment to the inner (lumenal) face of this membrane requires two Aox subunits, namely Aox4p and Aox5p, and Pex16p.

3 The membrane-bound Aox-Pex16p protein complex regulates the division of mature peroxisomes

3.1 Abstract

A combination of electron microscopy, subcellular fractionation and pulse-chase analysis of the intracellular trafficking of peroxisomal proteins provided evidence that the inability of the Aox complex to titrate all membrane-bound Pex16p causes a defect in the division of mature peroxisomes. Furthermore, I found that lack of Pex16p results in excessive proliferation of immature peroxisomal vesicles. My findings imply that Pex16p negatively regulates the membrane scission event required for the division of mature peroxisomes. Moreover, my data strongly suggest that scission of the membrane of mature peroxisomes, which results in their division, can occur only if all the Pex16p inside mature peroxisomes is titrated by its interaction with Aox complex that has relocated from the matrix to the membrane.

3.2 Introduction

Data presented in Chapter 2 provided evidence that relocation of a significant portion of Aox from the matrix to the membrane at the last step of assembly of mature peroxisomes from immature intermediates leads to the formation of a supramolecular protein complex at the inner (lumenal) face of the peroxisomal membrane. This protein complex contains

two molecules of Aox complex and two molecules of the peripheral membrane peroxin Pex16p exposed towards the matrix of the peroxisome. It was unclear whether the Aox-Pex16p complex plays a role in regulating the division of mature peroxisomes. Therefore, I decided to use a combination of several experimental approaches for monitoring the dynamics of peroxisome division in various mutant strains affected in the formation of the Aox-Pex16p complex.

3.3 Materials and methods

The *Y. lipolytica* wild-type strain *P01d* (*MatA ura3-302 leu2-270 xpr2-302*) [176], the mutant strains *aox5KO* (*MatA ura3-302 leu2-270 xpr2-3 aox5::URA3*) [175], *pex16KO* (*MatA ura3-302 leu2-270 xpr2-3 pex16::LEU2*) and *pex16-TH* (*MatA ura3-302::PEX16TH-URA3 leu2-270 xpr2-3 pex16-1*) [123], and the single *AOX* gene knock-out strains *aox1KO* (*MatA ura3-302 leu2-270 xpr2-3 aox1::URA3*), *aox2KO* (*MatA ura3-302 leu2-270 xpr2-3 aox2::URA3*), *aox3KO* (*MatA ura3-302 leu2-270 xpr2-3 aox3::URA3*), *aox4KO* (*MatA ura3-302 leu2-270 xpr2-3 aox4::URA3*) [176] were used. Growth was at 30°C. Yeast strains were initially grown in YPD (1% yeast extract, 2% peptone, 2% glucose) medium to an OD_{600} of ~1.5 and then shifted to YPBO (0.3% yeast extract, 0.5% peptone, 0.5% K_2HPO_4, 0.5% KH_2PO_4, 1% Brij-35, 1% [wt/ vol] oleic acid) medium to proliferate peroxisomes.

Rabbit polyclonal antibodies to the Aox1p, -3p and –5p subunits of the Aox complex [175], Pex2p [177], Pex5p [178], Pex16p [123], isocitrate lyase (ICL) [48], thiolase (THI) [178] and malate synthase (MLS) [48] have been described.

The initial step in the subcellular fractionation of YPBO-grown cells included the

differential centrifugation of lysed and homogenized spheroplasts at 1,000 x *g* for 8 min at 4°C in a rotor (model JS13.1; Beckman Instrs., Inc., Palo Alto, CA) to yield a postnuclear supernatant (PNS) fraction. The PNS fraction was further subjected to differential centrifugation at 20,000 x *g* for 30 min at 4°C in a rotor (model JS13.1; Beckman Instrs.) to yield pellet (20KgP) and supernatant (20KgS) fractions. The 20KgS fraction was further subfractionated by differential centrifugation at 200,000 x *g* for 1 h at 4°C in a rotor (model TLA120.2; Beckman Instrs., Inc.) to yield pellet (200KgP) and supernatant (200KgS) fractions.

To purify mature peroxisomes P6, the 20 KgP was further fractionated by flotation on a there-step sucrose gradient. Specifically, the 20 KgP was resuspended in 400 µl of 60% (wt/wt) sucrose in buffer H (5 mM MES, pH 5.5, 1 mM KCl, 0.5 mM EDTA, 0.1% [vol/vol] ethanol), overlaid with 2.3 ml of 50% (wt/wt) sucrose and 2.3 ml of 20% (wt/wt) sucrose (both in buffer H), and subjected to centrifugation in a rotor (model SW50.1; Beckman Instrs.) at 200,000 x *g* for 18 h at 4°C. Gradients were fractionated from the bottom, and 18 fractions of ~270 µl each were collected. To further purify mature peroxisomes P6, 4 vol of 0.5 M sucrose in buffer H were added to the peak peroxisomal fraction 4 recovered after isopycnic centrifugation on a discontinuous sucrose gradient. Peroxisomes were sedimented through a 150-µl cushion of 2 M sucrose in buffer H by centrifugation at 200,000 x *g* for 20 min at 4°C in a TLA120.2 rotor. The resultant pellet was resuspended in buffer H containing 1 M sorbitol and was subjected to further centrifugation on a linear 20-60% (wt/wt) sucrose gradient (in buffer H) at 197,000 x *g* for 18 h at 4°C in a rotor (model SW41Ti; Beckman Instrs., Inc.). Peak

peroxisomal fraction 5 equilibrating at a density of 1.21 g/cm^3 was recovered, and purified mature peroxisomes were pelleted at 200,000 x *g* for 20 min at 4°C in a TLA120.2 rotor, as described above. Pelleted peroxisomes were resuspended in 400 µl of 60% (wt/wt) sucrose in buffer H and subjected to flotation on a three-step sucrose gradient as described above. Peak peroxisomal fraction 4 was recovered and used for biochemical analyses. Peroxisomes isolated by this multistep method were greater than 97% pure, as judged by the presence of marker proteins of other organelles.

To purify immature peroxisomes P1 to P5, a 200,000-*g* pellet fraction (200KgP) was subjected to centrifugation on a discontinuous sucrose (18, 25, 30, 35, 40, and 53%, wt/wt) gradient at 120,000 x *g* for 18 h at 4°C in a Beckman SW28 rotor. 36 fractions of 1 ml each were collected. Fractions containing different subforms of immature peroxisomes were recovered, and 4 vol of 0.5 M sucrose in buffer H (5 mM MES, pH 5.5, 1 mM KCl, 0.5 mM EDTA, 0.1% ethanol, and a mixture of protease inhibitors) were added. Immature peroxisomes were pelleted onto a 150-µl cushion of 2 M sucrose in buffer H by centrifugation at 200,000 x *g* for 20 min at 4°C in a Beckman TLA120.2 rotor. Individual pellets of different subforms of immature peroxisomes were resuspended in 3 ml of 50% (wt/wt) sucrose in buffer H.

For purification of immature peroxisomes P1 and P2, pellets of P1 and P2 resuspended in 50% (wt/wt) sucrose in buffer H were overlaid with 30, 28, 26, 24, 22, and 10% sucrose (all wt/wt in buffer H). After centrifugation at 120,000 x *g* for 18 h at 4°C in a SW28 rotor, 18 fractions of 2 ml each were collected. P1 and P2 were pelleted,

resuspended and subjected to a second flotation on the same multistep sucrose gradient. Gradients were fractionated into 2-ml fractions as above, and P1 and P2 were recovered and pelleted.

For purification of immature peroxisomes P3 and P4, pellets of P3 and P4 resuspended in 50% (wt/wt) sucrose in buffer H were overlaid with 38%, 35%, 33% and 20% sucrose (all wt/wt in buffer H). After centrifugation at 120,000 x *g* for 18 h at 4°C in a SW28 rotor, 18 fractions of 2 ml each were collected. P3 and P4 were pelleted, resuspended in 3 ml of 50% (wt/wt) sucrose in buffer HE (20 mM MES, pH 5.5, 20 mM EDTA, 0.1% ethanol), overlaid with 39, 37, 35, 33, and 20% sucrose (all wt/wt in buffer HE), and subjected to centrifugation as above. Gradients were fractionated into 2-ml fractions, and P3 and P4 were recovered and pelleted. After resuspension in 3 ml of 50% (wt/wt) sucrose in buffer H, P3 and P4 were again subjected to flotation on the second multistep sucrose gradient described above. Gradients were fractionated into 2-ml fractions, and P3 and P4 were recovered and pelleted. Covalent coupling of affinity-purified antibodies to protein A-Sepharose for immunoaffinity chromatography was performed as described previously [175]. For immunoaffinity chromatography under native conditions, peroxisomal matrix proteins recovered in the supernatant fraction after centrifugation of osmotically lysed peroxisomes and peroxisomal liposomes were diluted with an equal volume of 50 mM Tris-HCl, pH 7.5, buffer containing 300 mM NaCl, 1% (v/v) Triton X-100 and protease inhibitor cocktail. The pellets of PMPs recovered after centrifugation of osmotically lysed peroxisomes and peroxisomal liposomes were

resuspended in 25 mM Tris-HCl, pH 7.5, buffer containing 150 mM NaCl, 0.5% (v/v) Triton X-100 and protease inhibitor cocktail. Samples were cleared of any nonspecifically binding proteins by incubation for 20 min at 4°C with protein A-Sepharose washed five times with 10 mM Tris-HCl, pH 7.5. The cleared samples were then subjected to immunoaffinity chromatography. Bound proteins were washed five times with 25 mM Tris-HCl, pH 7.5, 150 mM NaCl, 0.5% (v/v) Triton X-100, and eluted with 100 mM glycine, pH 2.8. Proteins were precipitated by addition of trichloroacetic acid to 10%, washed in ice-cold 80% (v/v) acetone, and then subjected to SDS-PAGE followed by immunoblotting.

For electron microscopy, whole cells were fixed in 1.5% $KMnO_4$ for 20 min at room temperature, dehydrated by successive incubations in increasing concentrations of ethanol, and embedded in TAAB 812 resin (Marivac, Halifax, Nova Scotia, Canada). Ultrathin sections were cut using an Ultra-Cut E Microtome (Reichert-Jung) and examined in a Phillips 410 electron microscope. For morphometric analysis of random electron microscopic sections of cells, 12 × 14-cm prints and 8 × 10-cm negatives of 35-40 cell sections of each strain at 24,000-29,000 magnification were scanned and converted to digitized images with an HP Scanjet 4400c scanner and Adobe Photoshop 6.0 software. Quantitation of digitized images was performed using NIH Image 1.55 software (National Institutes of Health, Bethesda, MD). Relative area of peroxisome section (%) was calculated as "area of peroxisome section/area of cell section × 100". Peroxisomes were counted in electron micrographs, and data are expressed as the number

of peroxisomes per μm^3 of cell section volume.

For pulse-chase experiments, YPBO-grown cells were pelleted at 10,000 x *g* for 8 min at room temperature, washed three times with water, incubated in 50 mM potassium phosphate buffer, pH 7.5, containing 10 mM DTT for 10 min at 30°C, and repelleted at 10,000 x *g* for 8 min at room temperature. Cells were resuspended at a concentration of 0.25 g/ml in 25 mM potassium phosphate buffer, pH 7.5, containing 0.55 M $MgSO_4$, and converted to spheroplasts by digestion at 30°C with Zymolyase 100T (ICN Biochemicals, Inc., Mississauga, Ontario, Canada) at 1 mg/ml of cells. Spheroplasts were harvested at 10,000 x *g* for 8 min at room temperature and resuspended at a concentration of 6 OD_{600}/ml in YNO medium supplemented with 1 M sucrose. Spheroplasts were incubated for 90 min at 30°C, labeled with L-[^{35}S]methionine (ICN Biochemicals, Inc.) at 40 $\mu Ci/OD_{600}$ for 1.5 min or 3 min at 30°C, and chased with an equal volume of 2× YPBO medium supplemented with 1 M sucrose and 10 mM unlabeled L-methionine. Samples were taken at various times of chase, and spheroplasts were immediately pelleted in a rotor (model F241.5; Beckman Instrs., Inc.) at 20,000 x *g* for 2 min at 4°C. All subsequent steps were performed at 4°C, and all solutions contained unlabeled L-methionine. Spheroplasts were resuspended in 150 µl of buffer H containing 1 M sorbitol and a mixture of protease inhibitors. Spheroplasts were osmotically lysed by addition of 300 µl of buffer H containing 0.1 M sorbitol and protease inhibitors. Lysis was greater than 90%, as determined by microscopy and enzymatic assay of the cytosolic marker glucose-6-phosphate dehydrogenase. The original osmolarity was reestablished by

addition of 300 µl of buffer H containing 1.9 M sorbitol and protease inhibitors. The lysate was subjected to centrifugation at 1,000 x *g* for 3 min at 4°C in a rotor (model F241.5; Beckman Instrs., Inc.) to yield a PNS fraction. The PNS fraction was loaded onto a 150-µl cushion of 1.2 M sucrose in buffer H containing protease inhibitors and subjected to centrifugation at 20,000 x *g* for 20 min at 4°C in a rotor (model TLA120.2; Beckman Instrs., Inc.) to yield pellet (20KgP) and supernatant (20KgS) fractions. The 20KgS fraction was further sedimented through a 150-µl cushion of 1.2 M sucrose in buffer H containing protease inhibitors at 200,000 x *g* for 20 min at 4°C in a rotor (model TLA120.2; Beckman Instrs., Inc.) to yield pellet (200KgP) and supernatant (200KgS) fractions. Immunoprecipitation under native conditions was performed by immunoaffinity chromatography with antibodies covalently coupled to protein A-Sepharose, as described above in this chapter. For immunoprecipitation under denaturing conditions, SDS was added to 2%, and samples were warmed at 65°C for 10 min. Samples were allowed to cool to room temperature, and 4 vol of 60 mM Tris-HCl, pH 7.4, buffer containing 1.25% (vol/vol) Triton X-100, 190 mM NaCl, and 6 mM EDTA were added. Samples were subsequently processed for immunoprecipitation, as described above in this chapter.

3.4 Results

3.4.1. The inability of the Aox complex to titrate all membrane-bound Pex16p causes a defect in the division of mature peroxisomes

Overexpression of the *PEX16* gene by the highly active thiolase promoter in the strain *pex16-TH* results in a reduced number of greatly enlarged mature peroxisomes

(Figure 3.1) [123]. Similar to Aox in mature peroxisomes of wild-type cells, a significant portion of all five Aox subunits inside the mature peroxisomes of *pex16-TH* cells is relocated from the matrix to the membrane (Figure 2.1 H), where they form a complex with each other and with Pex16p. In fact, all five Aox subunits and Pex16p recovered from the membranes of mature peroxisomes of *pex16-TH* cells coimmunoprecipitated under native conditions with anti-Aox3p or anti-Pex16p antibodies (Figure 2.1 I). However, unlike the membrane-attached Pex16p in mature peroxisomes of wild-type cells, which is present only as a component of the Aox-Pex16p complex (Figure 2.1 F), most of the Pex16p in mature peroxisomes of *pex16-TH* cells cannot be immunoprecipitated under native conditions with anti-Aox3p antibodies (Figure 2.1 I) and, therefore, does not interact with the membrane-bound Aox complex.

These findings suggest that scission of the membrane of mature peroxisomes, which results in their division, can occur only if all the Pex16p inside mature peroxisomes is titrated by its interaction with Aox complex that has relocated from the matrix to the membrane. Thus, Pex16p negatively regulates the membrane scission event required for the division of mature peroxisomes. In wild-type cells, the Aox complex that has relocated from the matrix to the membrane of mature peroxisomes interacts with Pex16p and terminates its negative effect on peroxisome division. This hypothesis is further supported by the observation that lack of either Aox4p or Aox5p prevented such a relocation of Aox complex (Figure 2.1, panels D and E) and resulted in fewer, but greatly enlarged, mature peroxisomes (Figure 3.1). On the other hand, lack of Aox1p, Aox2p or Aox3p did not impair the redistribution of Aox complex from the matrix to the membrane

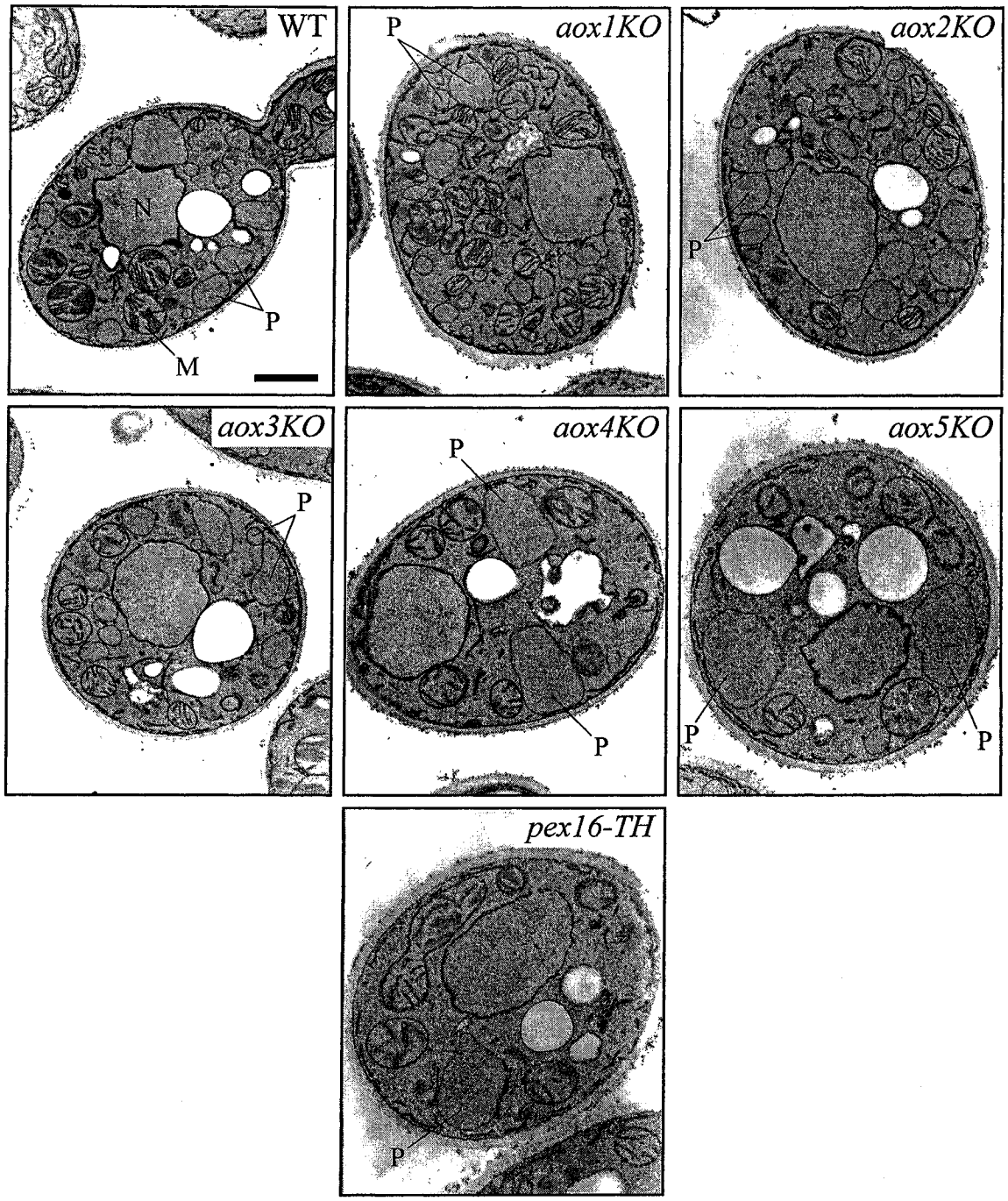

Figure 3.1. Lack of either the Aox4p or the Aox5p subunit of the Aox complex, similar to the overexpression of Pex16p, results in a reduced number of greatly enlarged peroxisomes. Transmission electron micrographs of the wild-type (*WT*), *aox1* to *aox5*, and *pex16-TH* strains grown for 9 h in oleic acid-containing medium. *M*, mitochondrion; *N*, nucleus; *P*, peroxisome. Bar, 1 μm.

inside mature peroxisomes (Figure 2.1 C) and did not affect the division of peroxisomes (Figure 3.1). All Pex16p in the membrane of mature peroxisomes recovered from *aox1KO*, *aox2KO* or *aox3KO* cells was titrated by its interaction with the Aox complex (Figure 2.3).

Importantly, the accumulation of greatly enlarged peroxisomes in *aox4KO* and *aox5KO* cells was not due to a deficiency in peroxisomal fatty acid β-oxidation. In fact, no mutation knocking out a single *Y. lipolytica AOX* gene affected the enzymatic activity of Aox, one of the key enzymes of peroxisomal β-oxidation, or impaired the utilization of oleic acid as a carbon source [176]. Thus, the observed changes in peroxisome size and number in *aox4KO* and *aox5KO* cells (Figure 3.1) cannot be attributed to a defect in the so called metabolic control of peroxisome abundance [117], which operates in yeast, mammalian and human cells [115, 117, 118, 120, 121].

Morphometric analysis of random electron microscopy sections was used to evaluate the dynamics of change in the size and number of peroxisomes in wild-type and *aox* mutant cells transferred from glucose- to oleic acid-containing medium. In wild-type cells of *Y. lipolytica*, such a transfer greatly increases peroxisome size and number (Figure 3.2) [121]. Data from morphometric analysis further confirmed that the inability of the Aox complex to relocate from the matrix to the membrane at the last step of the assembly of mature peroxisomes impairs their ability to divide. During the first 3 h of incubation in oleic acid-containing medium, the size of peroxisomes in wild-type, *aox4KO* and *aox5KO* cells significantly increased (Figure 3.3 A, Figure 3.2, Figure 3.4, Figure 3.5), while their number did not change (Figure 3.3 B, Figure 3.2, Figure 3.4,

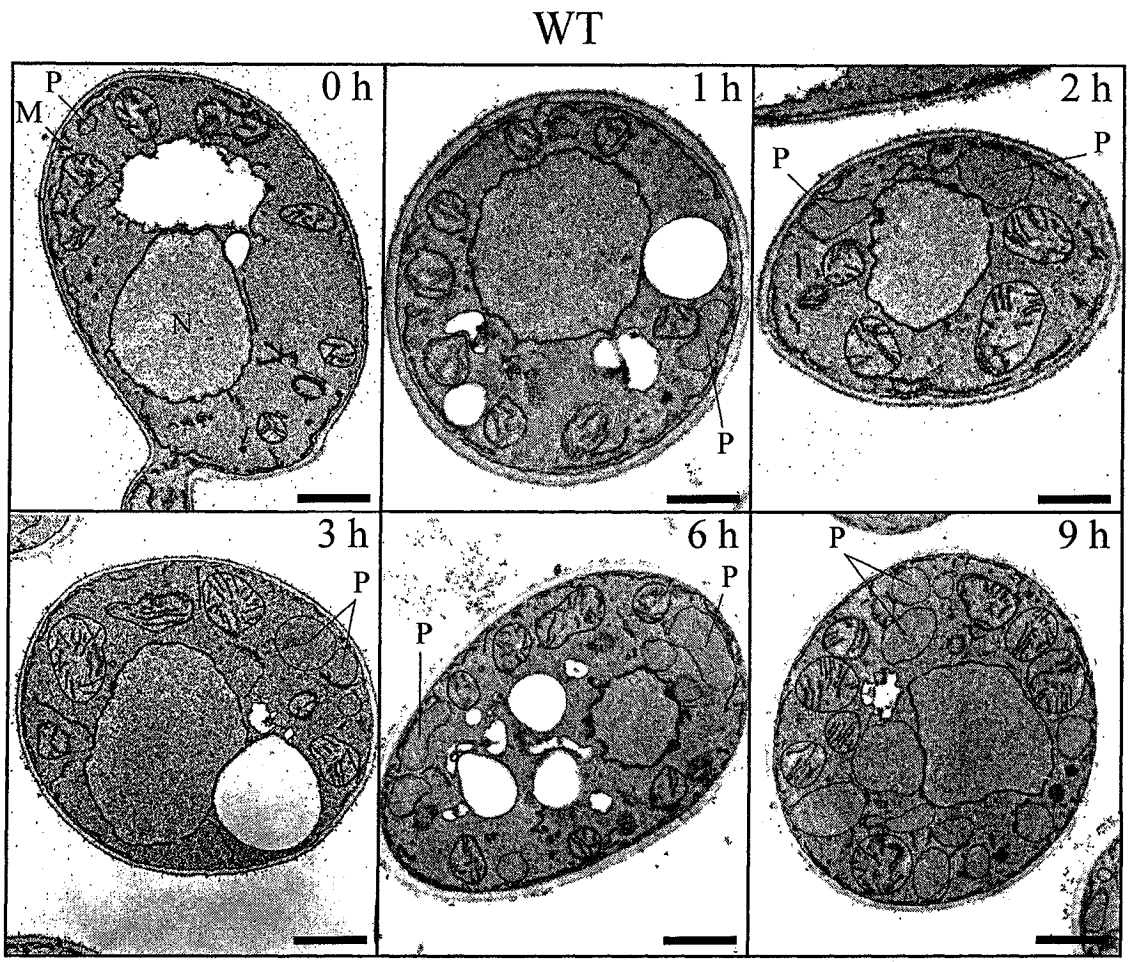

Figure 3.2. The dynamics of change in the size and number of peroxisomes in wild-type cells transferred from glucose- to oleic acid-containing medium. Cells were grown in glucose-containing medium overnight, transferred to oleic acid-containing medium, and incubated at 30°C. Aliquots of cells were taken at the times indicated, and the cells were fixed and processed for electron microscopy. *M*, mitochondrion; *N*, nucleus; *P*, peroxisome. Bar, 1 μm.

Figure 3.5). Similar dynamics of change in peroxisome size and number by 3 h after the shift from glucose- to oleic acid-containing medium was observed in *aox1KO*, *aox2KO* and *aox3KO* cells (data not shown). By 6 and 9 h after the shift to oleic-acid containing medium, the number of peroxisomes in wild-type, and in *aox1KO*, *aox2KO* and *aox3KO* cells, dramatically increased, attaining 14.6 ± 2.0 peroxisomes per μm^3 of cell section

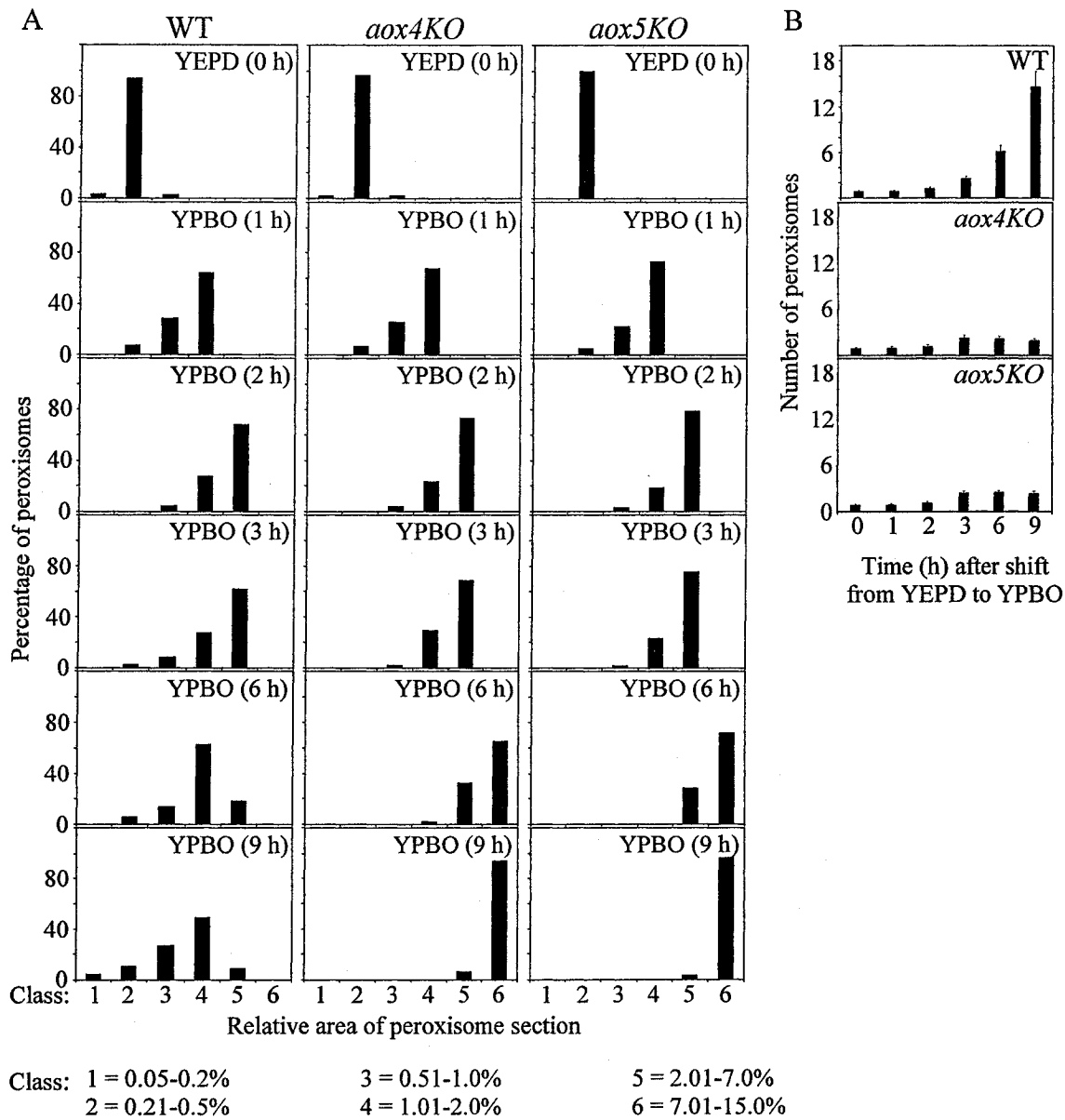

Figure 3.3. The dynamics of change in the size and number of peroxisomes in wild-type, *aox4KO* and *aox5KO* cells transferred from glucose- to oleic acid-containing medium. For each strain, morphometric analysis was performed on electron micrographs of 60 randomly selected cells. (A) Percentage of peroxisomes having the indicated relative area of peroxisome section. The relative area of peroxisome section was calculated as the [(area of peroxisome section/area of cell section) × 100]. (B) Numbers of peroxisomes. The data of morphometric analysis are expressed as the number of peroxisomes per μm^3 of cell section volume.

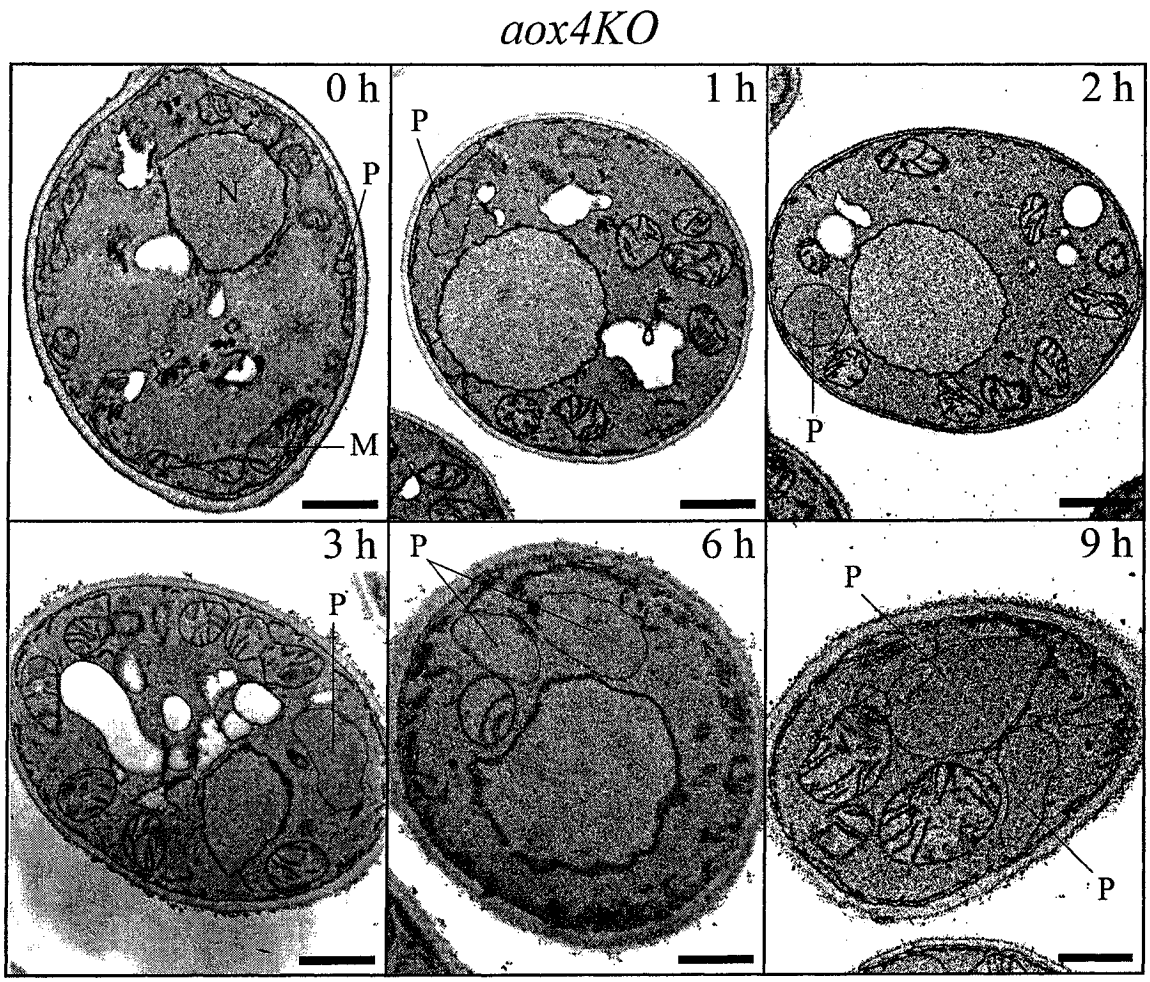

Figure 3.4. The dynamics of change in the size and number of peroxisomes in *aox4KO* mutant cells transferred from glucose- to oleic acid-containing medium. Cells were grown in glucose-containing medium overnight, transferred to oleic acid-containing medium, and incubated at 30°C. Aliquots of cells were taken at the times indicated, and the cells were fixed and processed for electron microscopy. *M*, mitochondrion; *N*, nucleus; *P*, peroxisome. Bar, 1 μm.

volume (Figure 3.2, Figure 3.3 B). Concomitantly, the proportion of small peroxisomes in these cells gradually increased, leading to significant variability in peroxisome size by 9 h after the shift (Figure 3.2, Figure 3.3 A). In contrast, the size of peroxisomes in *aox4KO* and *aox5KO* mutant cells continued to increase by 6 and 9 h after the shift to

aox5KO

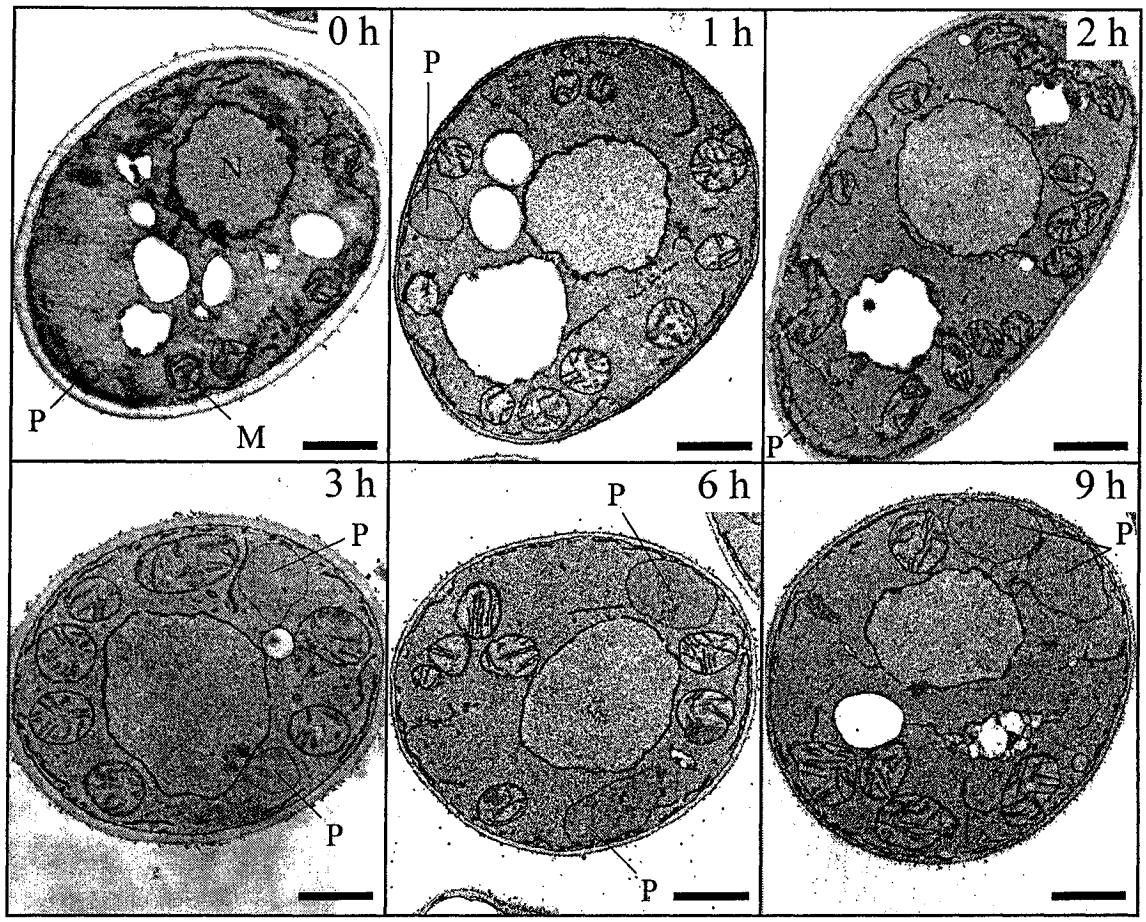

Figure 3.5. The dynamics of change in the size and number of peroxisomes in *aox5KO* mutant cells transferred from glucose- to oleic acid-containing medium. Cells were grown in glucose-containing medium overnight, transferred to oleic acid-containing medium, and incubated at 30°C. Aliquots of cells were taken at the times indicated, and the cells were fixed and processed for electron microscopy. *M*, mitochondrion; *N*, nucleus; *P*, peroxisome. Bar, 1 μm.

oleic acid-containing medium (Figure 3.3 A, Figure 3.4, Figure 3.5), with only greatly enlarged peroxisomes visible by 9 h after the shift. During the entire period of incubation after the shift from glucose- to oleic acid-containing medium, the number of peroxisomes in *aox4KO* and *aox5KO* cells did not change significantly, attaining only 1.7 ± 0.3 and

2.3 ± 0.4 peroxisomes per μm^3 of cell section volume, respectively, by the end of the incubation (Figure 3.3 B, Figure 3.4, Figure 3.5). Thus, the inability of the Aox complex lacking either the Aox4p or the Aox5p subunit to relocate from the matrix to the membrane and, therefore, to titrate all membrane-bound Pex16p results in the inability of Aox to prevent the negative effect of Pex16p on the division of mature peroxisomes.

3.4.2 Lack of Pex16p results in excessive proliferation of immature peroxisomal vesicles

The *pex16KO* mutant strain deleted for the *PEX16* gene accumulates a considerable number of very small peroxisomes [123] that are reminiscent of immature peroxisomal vesicles [55]. These immature peroxisomal vesicles can be pelleted only by centrifugation at 200,000 × *g*, whereas mature peroxisomes are completely pelletable even at 20,000 × *g* [48, 55]. In wild-type cells, immature peroxisomes represent only a minor portion of the peroxisome population, as judged from the relative distribution of malate synthase (MLS), a protein marker of both immature and mature peroxisomes, between the low-speed (20,000 × *g*) and high-speed (200,000 × *g*) organellar fractions (Figure 3.6 A). Data on the relative distribution of other peroxisomal protein markers and from immunofluorescence microscopy support this conclusion [48, 55]. In *pex16KO* cells, the steady-state level of immature peroxisomes is dramatically increased compared to their level in wild-type cells, with about half of the peroxisome population present as immature peroxisomal vesicles (Figure 3.6 A). These data strongly suggest that Pex16p negatively regulates the membrane scission event required for the division of early peroxisomal precursors, the immature peroxisomal vesicles P1 to P5. Inside the immature

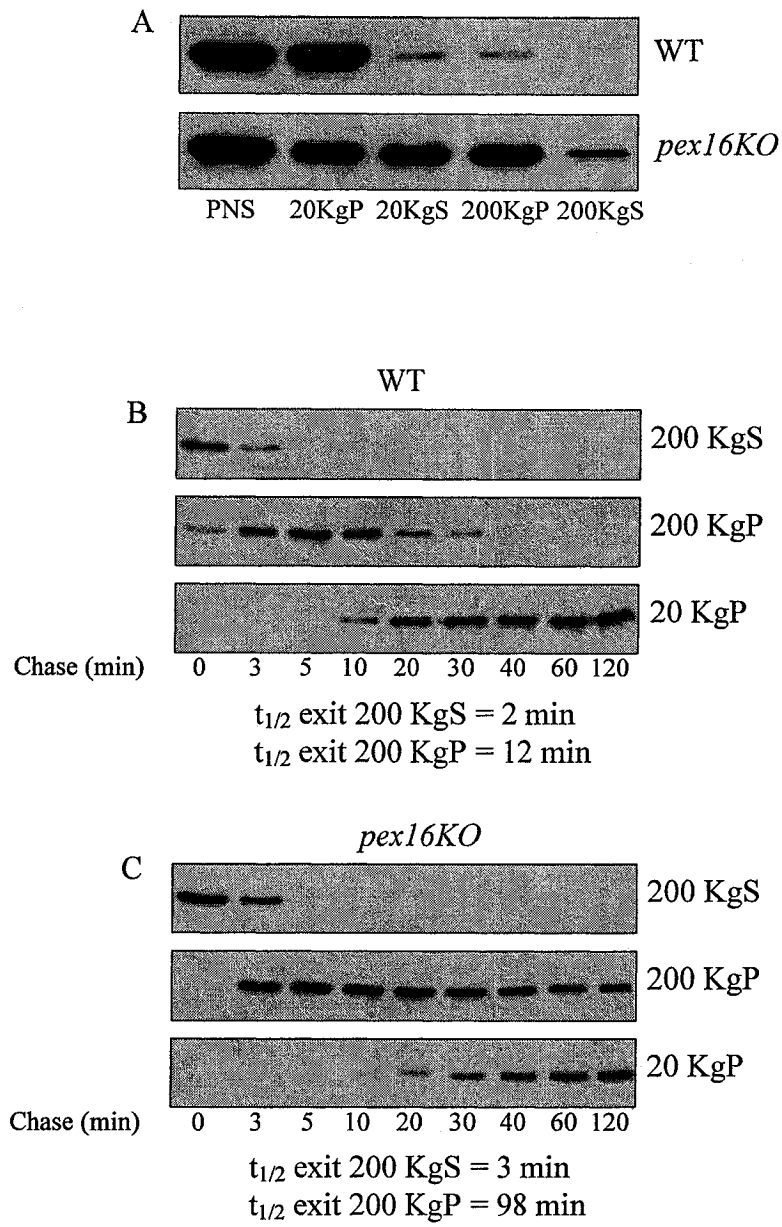

Figure 3.6. Lack of Pex16p results in excessive proliferation of immature peroxisomal vesicles and significantly decreases the rate and efficiency of their conversion to mature peroxisomes. (A) Recoveries of malate synthase (MLS), a protein marker of both immature and mature peroxisomes, in different subcellular fractions of wild-type and *pex16KO* mutant cells. Immature peroxisomal vesicles are recovered only in the 200KgP fraction, whereas mature peroxisomes are found only in the 20KgP fraction [48, 55]. (B and C) Pulse-chase analysis of the trafficking of MLS in vivo. Radiolabeled MLS was immunoprecipitated from the 200KgS (cytosolic), 200KgP and 20KgP fractions of wild-type (B) and *pex16KO* mutant (C) cells pulse-labeled with *L*-[^{35}S]methionine and chased with unlabeled *L*-methionine. Samples were taken at the indicated times after chase. Half-times for the exit from the 200KgS and 200KgP by MLS are presented.

peroxisomes of wild-type cells, the Aox complex cannot abolish the negative effect of Pex16p on scission of the membrane, because in this peroxisomal population Aox resides only in the matrix (Figure 2.1 A). Therefore, the lack of Pex16p in *pex16KO* cells results in the excessive proliferation of immature peroxisomal vesicles.

Pulse-chase analysis of the trafficking of MLS in vivo demonstrated that the excessive proliferation of immature peroxisomes in *pex16KO* cells significantly decreased the rate and efficiency of their conversion to mature peroxisomes (Figure 3.6, panels B and C). In contrast, the *pex16KO* mutation did not abolish the import of MLS (Figure 3.6, panels B and C) or of other peroxisomal proteins, including Aox1p, -2p, -3p, -4p, -5p, ICL, THI and Pex2p, from the cytosol to the matrix of immature peroxisomes. The excessive proliferation of immature peroxisomal vesicles could be suggested to decrease substantially the concentration of vesicle-associated complexes required for the conversion of these vesicles to mature peroxisomes.

3.5 Discussion

Data presented in Figure 3.1, along with findings reported in Figure 2.1, provide evidence that scission of the membrane of mature peroxisomes, which results in their division, can occur only if all the Pex16p inside mature peroxisomes is titrated by its interaction with Aox complex that has relocated from the matrix to the membrane. In fact, the division of mature peroxisomes is abolished in the *pex16-TH* mutant strains, whose Aox in mature peroxisomes is unable to titrate all the Pex16p due to the greatly elevated level of Pex16p in this mutant strain. Findings reported in Figure 3.1, in conjunction with data presented in Figures 2.1 and 2.3, further support the above conclusion as lack of either

Aox4p or Aox5p, the only two subunits required for the attachment of Aox to Pex16p, impairs the division of mature peroxisomes. Moreover, my hypothesis that the membrane-attached Aox inside mature peroxisomes must titrate all the Pex16p inside mature peroxisomes in order to abrogate the negative effect of Pex16p on membrane scission is also supported by results of the electron microscopic analysis shown in Figures 3.2 to 3.5. Specifically, using morphometric analysis of random electron microscopy sections, I confirmed the above hypothesis by evaluating the dynamics of change in the size and number of peroxisomes in wild-type and *aox* mutant cells transferred from glucose- to oleic acid-containing medium. My data also imply that Pex16p negatively regulates the membrane scission event required for the division of early peroxisomal precursors, the immature peroxisomal vesicles P1 to P5 (Figure 3.6). This conclusion is based on the observation that the lack of Pex16p in *pex16KO* cells results in the excessive proliferation of immature peroxisomal vesicles, thereby significantly decreased the rate and efficiency of their conversion to mature peroxisomes (Figure 3.6). It seems likely that the lack of Pex16p in *pex16KO* cells leads to substantial decrease of the concentration of vesicle-associated complexes required for the conversion of immature peroxisomal vesicles to mature peroxisomes.

3.6 Conclusions

Taken together, the data presented in Chapter 3 strongly suggest that Pex16p negatively regulates the membrane scission event required for peroxisome division. In immature peroxisomal vesicles, this negative effect of Pex16p on membrane scission is not suppressed by its interaction with Aox, which is located exclusively in the lumen of these

vesicles. In contrast, relocation of a significant portion of Aox from the matrix to the membrane at the last step of peroxisome maturation results in its binding to Pex16p, thereby titrating all the Pex16p and abrogating its negative effect on peroxisome division.

4 The mechanism of the relocation of Aox from the matrix to the membrane of mature peroxisomes

4.1 Abstract

Comparison of the spectra and relative distributions of peroxisomal matrix and membrane proteins present in immature peroxisomal vesicles and in mature peroxisomes strongly suggest that the stepwise import of distinct subsets of matrix proteins into different immature intermediates along the peroxisome assembly pathway provides them with an increasing fraction of the matrix proteins present in mature peroxisomes, P6. By reconstituting peroxisomal liposomes from matrix proteins, detergent-solubilized PMPs and membrane lipids of mature peroxisomes, I reconstructed in vitro the processes of relocation of Aox from the matrix to the membrane and its interaction with membrane-bound Pex16p. My findings provide evidence that overloading mature peroxisomes with matrix proteins other than Aox is a major factor in the relocation of Aox complex from the matrix to the membrane.

4.2 Introduction

Data presented in Chapters 2 and 3 provided evidence that relocation of a significant portion of Aox from the matrix to the membrane at the last step of assembly of mature peroxisomes from immature intermediates leads to the formation of the Aox-Pex16p

protein complex that plays a pivotal role in promoting the membrane scission event required for peroxisome division. But what pushes a significant portion of Aox from the matrix to the membrane and why such relocation of Aox occurs only in mature peroxisomes? To find an answer to this question, I decided to compare the spectra and relative distributions of peroxisomal matrix and membrane proteins present different intermediates of the peroxisome assembly pathway. In addition, I attempted to reconstruct the processes of relocation of Aox from the matrix to the membrane and its interaction with membrane-bound Pex16p by reconstituting peroxisomal liposomes from matrix proteins, detergent-solubilized PMPs and membrane lipids of mature peroxisomes.

4.3 Materials and methods

The *Y. lipolytica* wild-type strain *P01d* (*MatA ura3-302 leu2-270 xpr2-302*) [176] was used. This strain was initially grown in at 30°C YPD (1% yeast extract, 2% peptone, 2% glucose) medium to an OD_{600} of ~1.5 and then shifted to YPBO (0.3% yeast extract, 0.5% peptone, 0.5% K_2HPO_4, 0.5% KH_2PO_4, 1% Brij-35, 1% [wt/ vol] oleic acid) medium to proliferate peroxisomes.

Rabbit polyclonal antibodies to the Aox1p, -3p and –5p subunits of the Aox complex [175], Pex2p [177], Pex5p [178], Pex16p [123], isocitrate lyase (ICL) [48], thiolase (THI) [178] and malate synthase (MLS) [48] have been described.

The initial step in the subcellular fractionation of YPBO-grown cells included the differential centrifugation of lysed and homogenized spheroplasts at 1,000 x *g* for 8 min at 4°C in a rotor (model JS13.1; Beckman Instrs., Inc., Palo Alto, CA) to yield a postnuclear supernatant (PNS) fraction. The PNS fraction was further subjected to

differential centrifugation at 20,000 x *g* for 30 min at 4°C in a rotor (model JS13.1; Beckman Instrs.) to yield pellet (20KgP) and supernatant (20KgS) fractions. The 20KgS fraction was further subfractionated by differential centrifugation at 200,000 x *g* for 1 h at 4°C in a rotor (model TLA120.2; Beckman Instrs., Inc.) to yield pellet (200KgP) and supernatant (200KgS) fractions.

To purify mature peroxisomes P6, the 20 KgP was further fractionated by flotation on a three-step sucrose gradient. Specifically, the 20 KgP was resuspended in 400 µl of 60% (wt/wt) sucrose in buffer H (5 mM MES, pH 5.5, 1 mM KCl, 0.5 mM EDTA, 0.1% [vol/vol] ethanol), overlaid with 2.3 ml of 50% (wt/wt) sucrose and 2.3 ml of 20% (wt/wt) sucrose (both in buffer H), and subjected to centrifugation in a rotor (model SW50.1; Beckman Instrs.) at 200,000 x *g* for 18 h at 4°C. Gradients were fractionated from the bottom, and 18 fractions of ~270 µl each were collected. To further purify mature peroxisomes P6, 4 vol of 0.5 M sucrose in buffer H were added to the peak peroxisomal fraction 4 recovered after isopycnic centrifugation on a discontinuous sucrose gradient. Peroxisomes were sedimented through a 150-µl cushion of 2 M sucrose in buffer H by centrifugation at 200,000 x *g* for 20 min at 4°C in a TLA120.2 rotor. The resultant pellet was resuspended in buffer H containing 1 M sorbitol and was subjected to further centrifugation on a linear 20-60% (wt/wt) sucrose gradient (in buffer H) at 197,000 x *g* for 18 h at 4°C in a rotor (model SW41Ti; Beckman Instrs., Inc.). Peak peroxisomal fraction 5 equilibrating at a density of 1.21 g/cm^3 was recovered, and purified mature peroxisomes were pelleted at 200,000 x *g* for 20 min at 4°C in a TLA120.2 rotor, as described above. Pelleted peroxisomes were resuspended in 400 µl of

60% (wt/wt) sucrose in buffer H and subjected to flotation on a three-step sucrose gradient as described above. Peak peroxisomal fraction 4 was recovered and used for biochemical analyses. Peroxisomes isolated by this multistep method were greater than 97% pure, as judged by the presence of marker proteins of other organelles.

To purify immature peroxisomes P1 to P5, a 200,000-*g* pellet fraction (200KgP) was subjected to centrifugation on a discontinuous sucrose (18, 25, 30, 35, 40, and 53%, wt/wt) gradient at 120,000 x *g* for 18 h at 4°C in a Beckman SW28 rotor. 36 fractions of 1 ml each were collected. Fractions containing different subforms of immature peroxisomes were recovered, and 4 vol of 0.5 M sucrose in buffer H (5 mM MES, pH 5.5, 1 mM KCl, 0.5 mM EDTA, 0.1% ethanol, and a mixture of protease inhibitors) were added. Immature peroxisomes were pelleted onto a 150-µl cushion of 2 M sucrose in buffer H by centrifugation at 200,000 x *g* for 20 min at 4°C in a Beckman TLA120.2 rotor. Individual pellets of different subforms of immature peroxisomes were resuspended in 3 ml of 50% (wt/wt) sucrose in buffer H.

For purification of immature peroxisomes P1 and P2, pellets of P1 and P2 resuspended in 50% (wt/wt) sucrose in buffer H were overlaid with 30, 28, 26, 24, 22, and 10% sucrose (all wt/wt in buffer H). After centrifugation at 120,000 x *g* for 18 h at 4°C in a SW28 rotor, 18 fractions of 2 ml each were collected. P1 and P2 were pelleted, resuspended and subjected to a second flotation on the same multistep sucrose gradient. Gradients were fractionated into 2-ml fractions as above, and P1 and P2 were recovered and pelleted.

For purification of immature peroxisomes P3 and P4, pellets of P3 and P4

resuspended in 50% (wt/wt) sucrose in buffer H were overlaid with 38%, 35%, 33% and 20% sucrose (all wt/wt in buffer H). After centrifugation at 120,000 x *g* for 18 h at 4°C in a SW28 rotor, 18 fractions of 2 ml each were collected. P3 and P4 were pelleted, resuspended in 3 ml of 50% (wt/wt) sucrose in buffer HE (20 mM MES, pH 5.5, 20 mM EDTA, 0.1% ethanol), overlaid with 39, 37, 35, 33, and 20% sucrose (all wt/wt in buffer HE), and subjected to centrifugation as above. Gradients were fractionated into 2-ml fractions, and P3 and P4 were recovered and pelleted. After resuspension in 3 ml of 50% (wt/wt) sucrose in buffer H, P3 and P4 were again subjected to flotation on the second multistep sucrose gradient described above. Gradients were fractionated into 2-ml fractions, and P3 and P4 were recovered and pelleted.

Covalent coupling of affinity-purified antibodies to protein A-Sepharose for immunoaffinity chromatography was performed as described previously [175]. For immunoaffinity chromatography under native conditions, peroxisomal matrix proteins recovered in the supernatant fraction after centrifugation of osmotically lysed peroxisomes and peroxisomal liposomes were diluted with an equal volume of 50 mM Tris-HCl, pH 7.5, buffer containing 300 mM NaCl, 1% (v/v) Triton X-100 and protease inhibitor cocktail. The pellets of PMPs recovered after centrifugation of osmotically lysed peroxisomes and peroxisomal liposomes were resuspended in 25 mM Tris-HCl, pH 7.5, buffer containing 150 mM NaCl, 0.5% (v/v) Triton X-100 and protease inhibitor cocktail. Samples were cleared of any nonspecifically binding proteins by incubation for 20 min at 4°C with protein A-Sepharose washed five times with 10 mM Tris-HCl, pH 7.5. The cleared samples were then subjected to immunoaffinity chromatography. Bound

proteins were washed five times with 25 mM Tris-HCl, pH 7.5, 150 mM NaCl, 0.5% (v/v) Triton X-100, and eluted with 100 mM glycine, pH 2.8. Proteins were precipitated by addition of trichloroacetic acid to 10%, washed in ice-cold 80% (v/v) acetone, and then subjected to SDS-PAGE followed by immunoblotting.

For preparing peroxisomal liposomes, mature peroxisomes P6 were purified from the 20KgP fraction as described above in this Chapter. Peroxisomes were lysed by incubation on ice for 20 min in 20 mM HEPES-KOH buffer, pH 8.0, containing 50 mM NaCl and protease inhibitor cocktail. The lysate was subjected to centrifugation at 100,000 × *g* for 20 min at 4°C in a TLA120.2 rotor (Beckman) to yield a supernatant containing peroxisomal matrix proteins and a pellet of PMPs. Matrix proteins of mature peroxisomes were dialyzed against buffer R (20 mM MES-KOH, pH 6.0, 150 mM NaCl, 5 mM DTT, 10% glycerol) containing 1% (w/v) n-octyl-β-D-glucopyranoside (OG). Immunoaffinity chromatography under native conditions (see the protocol described above in this Chapter) using anti-Aox1p antibodies covalently linked to protein A-Sepharose was used to deplete these peroxisomal matrix proteins of Aox. Aox complex for the reconstitution of peroxisomal liposomes was purified from the matrix of mature peroxisomes by immunoaffinity chromatography using anti-Aox3p antibodies covalently linked to protein A-Sepharose, as described above in this Chapter. After elution with buffer E (20 mM HEPES-KOH, pH 7.5, 250 mM $MgCl_2$, 5 mM DTT, 10% glycerol), purified Aox complex was dialyzed against buffer R containing 1% (w/v) OG. The pellet of PMPs recovered after centrifugation of osmotically lysed mature peroxisomes was resuspended in ice-cold buffer R containing 1% (w/v) OG. After incubation on ice for 20

min with occasional agitation, the sample of detergent-solubilized PMPs was subjected to centrifugation at 100,000 × *g* for 20 min at 4°C in a TLA120.2 rotor. The resulting supernatant of solubilized PMPs was depleted of the Aox-Pex16p complex by immunoaffinity chromatography under native conditions (see the protocol described above in this chapter) using anti-Aox1p antibodies covalently linked to protein A-Sepharose. For the reconstitution of peroxisomal liposomes PLA to PLC, detergent-solubilized PMPs immunodepleted of the Aox-Pex16p complex were supplemented with Pex16p, which was purified from membranes of osmotically lysed peroxisomes P4 by immunoaffinity chromatography under native conditions using anti-Pex16p antibodies covalently linked to protein A-Sepharose. After elution with buffer E containing 1% (w/v) OG, purified Pex16p was dialyzed against buffer R containing 1% (w/v) OG. For the reconstitution of peroxisomal liposomes PLD lacking Pex16p, detergent-solubilized PMPs immunodepleted of the Aox-Pex16p complex were supplemented only with buffer R containing 1% (w/v) OG.

Detergent-solubilized PMPs immunodepleted of the Aox-Pex16p complex and either supplemented or not supplemented with purified Pex16p were mixed with dialyzed matrix proteins immunodepleted of Aox and with purified Aox complex. After incubation on ice for 20 min with occasional agitation, the mixture of matrix proteins and PMPs in buffer R containing 1% (w/v) OG was added to the lipids extracted from the membranes of P6 peroxisomes and dried down by a gentle stream of nitrogen. The lipid film was dissolved by gentle agitation for 20 min at room temperature.

To dilute the detergent OG below its critical micellar concentration, thereby

promoting the formation of peroxisomal liposomes, 3 volumes of buffer D (20 mM MES-KOH, pH 6.0, 150 mM NaCl) were added to the mixture of peroxisomal matrix proteins, detergent-solubilized PMPs and membrane lipids dissolved in buffer R containing 1% (w/v) OG. To remove the detergent, the samples were dialyzed in a Tube-O-Dialyzer (7.5-kD cutoff) (Chemicon) against buffer D containing 0.1% Biobeads SM2 (Bio-Rad). After overnight dialysis at 4°C, samples were transferred to the bottom of ultraclear centrifuge tubes (Beckman) and supplemented with 4 volumes of 65% (w/w) sucrose in buffer D in order to adjust the sucrose concentration of the samples to 52% (w/w). Samples were then overlaid with 40% and then with 20% sucrose (both w/w in buffer D) and lastly with buffer D alone. After centrifugation at 200,000 × *g* for 18 h at 4°C in a SW50.1 rotor (Beckman), 18 fractions of 275 µl each were collected. Peroxisomal liposomes were recovered at the 52%/40% sucrose interface.

Four types of peroxisomal liposomes, termed PLA to PLD, were reconstituted. PLA were reconstituted from matrix proteins immunodepleted of Aox, Aox complex purified from the matrix of mature peroxisomes by immunoaffinity chromatography, detergent-solubilized PMPs immunodepleted of Aox and membrane lipids. Each component used for the reconstitution of PLA was recovered from 1 mg (1 equivalent) of peroxisomes. PLB were reconstituted from 0.2 equivalent of matrix proteins immunodepleted of Aox, 1 equivalent of purified Aox complex, 1 equivalent of detergent-solubilized PMPs immunodepleted of Aox and 1 equivalent of membrane lipids. PLC were reconstituted from 0.2 equivalent of matrix proteins immunodepleted of Aox, 5 equivalents of purified Aox complex, 1 equivalent of detergent-solubilized PMPs

immunodepleted of Aox and 1 equivalent of membrane lipids. PLD were reconstituted from 1 equivalent of matrix proteins immunodepleted of Aox, 1 equivalent of purified Aox complex, 1 equivalent of detergent-solubilized PMPs immunodepleted of both Aox and Pex16p and 1 equivalent of membrane lipids.

4.4 Results

4.4.1. Spectra and relative distributions of matrix and membrane proteins in peroxisomes P1 to P6

Comparison of the spectra and relative distributions of peroxisomal matrix and membrane proteins demonstrated that even the earliest intermediates in the multistep peroxisome assembly pathway, the immature peroxisomal vesicles P1 and P2, contain most of the peroxisomal membrane proteins (PMP) associated with mature peroxisomes, P6 (Figure 4.1 A). P1 and P2 undergo fusion to generate larger and more dense immature peroxisomal vesicles, P3 [55], containing PMPs derived from both fusion partners. The quantities of PMPs in P4, P5 and P6 peroxisomes were significantly lower than in P1, P2 and P3 peroxisomes, and gradually decreased from P4 to P6 (Figure 4.1 B). In contrast, only a few matrix proteins found in mature peroxisomes were seen in the immature peroxisomal vesicles P1, P2 and P3 (Figure 4.1 A). Most matrix proteins were associated with P4, P5 and P6, and the complexity of their spectra increased from P4 to P6 (Figure 4.1 A). The quantities of matrix proteins in P4, P5 and P6 peroxisomes were significantly higher than in P1, P2 and P3 peroxisomes, and gradually increased from P4 to P6 (Figure 4.1 B). Taken together, these results strongly suggest that the stepwise import of distinct subsets of matrix proteins into different immature intermediates along the peroxisome

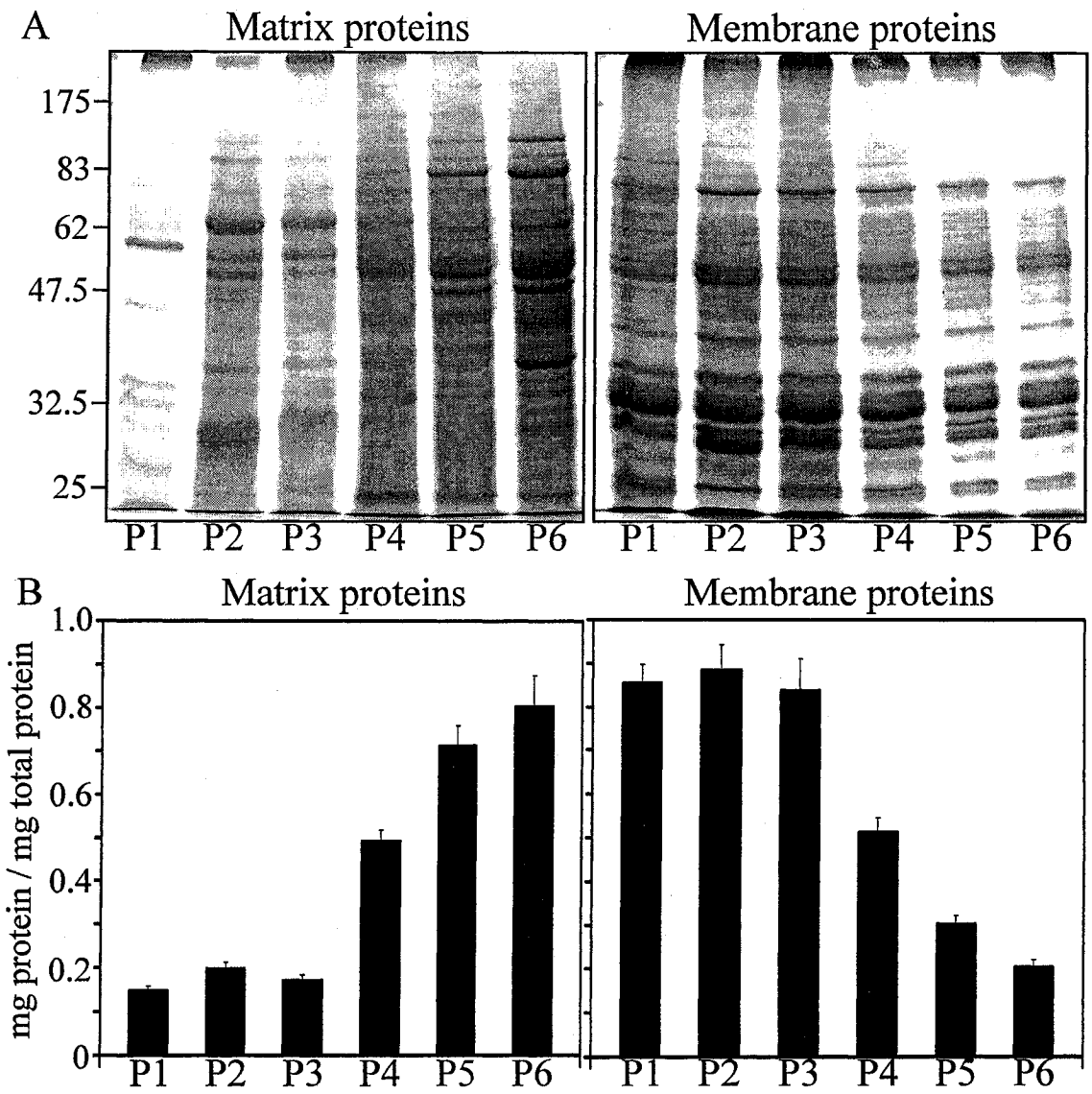

Figure 4.1. Spectra and relative distributions of matrix and membrane proteins in peroxisomes P1 to P6 recovered from wild-type cells. Purified peroxisomal subforms were osmotically lysed and subjected to centrifugation to yield supernatant (matrix proteins) and pellet (membrane proteins) fractions. Recovered proteins were resolved by SDS-PAGE and stained with Coomassie Blue (A) or quantitated with a protein assay kit (B).

assembly pathway provides them with an increasing fraction of the matrix proteins present in mature peroxisomes, P6. P6 peroxisomes contain the highest levels of matrix

proteins (Figure 4.1, panels A and B).

4.4.2 Relocation of Aox from the matrix to the membrane of mature peroxisomes is due to an increase in the total mass of matrix proteins above a critical level

Based on the findings reported in Chapter 4.4.1, I hypothesized that the observed relocation of Aox complex from the matrix to the membrane of mature peroxisomes (Figure 2.1 A) is due to an increase in the total mass of matrix proteins above a critical level, and that overloading mature peroxisomes with matrix proteins is a major factor in the relocation of Aox. To test this hypothesis, I attempted to reconstruct in vitro the relocation of Aox from the matrix to the membrane and its interaction with membrane-bound Pex16p by reconstituting peroxisomal liposomes from matrix proteins, detergent-solubilized PMPs and membrane lipids of mature peroxisomes. I reconstituted four types of peroxisomal liposomes, termed PLA to PLD (Figure 4.2 A). PLA were reconstituted from matrix proteins immunodepleted of Aox, Aox complex purified from the matrix of mature peroxisomes by immunoaffinity chromatography, detergent-solubilized PMPs immunodepleted of Aox and membrane lipids. Each component used for the reconstitution of PLA was recovered from 1 mg (1 equivalent) of peroxisomes. PLB were reconstituted from 0.2 equivalent of matrix proteins immunodepleted of Aox, 1 equivalent of purified Aox complex, 1 equivalent of detergent-solubilized PMPs immunodepleted of Aox and 1 equivalent of membrane lipids. PLC were reconstituted from 0.2 equivalent of matrix proteins immunodepleted of Aox, 5 equivalents of purified Aox complex, 1 equivalent of detergent-solubilized PMPs immunodepleted of Aox and 1 equivalent of membrane lipids. PLD were reconstituted from 1 equivalent of matrix

A

Liposome type	Equivalents per liposome reconstitution			
	Matrix proteins (id Aox)	Aox complex	Membrane proteins (id Aox)	Membrane lipids
PLA	1	1	1	1
PLB	0.2	1	1	1
PLC	0.2	5	1	1
PLD	1	1	1 (id Pex16p)	1

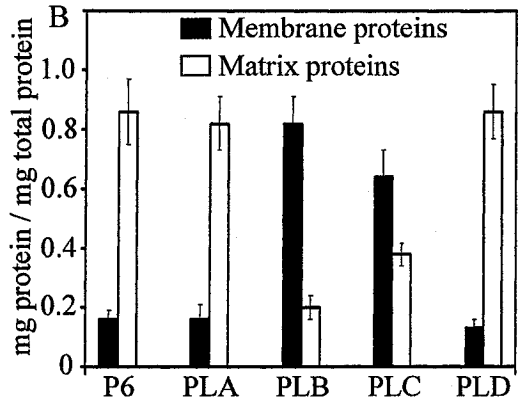

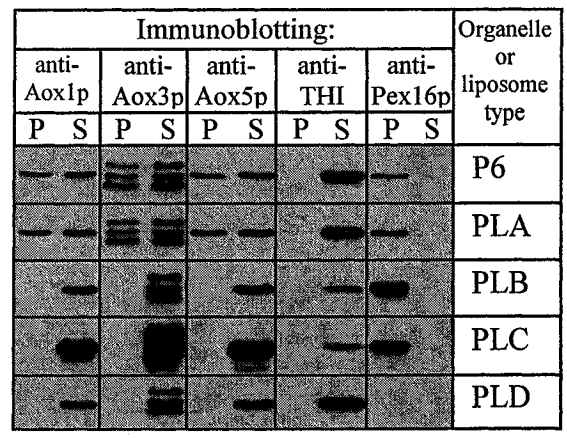

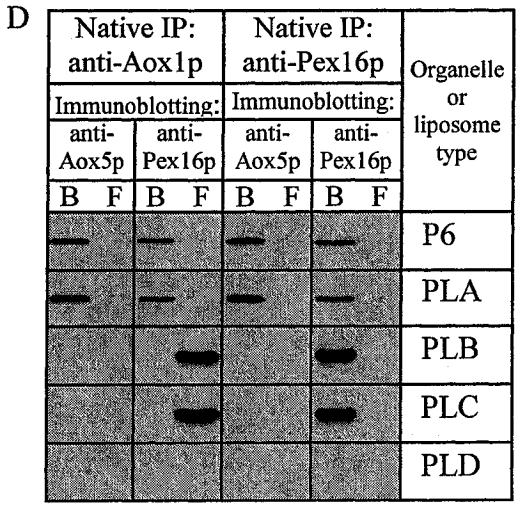

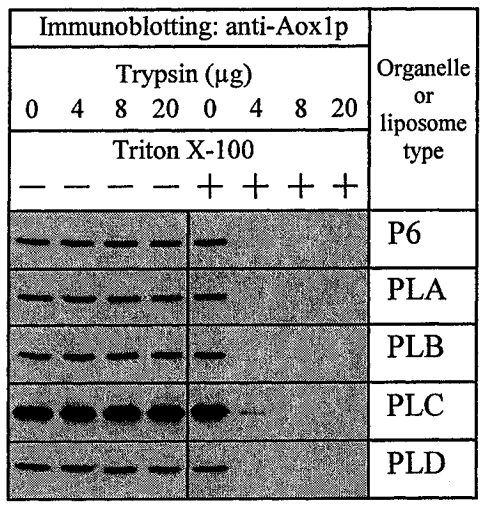

Figure 4.2. The increase in total mass of matrix proteins other then Aox causes the redistribution of Aox from the matrix to the membrane inside reconstituted peroxisomal liposomes. (A) The amounts of individual components of mature peroxisomes used for the reconstitution of four types of peroxisomal liposomes. *id Aox* and *id Pex16p*, samples immunodepleted of Aox and Pex16p, respectively. (B) Purified peroxisomes and peroxisomal liposomes were osmotically lysed and subjected to centrifugation to yield supernatant (matrix proteins) and pellet (membrane proteins) fractions. Recovered proteins were quantitated with a protein assay kit. (C) Peroxisomes and peroxisomal liposomes (20 μg of total protein) were osmotically lysed and subjected to centrifugation to yield supernatant (*S*, matrix proteins) and pellet

(*P*, membrane proteins) fractions. Recovered proteins were resolved by SDS-PAGE and immunoblotted with antibodies to the Aox1p, -3p and –5p subunits of the Aox complex, thiolase and Pex16p. (D) Membrane proteins recovered after centrifugation of osmotically lysed P6 peroxisomes and peroxisomal liposomes (20 μg of total peroxisomal protein) were subjected to immunoaffinity chromatography under native conditions using either anti-Aox1p or anti-Pex16p antibodies covalently coupled to protein A-Sepharose. Proteins bound to the column (*B*) and unbound proteins recovered in the flow-through (*F*) were immunoblotted with the indicated antibodies. (E) Peroxisomes and peroxisomal liposomes (20 μg of total protein) were treated with the indicated amounts of trypsin in the absence (-) or presence (+) of 1.0% (v/v) Triton X-100 for 30 min on ice. Samples were subjected to SDS-PAGE and immunoblotting with anti-Aox1p antibodies.

proteins immunodepleted of Aox, 1 equivalent of purified Aox complex, 1 equivalent of detergent-solubilized PMPs immunodepleted of both Aox and Pex16p and 1 equivalent of membrane lipids.

Electron microscopy revealed that all four types of peroxisomal liposomes were bound by a single membrane (Figure 4.3). Comparison of the relative distributions of peroxisomal matrix and membrane proteins demonstrated no significant difference between mature peroxisomes and PLA (Figure 4.2 B). In contrast, the quantities of matrix proteins in PLB were significantly lower than in mature peroxisomes or PLA (Figure 4.2 B). Even though the total amounts of all five Aox subunits in mature peroxisomes, PLA and PLB were similar (Figure 4.2 C), the Aox complex was attached to the membrane only in mature peroxisomes and PLA (Figure 4.2 C) in which membrane-bound Aox formed a complex with Pex16p (Figure 4.2 D). In contrast, no Aox subunits were attached to the membrane inside PLB (Figure 4.2 C), in which Pex16p was present only in its free form (Figure 4.2 D). Like the Aox complex in mature peroxisomes, Aox in PLA and PLB was resistant to digestion by external protease added to intact peroxisomes

A

Liposome type	Equivalents per liposome reconstitution reaction			
	Matrix proteins (id Aox)	Aox complex	Membrane proteins (id Aox)	Membrane lipids
PLA	1	1	1	1
PLB	0.2	1	1	1
PLC	0.2	5	1	1
PLD	1	1	1 (id Pex16p)	1

B

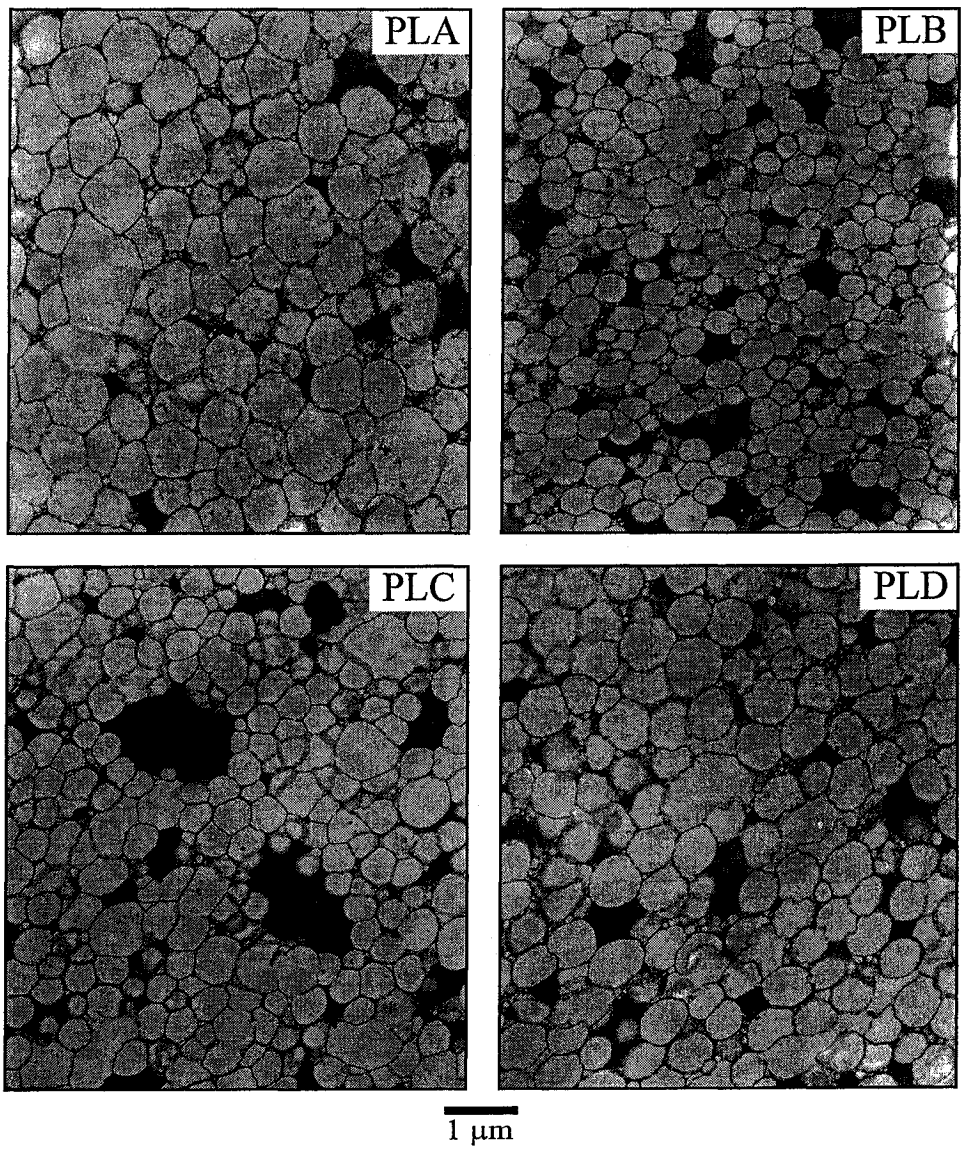

Figure 4.3. Size and morphology of peroxisomal liposomes reconstituted from components of mature peroxisomes P6. (A) The amounts of individual components of mature peroxisomes P6 used for the

reconstitution of four types of peroxisomal liposomes. *id Aox* and *id Pex16p*, samples immunodepleted of Aox and Pex16p, respectively. (B) Transmission electron micrographs of reconstituted peroxisomal liposomes PLA to PLD purified by flotation on a multi-step sucrose gradient. Bar, 1 μm.

or liposomes, i.e. was present in membrane-enclosed form (Figure 4.2 E). Because PLA and PLB differ only in their total amount of matrix proteins but contain the same amount of Aox, the increase in total mass of matrix proteins above a critical level can cause the observed relocation of Aox complex from the matrix to the membrane inside mature peroxisomes (Figure 2.1 A).

A comparative analysis of PLB and PLC, which differ in their amounts of Aox (Figure 4.2 C) but contain similar low amounts of other matrix proteins (Figure 4.2 B), showed that a significant increase in the amount of matrix-associated Aox did not result in its relocation to the membrane (Figure 4.2 C). Taken together, these findings suggest that overloading mature peroxisomes with matrix proteins other than Aox is a major factor in the relocation of Aox complex from the matrix to the membrane.

Finally, although PLA and PLD were loaded with very similar high amounts of matrix proteins (Figure 4.2 B), including Aox (Figure 4.2 C), the Aox complex was attached to the membrane only inside PLA (Figure 4.2 C). PLA contain Pex16p, while PLD lack this membrane-bound peroxin (Figure 4.2 C). Therefore, Pex16p is the only attachment factor for the Aox complex in the PLA liposomes containing high amounts of matrix proteins and, perhaps, also in mature peroxisomes P6 (Figure 2.1 G) containing the greatest percentage of matrix proteins as compared to immature peroxisomal vesicles P1 to P5 (Figure 4.1, panels A and B).

4.5 Discussion

Data presented in Figure 4.1 provide evidence that the stepwise import of distinct subsets of matrix proteins into different immature intermediates along the peroxisome assembly pathway provides them with an increasing fraction of the matrix proteins present in mature peroxisomes, P6. I found that mature peroxisomes P6 contain the highest levels of matrix proteins. Furthermore, as findings reported in Figures 4.2 and 4.3 imply, overloading mature peroxisomes with matrix proteins other than Aox is a major factor in the relocation of Aox complex from the matrix to the membrane. It should be noted that the data presented in this Chapter cannot rule out the possibility that a distinct yet unknown matrix protein or a limited set of such proteins rather than protein mass in the peroxisomal matrix initiates the relocation of Aox complex from the matrix to the membrane, thereby terminating the negative action of Pex16p on peroxisome division. Although Aox in the matrix of mature peroxisomes does not form a stable complex with any protein [175], even its transient interaction with a specific yet unknown soluble factor may promote the redistribution of Aox from the matrix to the membrane. Alternatively, overloading mature peroxisomes with matrix proteins may ultimately lead to the relocation of an unknown specific factor from the matrix to the membrane. Once bound to the peroxisomal membrane, this specific factor may cause perturbations in its physical properties, thereby promoting the assembly of the Aox-Pex16p complex at the matrix face of the membrane. The development of a reliable in vitro assay for reconstructing the relocation of Aox from the matrix to the membrane and its interaction with membrane-bound Pex16p creates the opportunity to test individual peroxisomal matrix proteins for

their ability to initiate these processes.

4.6 Conclusions

Taken together, the data presented in Chapters 2, 3 and 4 can be summarized in the following model for peroxisome growth and division in the yeast *Y. lipolytica* (Figure 4.4). Six subforms of peroxisomes, termed P1 to P6, are organized into a multistep peroxisome assembly pathway. The pathway operates by conversion of the subforms in a temporally ordered manner from P1 to P6 and leads to the formation of mature peroxisomes, P6, carrying the complete set of matrix and membrane proteins. The earliest intermediates in the assembly pathway, the immature peroxisomal vesicles P1 and P2, contain most of the PMPs associated with mature peroxisomes. P1 and P2 are competent for the import of a limited subset of matrix proteins and, therefore, contain only a few matrix proteins found in mature peroxisomes. P1 and P2 undergo fusion to generate larger and dense immature peroxisomal vesicles, P3. Conversion of P3 to mature peroxisomes P6 proceeds through several consecutive steps. At each of these steps, the import of a limited subset of matrix proteins results in the formation of a distinct peroxisomal subform that is larger and dense than its precursor.

The amounts of immature peroxisomal vesicles P1 to P5 are not more than 1-2% that of mature peroxisomes, based on protein mass [48, 55]. The peroxin Pex16p, which is attached to the matrix surface of the membrane, negatively regulates the division of immature peroxisomal vesicles, thereby preventing their excessive proliferation. The Pex16p-dependent negative control of the membrane scission event required for the division of immature peroxisomal vesicles is essential for cell growth in oleic acid-

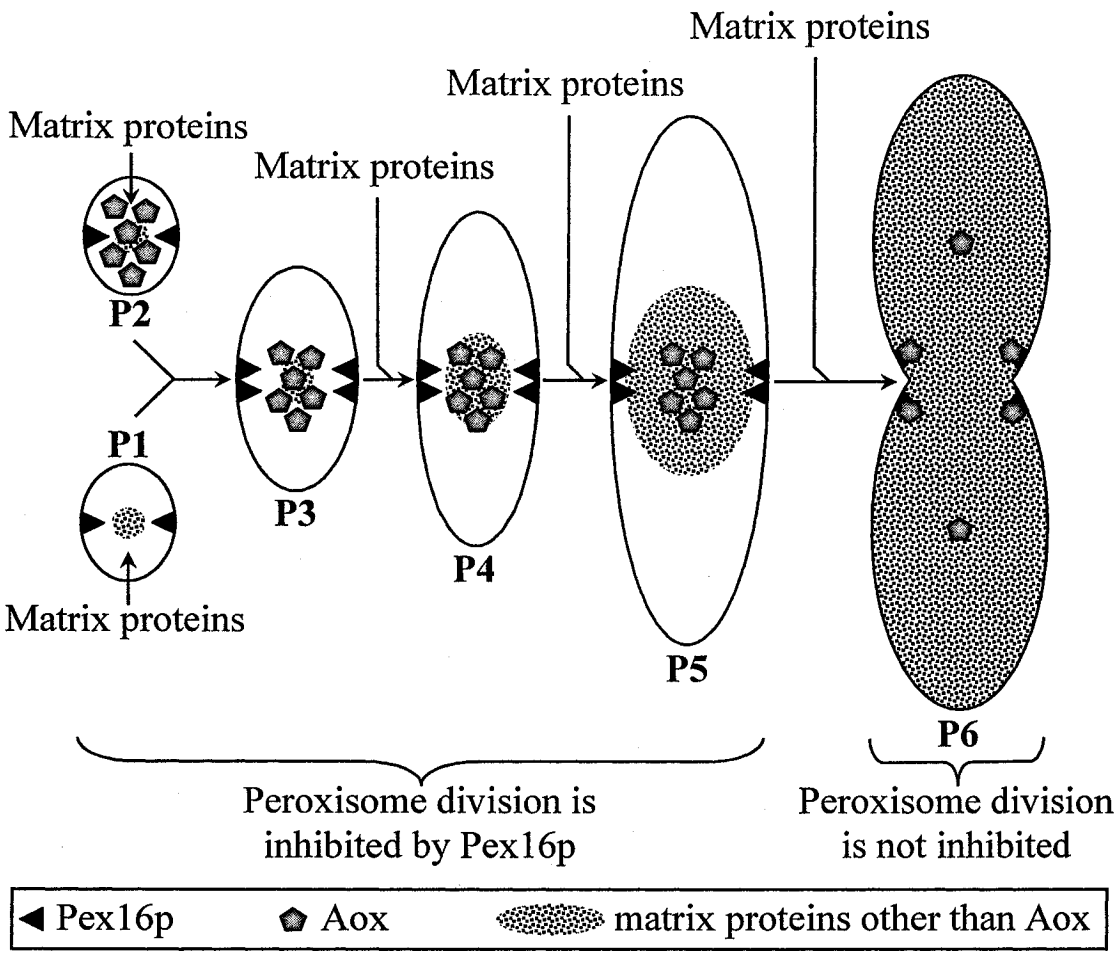

Figure 4.4. Temporally and spatially regulated interaction between membrane-attached Aox and Pex16p coordinates peroxisome growth and division in *Y. lipolytica*. Only mature peroxisomes, termed P6, contain the complete set of matrix proteins. P6 assemble from several immature peroxisomal vesicles, called P1 to P5, in a multistep pathway. The stepwise import of distinct subsets of matrix proteins into different immature intermediates along the pathway provides them with an increasing fraction of the matrix proteins present in mature peroxisomes.

containing medium. In fact, lack of Pex16p results in the excessive proliferation of immature peroxisomal precursors and impairs the utilization of oleic acid as a carbon source.

The stepwise import of distinct subsets of matrix proteins into P1 to P5

intermediates provides them with an increasing fraction of the matrix proteins present in mature peroxisomes. This increase in the total mass of matrix proteins above a critical level causes the redistribution of the heteropentameric complex of Aox, which is imported into the early intermediate P2, from the matrix to the matrix surface of the membrane. A significant redistribution of Aox complex from the matrix to the membrane occurs only in mature peroxisomes, which contain the greatest percentage of matrix proteins. Overloading mature peroxisomes with matrix proteins other than Aox can be a major factor in the relocation of Aox complex to the membrane. The available data cannot rule out the possibility that a distinct yet unknown matrix protein rather than protein mass in the peroxisomal matrix initiates the relocation of Aox complex from the matrix to the membrane.

Inside mature peroxisomes, the membrane-bound pool of Aox complex interacts, via its Aox4p and Aox5p subunits, with Pex16p. This interaction leads to the formation of a supramolecular complex containing two molecules of Aox complex and two molecules of Pex16p, and terminates the negative action of Pex16p on scission of the peroxisomal membrane, thereby allowing mature peroxisomes to divide. The temporally and spatially regulated interaction between membrane-attached Aox and Pex16p ensures the temporal and spatial separation of the processes of peroxisome assembly and division in the yeast *Y. lipolytica*. Such a separation may provide an important advantage for the efficient, stepwise assembly of mature, metabolically active peroxisomes.

5 The composition of peroxisomal membrane lipids and their transbilayer distribution are changed during peroxisome maturation

5.1 Abstract

Monitoring of specific changes in the membrane lipid compositions of different intermediates in the peroxisome assembly pathway provide evidence that: 1) the conversion of P5 to P6 in wild-type cells is marked by the biosynthesis of phosphatidic acid (PA) and diacylglycerol (DAG) in the peroxisomal membrane; 2) PA and DAG are formed in a two-step biosynthetic pathway, which includes two consecutive enzymatic reactions catalyzed by an LPA acyltransferase (LPAAT) and a PA phosphatase (PAP); 3) the LPAAT and PAP reactions are the only reactions leading to the formation of PA and DAG, respectively, in the peroxisomal membrane; 4) Pex16p, a negative regulator of the division of immature peroxisomal vesicles, inhibits LPAAT; 5) the binding of Aox to Pex16p in mature peroxisomes of wild-type cells greatly decreases the affinity between Pex16p and LPA, thereby allowing LPA to enter the two-step biosynthetic pathway leading to the formation of PA and DAG; 6) during peroxisome maturation, the movement of DAG from the lumenal to the cytosolic leaflet of the membrane bilayer coincides with the translocation of phosphatidylserine (PS) in the opposite direction, perhaps generating a lipid imbalance across the bilayer and thereby driving the process of membrane fission; 7) the Pex2p-dependent transfer of phosphatidylcholine (PC) from the P3- and P4-associated ER subcompartment to the acceptor membranes of P3 and P4 provides these membranes with the bulk quantities of PC and is essential for the conversion of P4 to P5; and 8) PC in the peroxisomal membrane is a positive regulator of

both the LPAAT and PAP reactions in the pathway for DAG biosynthesis.

5.2 Introduction

Data presented in Chapters 2, 3 and 4 provided evidence that relocation of a significant portion of Aox from the matrix to the membrane at the last step of assembly of mature peroxisomes from immature intermediates leads to the formation of the Aox-Pex16p protein complex that plays a pivotal role in promoting the membrane scission event required for peroxisome division. Scission of the peroxisomal membrane is mandatory for peroxisome division. Like any event of membrane scission [136, 153-156], scission of the peroxisomal membrane must be preceded by the destabilization of the membrane bilayer leading to membrane bending. Bending and scission of mitochondrial, chloroplast and Golgi membranes in yeasts, plants and mammals are energetically unfavorable processes that require several teams of proteins [156-168] and a distinct set of membrane lipids, including phosphoinositides [154, 159, 160, 169, 170], phosphatidic acid (PA) [136, 155, 158, 163, 171] and diacylglycerol (DAG) [136, 155, 158, 170]. Therefore, at that stage of my graduate research in Dr. Titorenko's laboratory, the major challenge was to find out whether the interaction between Pex16p and Aox promotes specific changes in the lipid composition of the peroxisomal membrane, thereby triggering the membrane destabilization, bending, scission and fission events required for the division of mature peroxisomes.

5.3 Materials and methods

The *Y. lipolytica* wild-type strain *P01d* (*MatA ura3-302 leu2-270 xpr2-302*) [176], the mutant strains *pex2KO* (*MatA ura3-302 leu2-270 xpr2-3 pex2::LEU2*), [177], *pex16KO*

(*MatA ura3-302 leu2-270 xpr2-3 pex16::LEU2*), *pex16-TH* (*MatA ura3-302::PEX16TH-URA3 leu2-270 xpr2-3 pex16-1*) [123] and *pex19KO* (*MatA ura3-302 leu2-270 xpr2-3 pex19::LEU2*) [180], and the single *AOX* gene knock-out strains *aox1KO* (*MatA ura3-302 leu2-270 xpr2-3 aox1::URA3*), *aox2KO* (*MatA ura3-302 leu2-270 xpr2-3 aox2::URA3*), *aox3KO* (*MatA ura3-302 leu2-270 xpr2-3 aox3::URA3*), *aox4KO* (*MatA ura3-302 leu2-270 xpr2-3 aox4::URA3*) [176] were used. Growth was at 30°C. Yeast strains were initially grown in YPD (1% yeast extract, 2% peptone, 2% glucose) medium to an OD_{600} of ~1.5 and then shifted to YPBO (0.3% yeast extract, 0.5% peptone, 0.5% K_2HPO_4, 0.5% KH_2PO_4, 1% Brij-35, 1% [wt/ vol] oleic acid) medium to proliferate peroxisomes.

Rabbit polyclonal antibodies to the Aox1p, -3p and –5p subunits of the Aox complex [175], Pex2p [177], Pex5p [178], Pex16p [123], Pex19p [180], isocitrate lyase (ICL) [48], thiolase (THI) [178] and malate synthase (MLS) [48] have been described. Monospecific antibodies to Vps1p and Pex10p were raised in rabbit against their amino- and carboxyl-terminal peptides MDKELISTVNKLQDALA and CRQGVREQNLLPIR, respectively. Anti-Vps1p and anti-Pex10p antibodies were made at the "Open Biosystems" Company. Monoclonal anti-phosphatidylserine antibody was purchased from Upstate USA. Fluorescein-conjugated anti-mouse IgM antibody was from Jackson ImmunoResearch Laboratories. Alexa Fluor 488 signal-amplification kit for fluorescein-conjugated probes was purchased from Molecular Probes.

The initial step in the subcellular fractionation of YPBO-grown cells included the differential centrifugation of lysed and homogenized spheroplasts at 1,000 x *g* for 8 min

at 4°C in a rotor (model JS13.1; Beckman Instrs., Inc., Palo Alto, CA) to yield a postnuclear supernatant (PNS) fraction. The PNS fraction was further subjected to differential centrifugation at 20,000 x *g* for 30 min at 4°C in a rotor (model JS13.1; Beckman Instrs.) to yield pellet (20KgP) and supernatant (20KgS) fractions. The 20KgS fraction was further subfractionated by differential centrifugation at 200,000 x *g* for 1 h at 4°C in a rotor (model TLA120.2; Beckman Instrs., Inc.) to yield pellet (200KgP) and supernatant (200KgS) fractions.

To purify mature peroxisomes P6, the 20 KgP was further fractionated by flotation on a three-step sucrose gradient. Specifically, the 20 KgP was resuspended in 400 µl of 60% (wt/wt) sucrose in buffer H (5 mM MES, pH 5.5, 1 mM KCl, 0.5 mM EDTA, 0.1% [vol/vol] ethanol), overlaid with 2.3 ml of 50% (wt/wt) sucrose and 2.3 ml of 20% (wt/wt) sucrose (both in buffer H), and subjected to centrifugation in a rotor (model SW50.1; Beckman Instrs.) at 200,000 x *g* for 18 h at 4°C. Gradients were fractionated from the bottom, and 18 fractions of ~270 µl each were collected. To further purify mature peroxisomes P6, 4 vol of 0.5 M sucrose in buffer H were added to the peak peroxisomal fraction 4 recovered after isopycnic centrifugation on a discontinuous sucrose gradient. Peroxisomes were sedimented through a 150-µl cushion of 2 M sucrose in buffer H by centrifugation at 200,000 x *g* for 20 min at 4°C in a TLA120.2 rotor. The resultant pellet was resuspended in buffer H containing 1 M sorbitol and was subjected to further centrifugation on a linear 20-60% (wt/wt) sucrose gradient (in buffer H) at 197,000 x *g* for 18 h at 4°C in a rotor (model SW41Ti; Beckman Instrs., Inc.). Peak peroxisomal fraction 5 equilibrating at a density of 1.21 g/cm^3 was recovered, and

purified mature peroxisomes were pelleted at 200,000 x *g* for 20 min at 4°C in a TLA120.2 rotor, as described above. Pelleted peroxisomes were resuspended in 400 µl of 60% (wt/wt) sucrose in buffer H and subjected to flotation on a three-step sucrose gradient as described above. Peak peroxisomal fraction 4 was recovered and used for biochemical analyses. Peroxisomes isolated by this multistep method were greater than 97% pure, as judged by the presence of marker proteins of other organelles.

To purify immature peroxisomes P1 to P5, a 200,000-*g* pellet fraction (200KgP) was subjected to centrifugation on a discontinuous sucrose (18, 25, 30, 35, 40, and 53%, wt/wt) gradient at 120,000 x *g* for 18 h at 4°C in a Beckman SW28 rotor. 36 fractions of 1 ml each were collected. Fractions containing different subforms of immature peroxisomes were recovered, and 4 vol of 0.5 M sucrose in buffer H (5 mM MES, pH 5.5, 1 mM KCl, 0.5 mM EDTA, 0.1% ethanol, and a mixture of protease inhibitors) were added. Immature peroxisomes were pelleted onto a 150-µl cushion of 2 M sucrose in buffer H by centrifugation at 200,000 x *g* for 20 min at 4°C in a Beckman TLA120.2 rotor. Individual pellets of different subforms of immature peroxisomes were resuspended in 3 ml of 50% (wt/wt) sucrose in buffer H.

For purification of immature peroxisomes P1 and P2, pellets of P1 and P2 resuspended in 50% (wt/wt) sucrose in buffer H were overlaid with 30, 28, 26, 24, 22, and 10% sucrose (all wt/wt in buffer H). After centrifugation at 120,000 x *g* for 18 h at 4°C in a SW28 rotor, 18 fractions of 2 ml each were collected. P1 and P2 were pelleted, resuspended and subjected to a second flotation on the same multistep sucrose gradient. Gradients were fractionated into 2-ml fractions as above, and P1 and P2 were recovered

and pelleted.

For purification of immature peroxisomes P3 and P4, pellets of P3 and P4 resuspended in 50% (wt/wt) sucrose in buffer H were overlaid with 38%, 35%, 33% and 20% sucrose (all wt/wt in buffer H). After centrifugation at 120,000 x *g* for 18 h at 4°C in a SW28 rotor, 18 fractions of 2 ml each were collected. P3 and P4 were pelleted, resuspended in 3 ml of 50% (wt/wt) sucrose in buffer HE (20 mM MES, pH 5.5, 20 mM EDTA, 0.1% ethanol), overlaid with 39, 37, 35, 33, and 20% sucrose (all wt/wt in buffer HE), and subjected to centrifugation as above. Gradients were fractionated into 2-ml fractions, and P3 and P4 were recovered and pelleted. After resuspension in 3 ml of 50% (wt/wt) sucrose in buffer H, P3 and P4 were again subjected to flotation on the second multistep sucrose gradient described above. Gradients were fractionated into 2-ml fractions, and P3 and P4 were recovered and pelleted.

For extraction of lipids, 1.2 ml of chloroform/methanol (1:1, v/v) were added to a 600-µl sample of each purified peroxisomal subform. After incubation on ice for 15 min, samples were subjected to centrifugation at 20,000 × g for 15 min at 4°C. The chloroform phase was separated and dried under nitrogen. The lipid film was dissolved in 60 µl of chloroform (for the analysis of ergosterol and ceramide) or 60 µl of chloroform/methanol (1:1, v/v) (for the analysis of glycerophospholipids). 20 µl of each sample were spotted on 60Å silica gel plates for TLC (Whatman). The lipids were developed in the following solvent systems: chloroform/acetone (4:1, v/v) (for the analysis of ergosterol and ceramide) and chloroform/methanol/water (65:25:4, v/v) (for the analysis of glycerophospholipids). All lipids were detected using 5% phosphomolybdic acid in

ethanol and visualized by heating for 30 min at 110°C.

To evaluate the distribution of DAG and PS between the two leaflets of the membrane bilayers in immature peroxisomal vesicles and mature peroxisomes, the suspension of a purified peroxisomal subform in ice-cold buffer H (10 mM MES-KOH, pH 5.5, 250 mM sorbitol, 1 mM KCl, 0.5 mM EDTA, protease inhibitor cocktail) at 1 mg protein/ml was divided into two equal aliquots. One aliquot remained untreated, whereas peroxisomal vesicles in the other aliquot were lysed by incubation on ice for 20 min in 20 mM HEPES-KOH buffer, pH 8.0, containing 50 mM NaCl and protease inhibitor cocktail. The pellet of membranes recovered after centrifugation of osmotically lysed P1, P2, P3, P4, P5 or P6 was resuspended in ice-cold buffer H at 1 mg protein/ml. Two-fold serial dilutions of intact peroxisomal subforms (from the first aliquot) and of the membranes recovered after osmotic lysis of these peroxisomal subforms (from the second aliquot) in the range of 10-160 μg protein/ml were made in ice-cold buffer H. The DAG-binding C1b domain of protein kinase C labeled with the fluorophore Alexa Fluor 488 or anti-PS mouse IgM were added to concentrations 5 and 1 μg/ml, respectively. For samples that were exposed to Alexa Fluor 488-tagged C1b domain, the Alexa Fluor 488 fluorescence at 510 nm was monitored. All samples that were initially exposed to anti-PS mouse IgM were initially incubated for 30 min on ice and then subjected to centrifugation at 100,000 × g for 8 min at 4°C. The pellets were resuspended in 200 μl of ice-cold buffer H and supplemented with fluorescein-conjugated goat anti-mouse IgM antibodies at 5 μg/ml, respectively. After incubation for 30 min on ice, samples were subjected to centrifugation at 100,000 × g for 8 min at 4°C. The pellets were resuspended in 200 μl of

ice-cold buffer H and supplemented with Alexa Fluor 488 rabbit anti-fluorescein/Oregon Green IgG at 15 μg/ml. Following incubation for 30 min on ice, samples were subjected to centrifugation at 100,000 × g for 8 min at 4°C. The pellets were resuspended in 200 μl of ice-cold buffer H and supplemented with Alexa Fluor 488 goat anti-rabbit IgG at 20 μg/ml. After incubation for 30 min on ice, samples were subjected to centrifugation at 100,000 × g for 8 min at 4°C. The pellets were resuspended in 200 μl of ice-cold buffer H and placed into the wells of a 96-well microplate. The fluorescence of samples was measured using the Wallac Victor 2 Multi-label microplate fluorescence reader with filters set at 485 (+/- 7.5) nm (excitation) and 510 (+/- 5) nm (emission). Controls were made for each dilution of intact peroxisomal subforms and of peroxisomal membranes recovered after osmotic lysis of these peroxisomal subforms. The controls included normal mouse IgM at 1 μg/ml added instead of anti-PS mouse IgM. Background fluorescence, which was due to the nonspecific binding of mouse IgM and/or fluorescein- or Alexa Fluor 488-labeled antibodies to the peroxisomal membrane, was subtracted. The ratio "fluorescence for intact peroxisomes (F_i)/fluorescence for osmotically lysed peroxisomes (F_{ol})" was calculated for each dilution of intact peroxisomal subforms and of the membranes recovered after osmotic lysis of these peroxisomal subform. This ratio is equal to the fraction of the total pool of a monitored lipid that is located in the outer (cytosolic) leaflet of the membrane.

To evaluate the phospholipid-binding specificity of Pex16p associated with different peroxisomal subforms, the pellet of membranes recovered after centrifugation of osmotically lysed peroxisomes was resuspended in buffer TBSO (10 mM Tris-HCl, pH

8.0, 150 mM NaCl, 0.5% n-OG) and incubated for 30 min on ice. Samples were subjected to centrifugation at 100,000 × g for 30 min at 4°C. Under these conditions, n-OG completely solubilized the vast majority of all membrane proteins. The supernatants of n-OG-solubilized proteins were then incubated at 5 μg/ml with the PIP-Strip (Echelon Biosciences) at 4°C overnight. After washing the PIP-Strip five times for 5 min each with TBSO, Pex16p was detected by immunoblotting with anti-Pex16p antibodies.

5.4 Results

5.4.1 Lipid composition of the peroxisomal membrane is changed during the last step of the assembly of a division-competent mature peroxisome

In wild-type cells, the levels of phosphatidic acid (PA) and diacylglycerol (DAG) in the peroxisomal membrane dramatically increased only during conversion of immature peroxisomal vesicles P5 to mature peroxisomes P6 (Figure 5.1 A). These two cone-shaped lipids are potent inducers of membrane fission [155, 159, 173, 174]. In contrast, the level of lysophosphatidic acid (LPA), an inverted-cone-shaped lipid [155], in the membrane greatly reduced during conversion of P5 to P6 (Figure 5.1 A). Importantly, the lack of Pex16p in *pex16KO* mutant cells resulted in the accumulation of PA and DAG and led to the disappearance of LPA even in the membrane of immature peroxisomal vesicles P3 (Figure 5.1 A). The *pex16KO* mutation, which causes the excessive proliferation of immature peroxisomal vesicles, impaired the conversion of P3 to P4 (see Chapter 3). On the contrary, the *PEX16-TH* mutation, which averts peroxisome division by dramatically elevating the intraperoxisomal pool of Pex16p (see Chapter 3), abolished the formation of PA and DAG and prevented the disappearance of LPA even in the

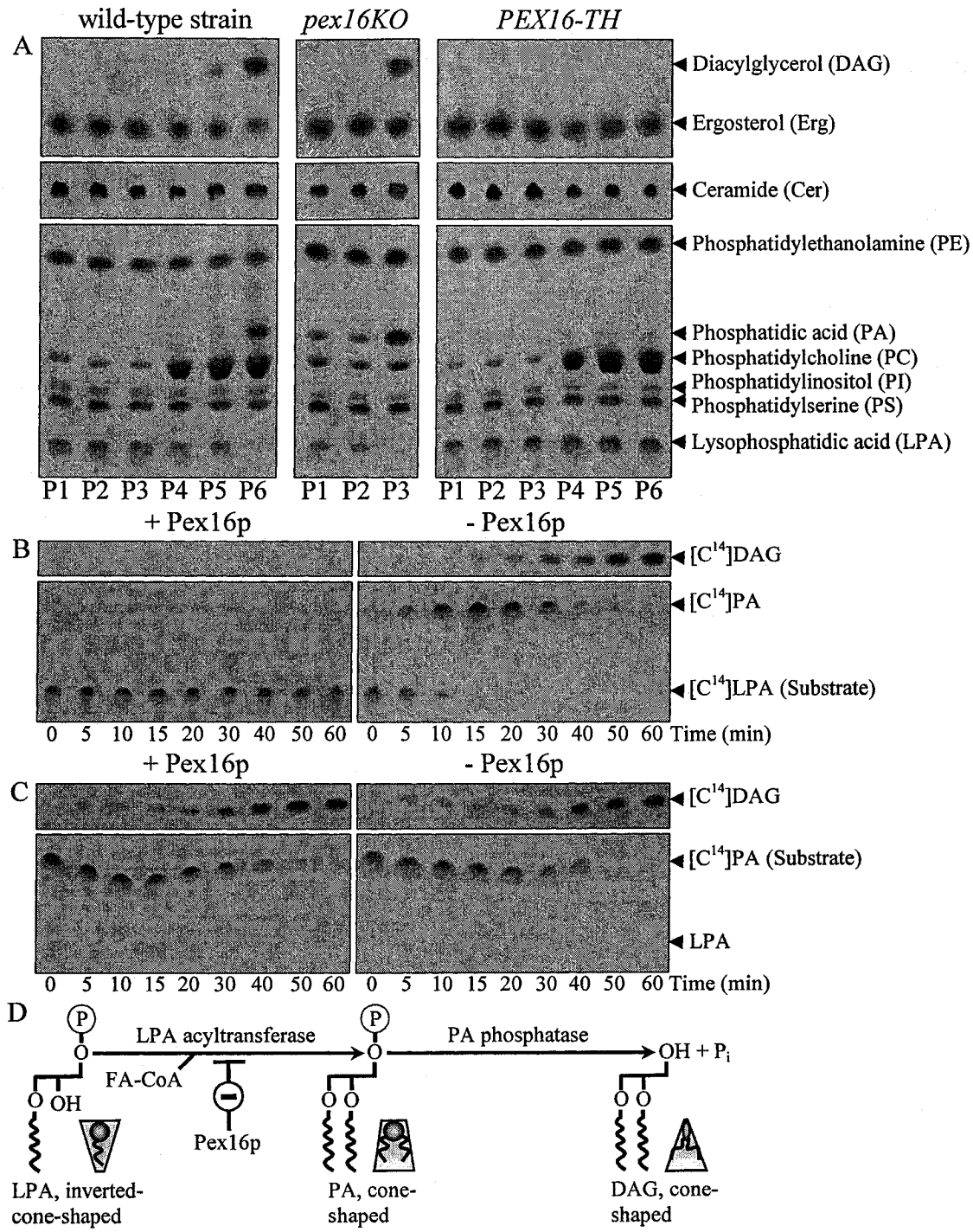

Figure 5.1. Pex16p regulates lipid metabolism in the peroxisomal membrane. (A) Spectra of membrane lipids in different peroxisomal subforms purified from wild-type, *pex16KO* and *PEX16-TH* cells. Peroxisomes were osmotically lysed and subjected to centrifugation. Lipids were extracted from equal quantities of the pelleted membrane proteins and analyzed by TLC. (B and C) Dynamics of radiolabeled

lipids in the membrane of P1 liposomes. Liposomes were reconstituted from peroxisomal membrane proteins immunodepleted (- Pex16p) or not immunodepleted (+ Pex16p) of Pex16p and non-radiolabeled lipids, all of which were extracted from the membrane of immature peroxisomal vesicles P1. [^{14}C]LPA (B) or [^{14}C]PA (C) were the only radiolabeled lipids incorporated into liposomes during their reconstitution. The [^{14}C]LPA-loaded liposomes (B) were also supplemented with unlabeled oleoyl-CoA, a co-substrate of LPAAT. Samples were taken at the indicated times after transfer of reconstituted liposomes from ice to 26°C. Lipids were extracted from the membrane and analyzed by TLC. (D) Pex16p inhibits LPAAT, the first enzyme in a two-step biosynthetic pathway that leads to the formation of DAG in the peroxisomal membrane during conversion of P5 to P6. Abbreviation: *FA-CoA*, acyl-CoA esters of fatty acids.

membrane of P6 (Figure 5.1 A). These findings suggest that the interaction between Aox and Pex16p at the matrix face of the membrane of mature peroxisomes P6 activates the biosynthesis of PA and DAG and promotes the catabolism of LPA.

To elucidate the mechanism that regulates the levels of PA, DAG and LPA in the peroxisomal membrane, I modified a procedure described in Chapter 4 in order to reconstitute peroxisomal liposomes from detergent-solubilized peroxisomal membrane proteins (PMPs) and membrane lipids of immature peroxisomal vesicles P1. No Aox subunits are attached to the membrane inside these P1-based liposomes (see Chapter 4), in which Pex16p is present only in its free form. In the membrane of P1 liposomes supplemented with [^{14}C]LPA as the only radiolabeled lipid, the decline in the level of [^{14}C]LPA coincided with the increase in the amount of newly synthesized [^{14}C]PA, which preceded the appearance of [^{14}C]DAG, only if these liposomes were reconstituted from PMPs immunodepleted of Pex16p (Figure 5.1 B). In contrast, if [^{14}C]PA was used as the only radiolabeled membrane lipid for reconstituting P1 liposomes, the decline in its level coincided with the increase in the amount of newly synthesized [^{14}C]DAG even if the PMPs taken for liposome reconstitution were not immunodepleted of Pex16p (Figure 5.1

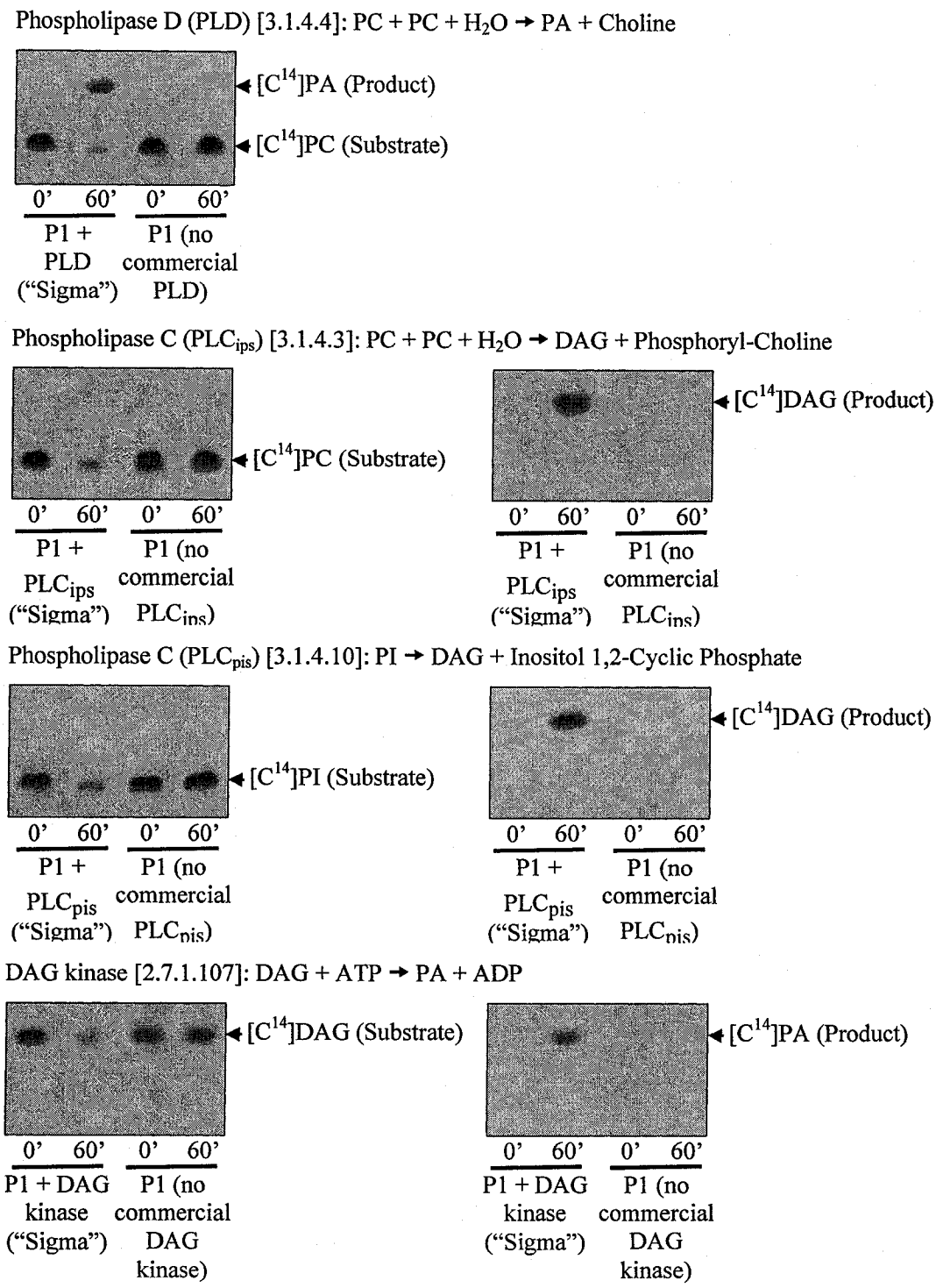

Figure 5.2. The peroxisomal membrane lacks the activities of enzymes that, in addition to LPAAT and PAP, can catalyze reactions resulting in the formation of PA or DAG. P1 liposomes that lack Pex16p were reconstituted as described in the legend to Figure 5.1. [^{14}C]-labeled lipid substrates were incorporated into

liposomes during their reconstitution. To provide a positive control, an aliquot of liposomes was supplemented with the commercial enzyme of interest. Samples were taken before and 60 min after transfer of reconstituted liposomes from ice to 26°C. Lipids were extracted from the membrane and analyzed by TLC. Abbreviations: PLC_{ips}, inositol phosphosphingolipid phospholipase C; PLC_{pis}, phosphoinositide-specific phospholipase C.

C).

Altogether, the above findings provide evidence that: 1) the conversion of P5 to P6 in wild-type cells is marked by the biosynthesis of PA and DAG in the peroxisomal membrane; 2) PA and DAG are formed in a two-step biosynthetic pathway, which includes two consecutive enzymatic reactions catalyzed by an LPA acyltransferase (LPAAT) and a PA phosphatase (PAP) (Figure 5.1 D); and 3) Pex16p, a negative regulator of the division of immature peroxisomal vesicles, inhibits LPAAT. The LPAAT and PAP reactions are the only reactions leading to the formation of PA and DAG, respectively, in the peroxisomal membrane. In fact, this membrane lacked the activities of phospholipase D, inositol phosphosphingolipid phospholipase C (PLC), phosphoinositide-specific PLC, and DAG kinase (Figure 5.2), all of which catalyze reactions that result in the formation of PA or DAG [155, 170, 181-183]. In addition, the peroxisomal membrane lacked two other enzymes that can promote the biosynthesis of PA or DAG (Figure 5.3), namely inositol phosphorylceramide synthase and inositolphosphotransferase 1 [181, 182, 184-187].

5.4.2 The binding of Pex16p to LPA prevents the formation of PA and DAG in the membranes of immature peroxisomal vesicles

Because Pex16p inhibits LPAAT in the membranes of P1 to P5, thereby preventing the

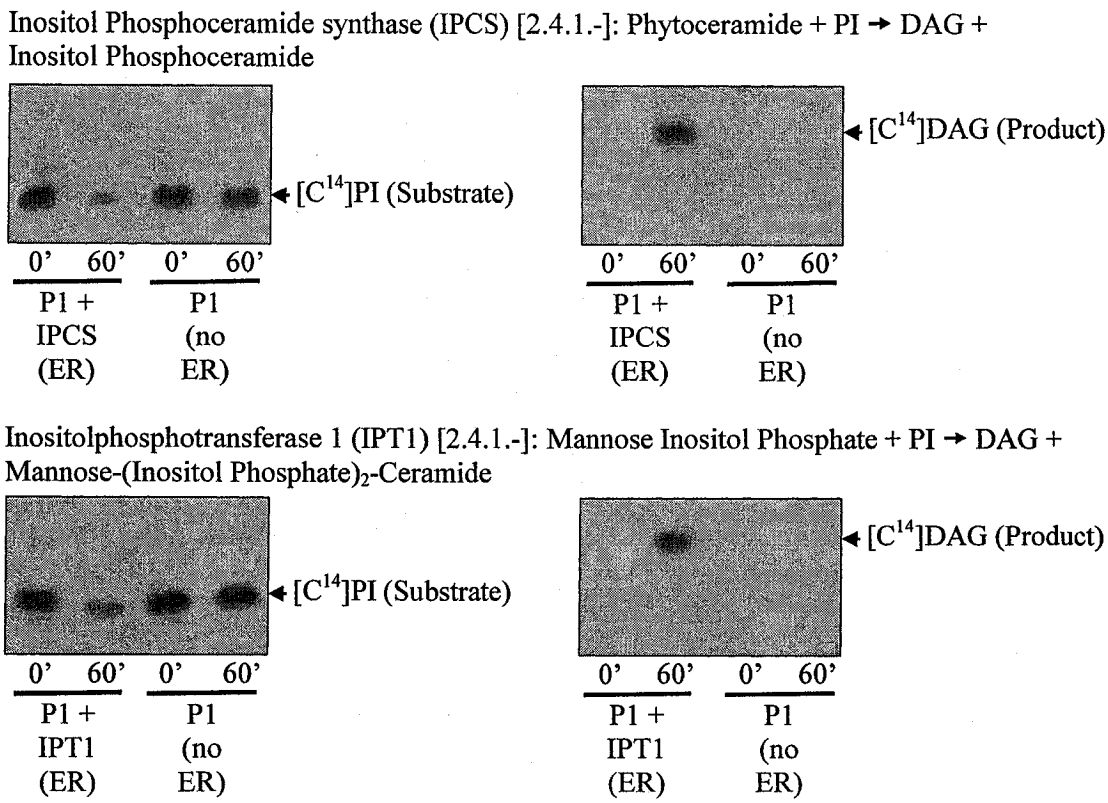

Figure 5.3. The peroxisomal membrane lacks enzymes that, in addition to LPAAT and PAP, can promote formation of PA or DAG. P1 liposomes that lack Pex16p were reconstituted as described in the legend to Figure 1. [^{14}C]PI, a radiolabeled lipid substrate, was incorporated into liposomes during their reconstitution. The [^{14}C]PI-loaded liposomes were also supplemented with unlabeled phytoceramide or mannose inositol phosphate, the two co-substrates of inositol phosphoceramide synthase or inositolphosphotransferase 1, respectively. To provide a positive control, an aliquot of liposomes was supplemented with detergent-solubilized membrane proteins and unlabeled membrane lipids of endoplasmic reticulum (ER) membranes purified from the yeast *Saccharomyces cerevisiae*. Samples were taken before and 60 min after transfer of reconstituted liposomes from ice to 26°C. Lipids were extracted from the membrane and analyzed by TLC.

formation of both PA and DAG, I sought to define the mechanism for the negative regulation of LPAAT by Pex16p in immature peroxisomal vesicles. Pex16p solubilized with the detergent n-octyl-β-D-glucopyranoside (n-OG) from the membranes of P1 to P5

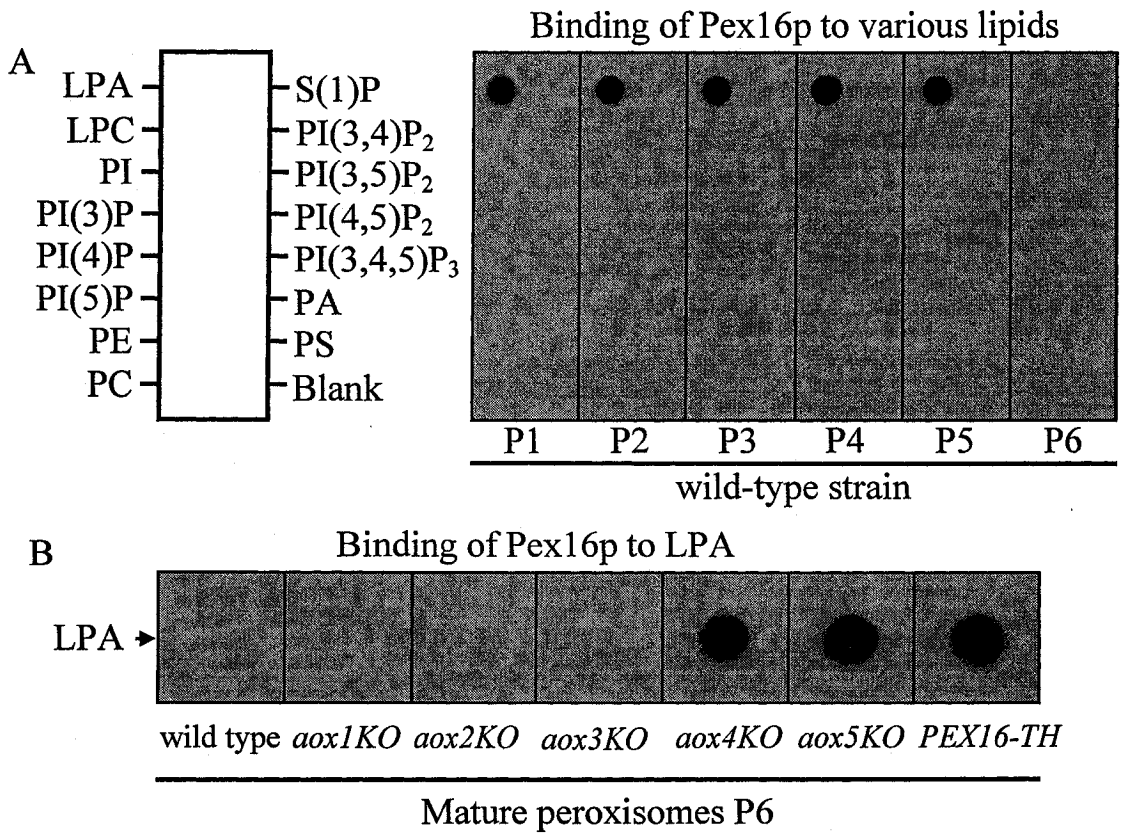

Figure 5.4. Pex16p binds to LPA only in the membranes of division-incompetent peroxisomal subforms. Different peroxisomal subforms purified from wild-type and mutant cells were osmotically lysed and subjected to centrifugation. The pellet of membranes after such centrifugation was solubilized with a detergent, n-OG. Equal quantities of detergent-soluble membrane proteins were analyzed by protein-lipid overlay assay using commercial PIP-Strips. Pex16p was detected by immunoblotting with anti-Pex16p antibodies.

purified from wild-type cells was able to bind only to LPA, a substrate of LPAAT, but not to any other lipid tested (Figure 5.4 A). In contrast, n-OG-soluble Pex16p of mature peroxisomes P6 did not bind to LPA if these peroxisomes were recovered from wild-type or *aox1KO*, *aox2KO* and *aox3KO* mutant strains (Figure 5.4). All these strains lack LPA and carry both PA and DAG in the membranes of their division-competent mature

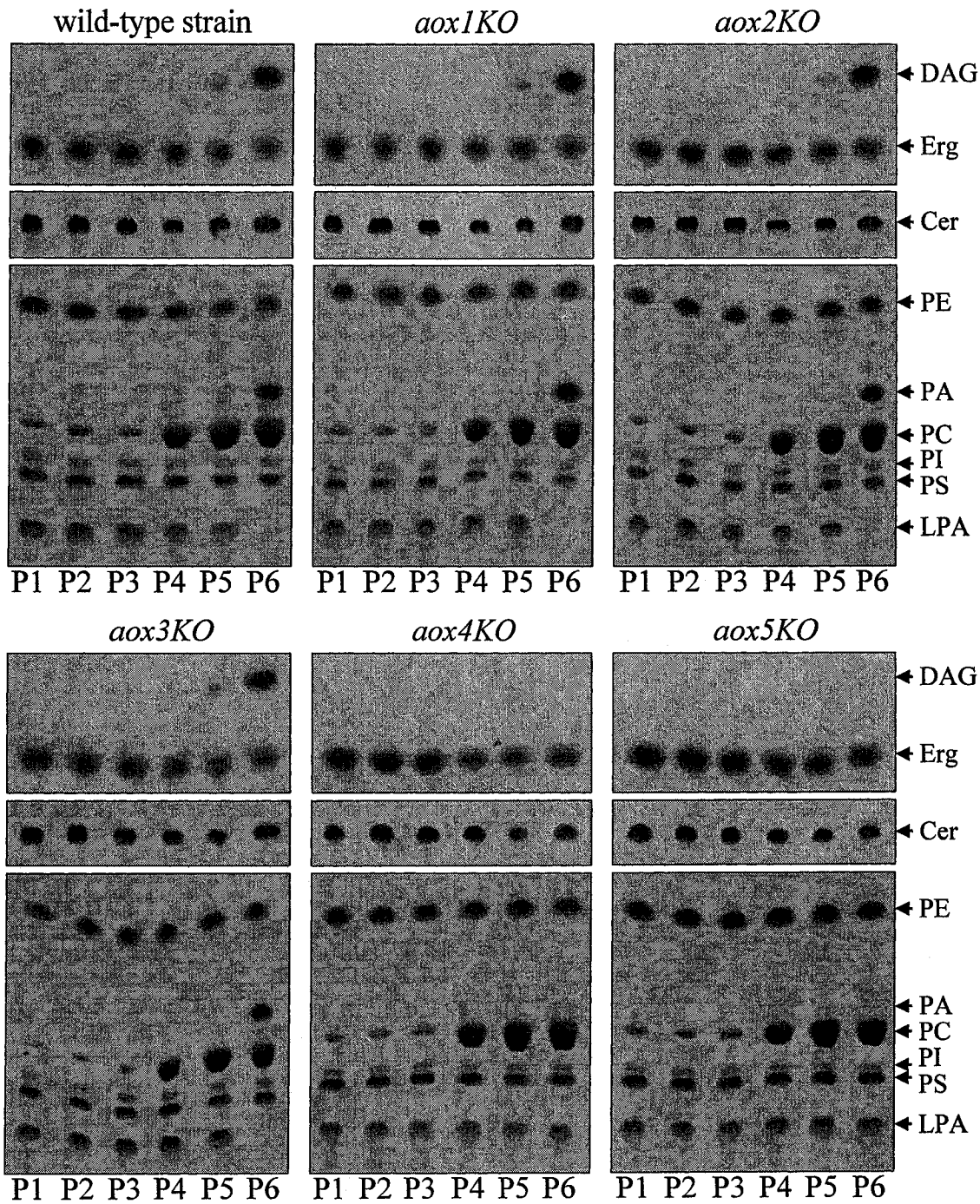

Figure 5.5. Mutations that abolish the binding of Aox to Pex16p, thereby impairing peroxisome division, prevent the biosynthesis of PA and DAG in the peroxisomal membrane. Highly purified peroxisomal subforms were osmotically lysed and subjected to centrifugation. Equal quantities of the pelleted membrane proteins recovered from different peroxisomal subforms were subjected to lipid extraction, which was followed by TLC and visualization of lipids.

peroxisomes (Figure 5.1 A and Figure 5.5). Of note, Pex16p is attached to the membranes of immature peroxisomal vesicles only in its free form, whereas all the Pex16p on the inner face of mature peroxisomes of wild-type or *aox1KO*, *aox2KO* and *aox3KO* mutant cells is titrated by its interaction with Aox (see Chapter 3). Importantly, the interaction between Pex16p and Aox is not affected by n-OG. Altogether, these data strongly suggest that the binding of Aox to Pex16p in mature peroxisomes of wild-type cells greatly decreases the affinity between Pex16p and LPA, thereby allowing LPA to enter the two-step biosynthetic pathway leading to the formation of PA and DAG. This hypothesis is supported by the observation that n-OG-soluble Pex16p of mature peroxisomes was capable of binding to LPA if these mature peroxisomes were purified from *aox4KO*, *aox5KO* or *PEX16-TH* mutant strains (Figure 5.4 B). All these mutant strains: 1) are deficient in the division of mature peroxisomes; 2) carry Pex16p in a free form that is not titrated by its interaction with Aox; and 3) accumulate a reduced number of greatly enlarged mature peroxisomes (see Chapter 3) that contain LPA but lack both PA and DAG (Figure 5.1 A and Figure 5.5).

5.4.3 Dynamics of changes in the transbilayer distribution of DAG and PS in the peroxisomal membrane during peroxisome maturation

My data suggest that LPA enters the two-step pathway for the biosynthesis of PA and DAG (Figure 5.1 D) only when the efficiency of its binding to Pex16p declines. Pex16p is a peripheral membrane protein that is attached only to the inner (lumenal) leaflet of the peroxisomal membrane [123]. Furthermore, it seems unlikely that LPA can translocate from the inner to the outer (cytosolic) leaflet of the peroxisomal membrane, as its

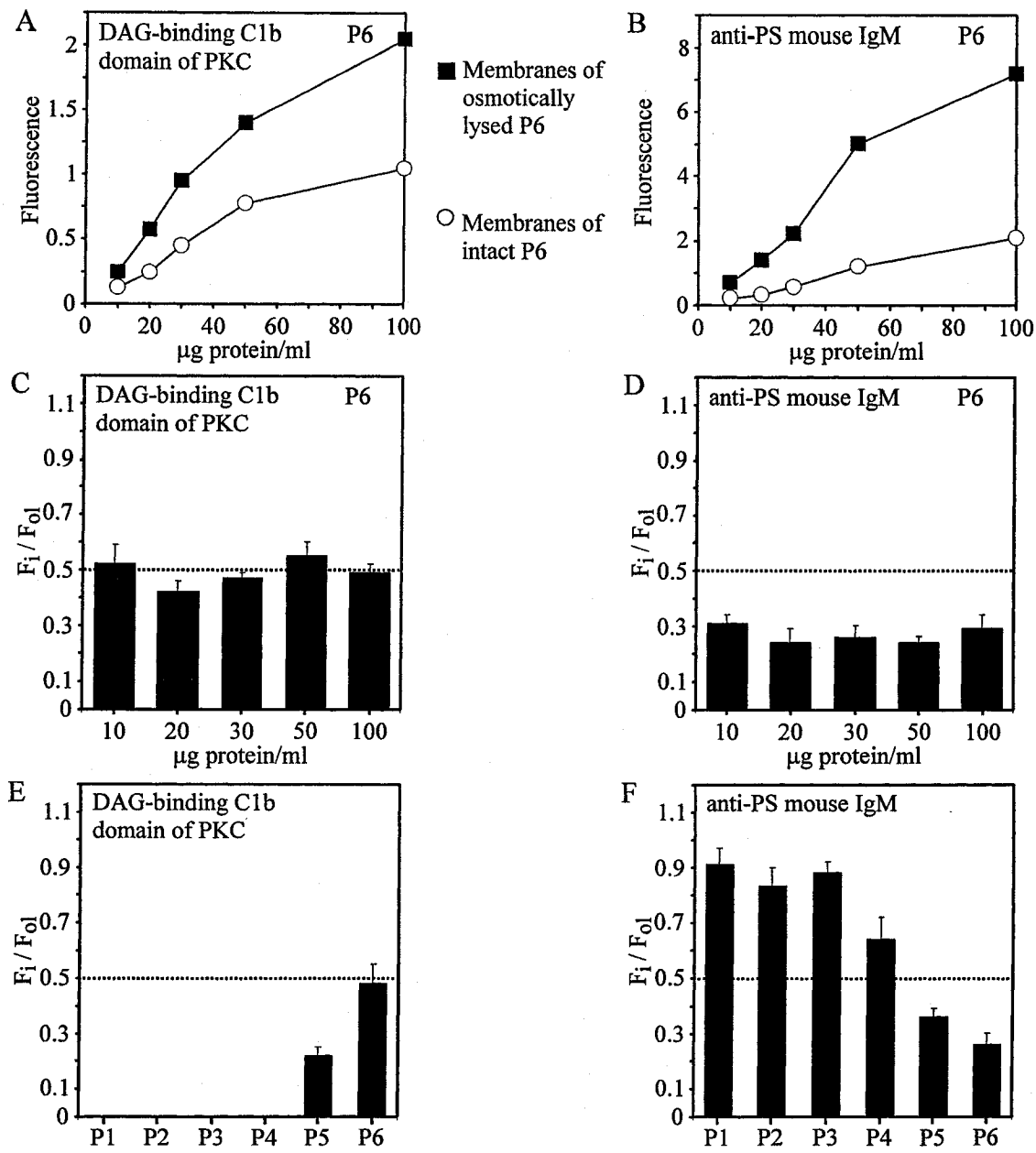

Figure 5.6. As peroxisomes mature, DAG and PS change their transbilayer distribution in the peroxisomal membrane. (A and B) A suspension of purified mature peroxisomes P6 was divided into two equal aliquots. One aliquot remained untreated, while peroxisomes in the other aliquot were osmotically lysed. Serial dilutions of intact P6 (from the first aliquot) and of the membranes recovered after centrifugation of osmotically lysed P6 (from the second aliquot) in the range of 10-100 µg protein/ml were exposed to the DAG-binding C1b domain of protein kinase C labeled with the fluorophore Alexa Fluor 488 (A) or anti-PS mouse IgM (B). For samples that were exposed to Alexa Fluor 488-tagged C1b domain, the Alexa Fluor 488 fluorescence at 510 nm was monitored. All samples that were initially exposed to anti-PS mouse IgM

were then treated with fluorescein-conjugated goat anti-mouse IgM antibodies, labeled with Alexa Fluor 488 rabbit anti-fluorescein/Oregon Green IgG, and finally exposed to Alexa Fluor 488 goat anti-rabbit IgG. The Alexa Fluor 488 fluorescence at 510 nm was monitored in individual samples. (C and D) The ratio "fluorescence for intact peroxisomes (F_i)/fluorescence for osmotically lysed peroxisomes (F_{ol})" was calculated for each dilution of intact P6 and of the membranes recovered after osmotic lysis of this peroxisomal subform. This ratio is equal to the fraction of the total pool of a monitored lipid that is located in the outer (cytosolic) leaflet of the membrane. (E and F) The ratio "F_i/F_{ol}" was calculated for each dilution of intact P1 to P6 and of the membranes recovered after osmotic lysis of each of these peroxisomal subforms.

spontaneous transbilayer movement is very slow [136, 148]. Altogether, these findings imply that the biosynthesis of PA and DAG is spatially restricted to the lumenal leaflet of the peroxisomal membrane. Using the DAG-binding C1b domain of protein kinase C [188], I evaluated the arrangement of DAG, a particularly potent cone-shaped inducer of membrane fission [154, 155, 172-174], between the two leaflets of the membrane bilayers in P5 and P6 peroxisomes. In the membranes of osmotically lysed peroxisomes, both leaflets of the bilayer were accessible to this DAG-specific probe. In contract, in the membranes of intact peroxisomes, this DAG sensor could detect only DAG molecules that resided in the cytosolic leaflet. In intact P5, only the minor portion of DAG was accessible to C1b domain of protein kinase C, with about 22% of this lipid located in the cytosolic leaflet of the bilayer (Figure 5.6 E). Thus, DAG resides predominantly in the lumenal leaflet of the membrane of P5. In contrast, DAG is distributed symmetrically between the two leaflets of the membrane bilayer in mature peroxisomes P6. In fact, about half of this lipid in intact P6 was accessible to C1b domain of protein kinase C (Figure 5.6, panels A, C and E).

I then used monoclonal antibodies to Phosphatidylserine (PS), a lipid that has a

cylindrical shape [154, 159], to monitor the transbilayer distribution of this lipid in the membranes of different peroxisomal subforms. PS in the membranes of immature peroxisomal vesicles P1 to P3 resides predominantly in their cytosolic leaflets, as the vast majority of this lipid was accessible to anti-PS antibodies in intact P1 to P3 (Figure 5.6 F). As peroxisomes mature, PS gradually moves from the cytosolic to the lumenal leaflets of their membranes, with only about 24% of this lipid being accessible to anti-PS antibodies in intact P6 (Figure 5.6, panels B, D and F).

In summary, my findings provide evidence for the specific redistribution of at least two lipids, namely DAG and PS, between the two leaflets of the peroxisomal membrane that occurs during peroxisome maturation. The movement of DAG from the lumenal to the cytosolic leaflet of the membrane bilayer coincides with the translocation of PS in the opposite direction, perhaps generating a lipid imbalance across the bilayer and thereby driving the process of membrane fission.

5.4.4 Endoplasmic reticulum-derived phosphatidylcholine in the peroxisomal membrane activates both LPAAT and PAP

The levels of phosphatidylcholine (PC), a major glycerophospholipid of the peroxisomal membrane [142, 147], in P4, P5 and P6 peroxisomes of wild-type cells were significantly higher than in P1, P2 and P3 peroxisomes (Figure 5.1 A). The observed increase in the levels of PC was not due to its *de novo* synthesis. In fact, the membranes of P3 and P4 did not contain PA and DAG (Figure 5.1 A), two substrates for PC biosynthesis via the PE methylation and CDP-choline pathways, respectively [181, 189]. Thus, PC is transported to the membranes of P3 and P4 during their conversion to P4 and P5,

respectively. Three established mechanisms of intracellular lipid transport to organellar membranes include: 1) transport catalyzed by cytosolic lipid transfer proteins [148, 190-194]; 2) vesicle-mediated transport [195-202] and 3) transport at regions of close apposition between specialized microdomains of the endoplasmic reticulum (ER) membrane, the principal site of glycerophospholipid synthesis [136, 148, 195-198], and the membranes of the trans Golgi [149-151, 199, 203, 204] or mitochondria [149, 150, 151, 205-207]. My data imply that the peroxisome-associated peroxin Pex2p [177] is required for the transfer of PC from the donor membrane of a distinct subcompartment of the ER to the acceptor membranes of P3 and P4 associated with this subcompartment. In fact, the *pex2KO* mutation significantly decreases the total levels of glycerophospholipids in the membranes of P3 and P4 peroxisomes and, at the same time, increases the levels of membrane glycerophospholipids in the P3- and P4-associated subcompartment of the ER [55, 75]. This ER subcompartment: 1) co-purifies with P3 and P4 peroxisomes [55, 75]; 2) can be separated from P3 and P4 by EDTA [55, 75]; and 3) can be distinguished from the free form of the ER by buoyant density [75], the total level of membrane glycerophospholipids [75], and protein spectrum (Figure 5.7 B). Furthermore, the *pex2KO* mutation, which substantially decreases the level of PC in P4 (Figure 5.7 A), impairs the conversion of P4 to P5 [75]. Altogether, these findings suggest that the Pex2p-dependent transfer of PC from the P3- and P4-associated ER subcompartment to the acceptor membranes of P3 and P4 provides these membranes with the bulk quantities of PC and is essential for the conversion of P4 to P5.

It seems that PC in the peroxisomal membrane is a positive regulator of both the

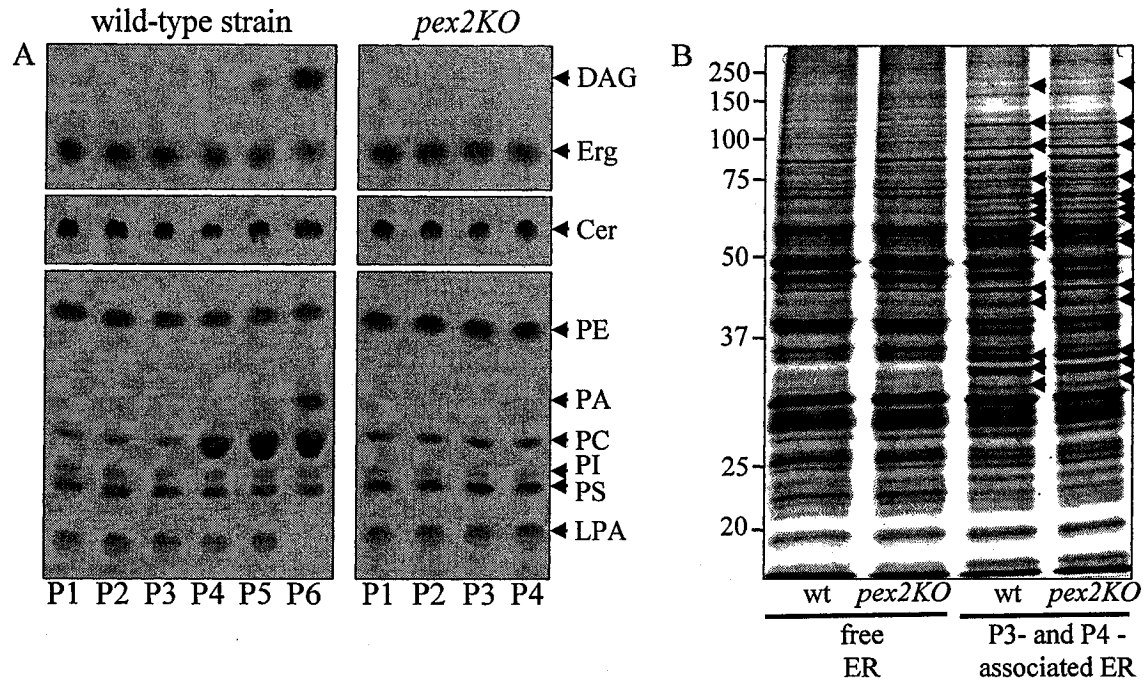

Figure 5.7. The Pex2p-dependent transfer of PC from a P3- and P4-associated subcompartment of the ER provides the peroxisomal membrane with the bulk quantities of this lipid. (A) The spectra of lipids found in the membranes of different peroxisomal subforms that were purified from wild-type and *pex2KO* mutant cells. (B) The spectra of proteins recovered in the free form of the ER and in the P3- and P4-associated subcompartment of the ER. Organelles were purified from wild-type and *pex2Δ* mutant cells as described in *Materials and Methods*. Arrowheads mark proteins found only in the ER subcompartment associated with P3 and P4 or significantly enriched in this subcompartment of the ER as compared with its free form.

LPAAT and PAP reactions in the pathway for DAG biosynthesis. In fact, the initial rates of both reactions in liposomes reconstituted from the Pex16p-immunodepleted PMPs and membrane lipids of P1, P2 and P3 were significantly lower than in liposomes reconstituted from membrane components of P4, P5 and P6 (Figure 5.8, panels A and B). Of note, the initial rates of both reactions were proportional to the steady-state levels of PC in the membranes of these peroxisomal liposomes (Figure 5.8, panels A and B). Importantly, the positive effect of PC on both LPAAT and PAP could be reconstructed in

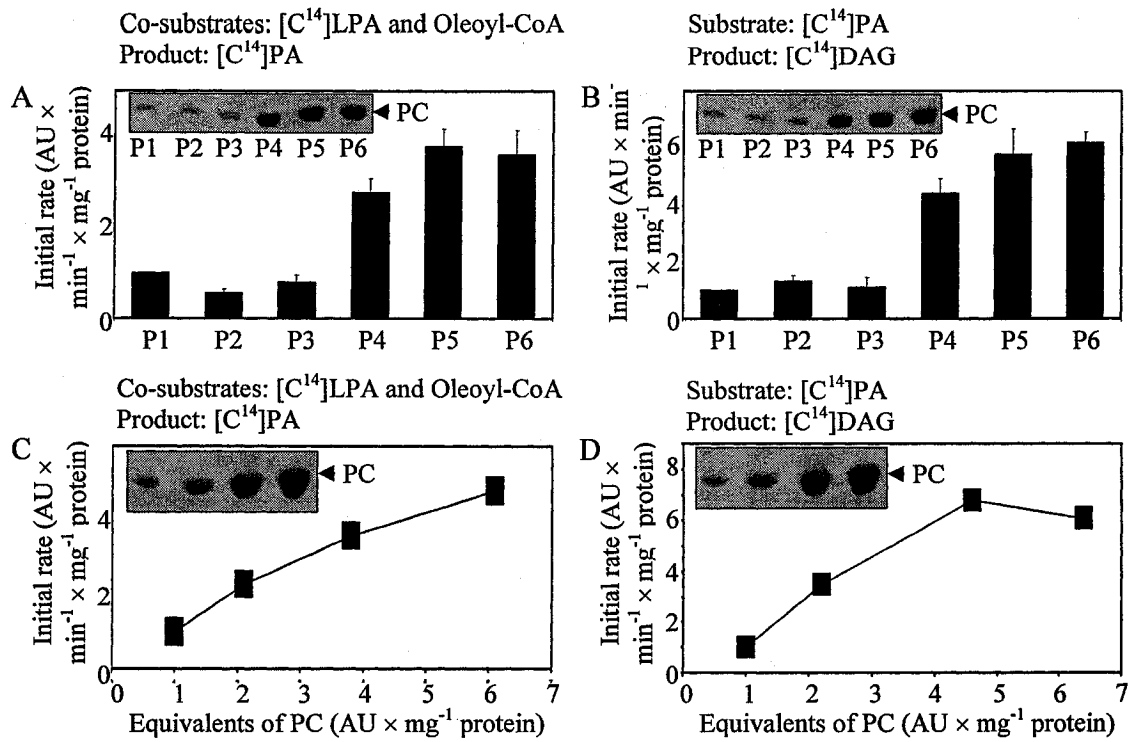

Figure 5.8. PC in the peroxisomal membrane is a positive regulator of both LPAAT and PAP. (A and B) The initial rates of the LPAAT (A) and PAP (B) reactions and the levels of PC in the membranes of liposomes reconstituted from the Pex16p-immunodepleted PMPs and membrane lipids of different peroxisomal subforms. Peroxisomal liposomes that lack Pex16p were reconstituted as described in the legend to Figure 5.1. [^{14}C]-labeled lipid substrates were incorporated into liposomes during their reconstitution. (C and D) The initial rates of the LPAAT (C) and PAP (D) reactions and the levels of PC in the membranes of four different types of liposomes reconstituted from the Pex16p-immunodepleted PMPs and membrane lipids of P1 peroxisomes. Four different types of liposomes varied only in the quantities of PC used for their reconstitution and recovered in their membranes after the reconstitution. To calculate the initial rates of the LPAAT and PAP reactions, the [^{14}C]-labeled LPA, PA and DAG were separated by TLC and quantified by autoradiography. To visualize non-radiolabeled PC, lipids were separated by TLC and detected using phosphomolybdic acid.

four different types of the Pex16p-immunodepleted P1 liposomes that varied only in the quantities of PC present in their membranes (Figure 5.8, panels C and D).

5.5 Discussion

Data presented in Figure 5.1 imply that the conversion of P5 to P6 in wild-type cells is marked by the biosynthesis of phosphatidic acid (PA) and diacylglycerol (DAG) in the peroxisomal membrane. This two lipid species are formed in a two-step biosynthetic pathway, which includes two consecutive enzymatic reactions catalyzed by an LPA acyltransferase (LPAAT) and a PA phosphatase (PAP). I found that the LPAAT and PAP reactions are the only reactions leading to the formation of PA and DAG, respectively, in the peroxisomal membrane (Figures 5.2 and 2.3). Importantly, LPAAT is inhibited by Pex16p, a negative regulator of the division of immature peroxisomal vesicles (Figure 5.1). Furthermore, findings reported in Figures 5.4 and 5.5 provide evidence that the binding of Aox to Pex16p in mature peroxisomes of wild-type cells greatly decreases the affinity between Pex16p and LPA, thereby allowing LPA to enter the two-step biosynthetic pathway leading to the formation of PA and DAG. Moreover, my data strongly suggest that the movement of DAG from the lumenal to the cytosolic leaflet of the membrane bilayer, which occurs during peroxisome maturation, coincides with the translocation of phosphatidylserine (PS) in the opposite direction (Figure 5.6). It is conceivable that such bidirectional movement of DAG and PS generates a lipid imbalance across the bilayer and thereby driving the process of membrane fission (Figure 5.6). Finally, the glycerophospholipid phosphatidylcholine (PC), which is transferred from the P3- and P4-associated ER subcompartment to the acceptor membranes of P3 and P4 (Figure 5.7), is a positive regulator of both the LPAAT and PAP reactions in the pathway for DAG biosynthesis (Figure 5.8).

5.6 Conclusions

Taken together, the data presented in Chapter 5 strongly suggest that the stepwise maturation of the peroxisome is accompanied by substantial changes in the composition of peroxisomal membrane lipids and in their transbilayer distribution. These changes are controlled by the Aox-Pex16p intraperoxisomal signaling acting from inside of the mature peroxisome. Importantly, the observed changes in the composition of peroxisomal membrane lipids and in their transbilayer distribution at the last step of the peroxisome assembly pathway trigger the membrane destabilization, bending, scission and fission events required for the division of mature peroxisomes.

6 Changes in the composition and transbilayer distribution of peroxisomal membrane lipids promote the recruitment of Vps1p from the cytosol to the mature peroxisome

6.1 Abstract

Lack of the dynamin-like protein Vps1p in the yeast *Y. lipolytica* results in a reduced number of greatly enlarged mature peroxisomes. Thus, Vps1p is essential for the division of mature peroxisomes in this yeast. The conversion of P5 to P6 in wild-type cells is marked by the recruitment of Vps1p from the cytosol to the surface of mature peroxisomes. This recruitment of Vps1p from the cytosol to the outer face of the mature peroxisome relies on the biosynthesis of PA and/or DAG in the inner (lumenal) leaflet of its membrane, which is triggered by the formation of the Aox/Pex16p complex at the inner (lumenal) face of this division-competent peroxisomal subform.

6.2 Introduction

Data presented in Chapter 5 provided evidence that the stepwise maturation of the peroxisome is accompanied by substantial changes in the composition of peroxisomal membrane lipids and in their transbilayer distribution. I found that these changes are controlled by the Aox-Pex16p intraperoxisomal signaling acting from inside of the mature peroxisome. Furthermore, my findings presented in Chapter 5 also strongly imply that the observed changes in the composition of peroxisomal membrane lipids and in their transbilayer distribution at the last step of the peroxisome assembly pathway trigger the membrane destabilization, bending, scission and fission events required for the division of mature peroxisomes. I thought that it would be interesting to see whether there are any protein constituents of mature peroxisomes that can promote the division of these peroxisomes in response to the Aox/Pex16p-dependent formation of PA and DAG in the peroxisomal membrane. The dynamin-like protein Vps1p would be a good candidate for such protein constituent. In fact, this member of the dynamin protein superfamily of large GTPases has been shown to be essential for peroxisome division in the yeast *S. cerevisiae* [25, 99, 208, 209]. However, it was not known whether Vps1p is required for peroxisome division in the yeast *Y. lipolytica*. Furthermore, it was not established whether Vps1p binds to mature peroxisomes in *Y. lipolytica* and, if it does, whether the recruitment of this predominantly cytosolic protein to the mature peroxisomes depends on the Aox/Pex16p-dependent formation of PA and DAG in the peroxisomal membrane.

6.3 Materials and methods

The *Y. lipolytica* wild-type strain *P01d* (*MatA ura3-302 leu2-270 xpr2-302*) [176], the mutant strains *vps1KO* (*MatA ura3-302 leu2-270 xpr2-3 vps1::URA3*), [177], *pex10KO* (*MatA ura3-302 leu2-270 xpr2-3 pex10::URA3*) and *pex16-TH* (*MatA ura3-302::PEX16TH-URA3 leu2-270 xpr2-3 pex16-1*) [123], and the single *AOX* gene knock-out strains *aox1KO* (*MatA ura3-302 leu2-270 xpr2-3 aox1::URA3*), *aox2KO* (*MatA ura3-302 leu2-270 xpr2-3 aox2::URA3*), *aox3KO* (*MatA ura3-302 leu2-270 xpr2-3 aox3::URA3*), *aox4KO* (*MatA ura3-302 leu2-270 xpr2-3 aox4::URA3*) [176] were used. Targeted integrative disruption of the *PEX10* and *VPS1* genes was performed with the *URA3* gene of *Y. lipolytica*, using a previously described modification of the sticky-end polymerase chain reaction procedure [176]. Growth was at 30°C. Yeast strains were initially grown in YPD (1% yeast extract, 2% peptone, 2% glucose) medium to an OD_{600} of ~1.5 and then shifted to YPBO (0.3% yeast extract, 0.5% peptone, 0.5% K_2HPO_4, 0.5% KH_2PO_4, 1% Brij-35, 1% [wt/ vol] oleic acid) medium to proliferate peroxisomes.

Rabbit polyclonal antibodies to the Aox1p, -3p and –5p subunits of the Aox complex [175], Pex2p [177], Pex5p [178], Pex16p [123], Pex19p [180], isocitrate lyase (ICL) [48], thiolase (THI) [178] and malate synthase (MLS) [48] have been described. Monospecific antibodies to Vps1p and Pex10p were raised in rabbit against their amino- and carboxyl-terminal peptides MDKELISTVNKLQDALA and CRQGVREQNLLPIR, respectively. Anti-Vps1p and anti-Pex10p antibodies were made at the "Open Biosystems" Company.

The initial step in the subcellular fractionation of YPBO-grown cells included the

differential centrifugation of lysed and homogenized spheroplasts at 1,000 x *g* for 8 min at 4°C in a rotor (model JS13.1; Beckman Instrs., Inc., Palo Alto, CA) to yield a postnuclear supernatant (PNS) fraction. The PNS fraction was further subjected to differential centrifugation at 20,000 x *g* for 30 min at 4°C in a rotor (model JS13.1; Beckman Instrs.) to yield pellet (20KgP) and supernatant (20KgS) fractions. The 20KgS fraction was further subfractionated by differential centrifugation at 200,000 x *g* for 1 h at 4°C in a rotor (model TLA120.2; Beckman Instrs., Inc.) to yield pellet (200KgP) and supernatant (200KgS) fractions.

To purify mature peroxisomes P6, the 20 KgP was further fractionated by flotation on a two-step sucrose gradient. Specifically, the 20 KgP was resuspended in 400 µl of 60% (wt/wt) sucrose in buffer H (5 mM MES, pH 5.5, 1 mM KCl, 0.5 mM EDTA, 0.1% [vol/vol] ethanol), overlaid with 2.3 ml of 50% (wt/wt) sucrose and 2.3 ml of 20% (wt/wt) sucrose (both in buffer H), and subjected to centrifugation in a rotor (model SW50.1; Beckman Instrs.) at 200,000 x *g* for 18 h at 4°C. Gradients were fractionated from the bottom, and 18 fractions of ~270 µl each were collected. To further purify mature peroxisomes P6, 4 vol of 0.5 M sucrose in buffer H were added to the peak peroxisomal fraction 4 recovered after isopycnic centrifugation on a discontinuous sucrose gradient. Peroxisomes were sedimented through a 150-µl cushion of 2 M sucrose in buffer H by centrifugation at 200,000 x *g* for 20 min at 4°C in a TLA120.2 rotor. The resultant pellet was resuspended in buffer H containing 1 M sorbitol and was subjected to further centrifugation on a linear 20-60% (wt/wt) sucrose gradient (in buffer H) at 197,000 x *g* for 18 h at 4°C in a rotor (model SW41Ti; Beckman Instrs., Inc.). Peak

peroxisomal fraction 5 equilibrating at a density of 1.21 g/cm^3 was recovered, and purified mature peroxisomes were pelleted at 200,000 x *g* for 20 min at 4°C in a TLA120.2 rotor, as described above. Pelleted peroxisomes were resuspended in 400 µl of 60% (wt/wt) sucrose in buffer H and subjected to flotation on a three-step sucrose gradient as described above. Peak peroxisomal fraction 4 was recovered and used for biochemical analyses. Peroxisomes isolated by this multistep method were greater than 97% pure, as judged by the presence of marker proteins of other organelles.

To purify immature peroxisomes P1 to P5, a 200,000-*g* pellet fraction (200KgP) was subjected to centrifugation on a discontinuous sucrose (18, 25, 30, 35, 40, and 53%, wt/wt) gradient at 120,000 x *g* for 18 h at 4°C in a Beckman SW28 rotor. 36 fractions of 1 ml each were collected. Fractions containing different subforms of immature peroxisomes were recovered, and 4 vol of 0.5 M sucrose in buffer H (5 mM MES, pH 5.5, 1 mM KCl, 0.5 mM EDTA, 0.1% ethanol, and a mixture of protease inhibitors) were added. Immature peroxisomes were pelleted onto a 150-µl cushion of 2 M sucrose in buffer H by centrifugation at 200,000 x *g* for 20 min at 4°C in a Beckman TLA120.2 rotor. Individual pellets of different subforms of immature peroxisomes were resuspended in 3 ml of 50% (wt/wt) sucrose in buffer H.

For purification of immature peroxisomes P1 and P2, pellets of P1 and P2 resuspended in 50% (wt/wt) sucrose in buffer H were overlaid with 30, 28, 26, 24, 22, and 10% sucrose (all wt/wt in buffer H). After centrifugation at 120,000 x *g* for 18 h at 4°C in a SW28 rotor, 18 fractions of 2 ml each were collected. P1 and P2 were pelleted, resuspended and subjected to a second flotation on the same multistep sucrose gradient.

Gradients were fractionated into 2-ml fractions as above, and P1 and P2 were recovered and pelleted.

For purification of immature peroxisomes P3 and P4, pellets of P3 and P4 resuspended in 50% (wt/wt) sucrose in buffer H were overlaid with 38%, 35%, 33% and 20% sucrose (all wt/wt in buffer H). After centrifugation at 120,000 x *g* for 18 h at 4°C in a SW28 rotor, 18 fractions of 2 ml each were collected. P3 and P4 were pelleted, resuspended in 3 ml of 50% (wt/wt) sucrose in buffer HE (20 mM MES, pH 5.5, 20 mM EDTA, 0.1% ethanol), overlaid with 39, 37, 35, 33, and 20% sucrose (all wt/wt in buffer HE), and subjected to centrifugation as above. Gradients were fractionated into 2-ml fractions, and P3 and P4 were recovered and pelleted. After resuspension in 3 ml of 50% (wt/wt) sucrose in buffer H, P3 and P4 were again subjected to flotation on the second multistep sucrose gradient described above. Gradients were fractionated into 2-ml fractions, and P3 and P4 were recovered and pelleted.

For electron microscopy, whole cells were fixed in 1.5% $KMnO_4$ for 20 min at room temperature, dehydrated by successive incubations in increasing concentrations of ethanol, and embedded in TAAB 812 resin (Marivac, Halifax, Nova Scotia, Canada). Ultrathin sections were cut using an Ultra-Cut E Microtome (Reichert-Jung) and examined in a Phillips 410 electron microscope. For morphometric analysis of random electron microscopic sections of cells, 12 × 14-cm prints and 8 × 10-cm negatives of 35-40 cell sections of each strain at 24,000-29,000 magnification were scanned and converted to digitized images with an HP Scanjet 4400c scanner and Adobe Photoshop

6.0 software. Quantitation of digitized images was performed using NIH Image 1.55 software (National Institutes of Health, Bethesda, MD). Relative area of peroxisome section (%) was calculated as "area of peroxisome section/area of cell section × 100". Peroxisomes were counted in electron micrographs, and data are expressed as the number of peroxisomes per μm^3 of cell section volume.

6.4 Results

The *Saccharomyces cerevisiae* dynamin-like protein Vps1p is essential for peroxisome division [25, 99, 208, 209]. Vps1p is a member of the dynamin protein superfamily of large GTPases that carry out a broad range of functions including organelle division and fusion, budding of transport vesicles, and cytokinesis [88, 92, 210-218]. Akin to its *S. cerevisiae* counterpart, *Y. lipolytica* Vps1p is required for peroxisome division. In fact, lack of Vps1p resulted in a reduced number of greatly enlarged peroxisomes in *Y. lipolytica* cells (Figure 6.1, panels A and B). Like most peroxisomes of wild-type cells, the majority of peroxisomes of *vps1KO* mutant cells could be pelleted by centrifugation at 20,000 x *g* (C. Gregg and V. Titorenko, unpublished data). These 20,000-g pelletable peroxisomes of *vps1KO* cells were very similar to mature peroxisomes purified from wild-type cells in regards to buoyant density, spectra of matrix and membrane proteins, and lipid composition of their membranes (C. Gregg and V. Titorenko, unpublished data). Data from morphometric analysis of random electron sections further confirmed that lack of Vps1p impairs the ability of completely assembled peroxisomes to divide, resulting in fewer, but greatly enlarged, mature peroxisomes (Figure 6.1, panels C, D and E).

S. cerevisiae Vps1p is mainly a cytosolic protein [219]. It can also be found in a

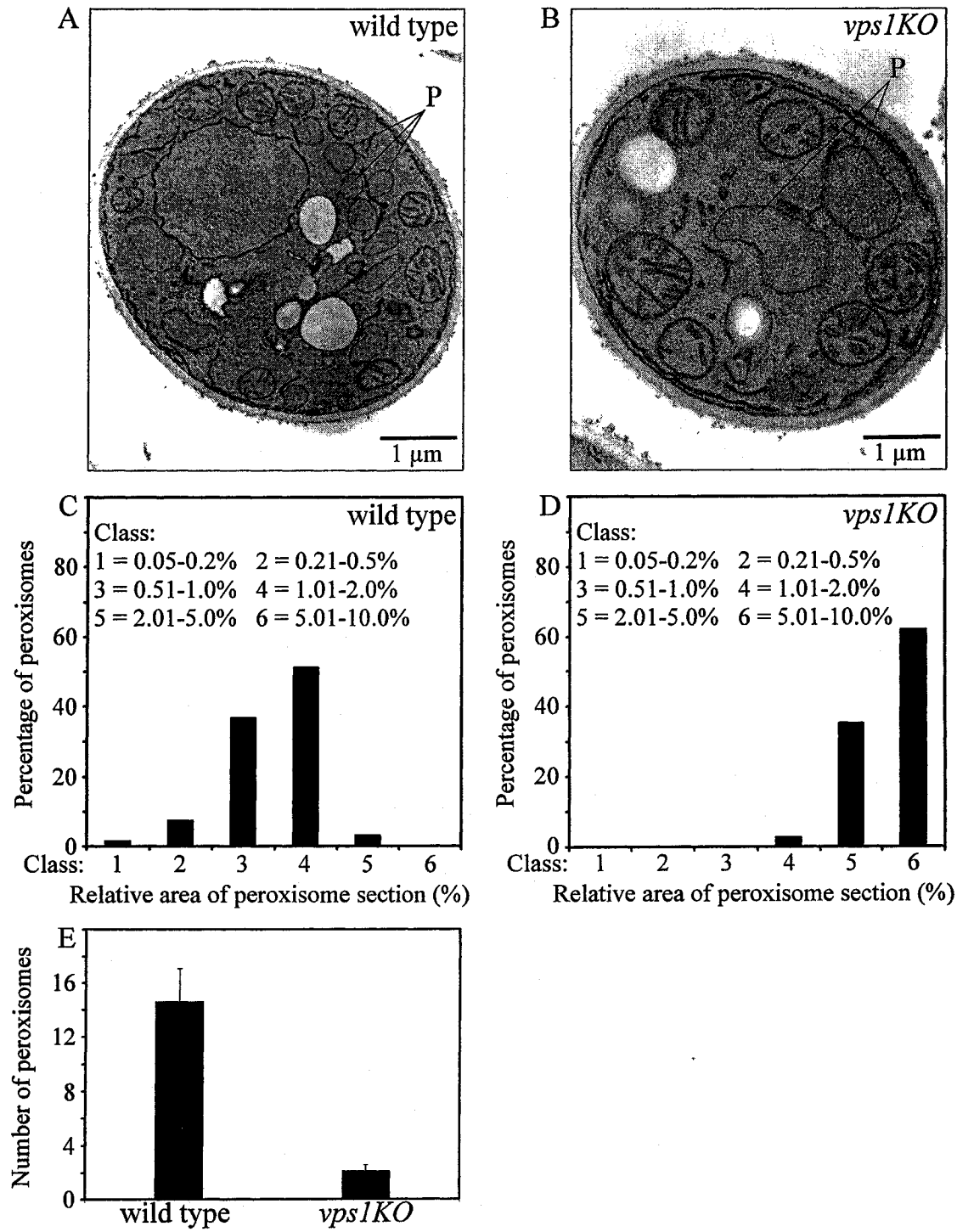

Figure 6.1. Lack of Vps1p greatly increases the size and dramatically reduces the number of peroxisomes. (A and B) Transmission electron micrographs of the wild-type and *vps1KO* strains grown for 9 h in oleic acid-containing medium. P, peroxisome. Bar, 1 μm. (C and D) Percentage of peroxisomes having the

indicated relative area of peroxisome section. The relative area of peroxisome section was calculated as (area of peroxisome section/area of cell section) × 100. (E) Numbers of peroxisomes. The data of morphometric analysis are expressed as the number of peroxisomes per μm^3 of cell section.

variety of cellular locations, including the Golgi and post-Golgi compartments [220], peroxisomes [99] and vacuoles [219]. Likewise, most of *Y. lipolytica* Vps1p localized to the cytosol, whereas the minor portion of this protein was associated with both low-speed (20,000 x *g*) and high-speed (200,000 x *g*) pelletable organelles (Figure 6.2 A). Using highly purified peroxisomal subforms of wild-type cells, we found that Vps1p was only present in mature peroxisomes (Figure 6.2 B). These peroxisomes are able to divide (see Chapters 2, 3 and 4). In contrast, the division-incompetent immature peroxisomal vesicles P1 to P5 lacked Vps1p (Figure 6.2 B). The P6-associated form of Vps1p is a peripheral membrane protein. In fact, it was solubilized completely by either 1 M NaCl or 0.1 M Na_2CO_3 (pH 11.0), whereas the peroxisomal integral membrane protein Pex2p was not (Figure 6.2 C). Furthermore, protease protection experiments revealed that Vps1p of mature peroxisomes was sensitive to trypsin digestion even in the absence of the detergent Triton X-100, whereas the membrane-enclosed protein thiolase was resistant to digestion by external protease added to intact peroxisomes (Figure 6.2 D). Taken together, these data provide evidence that the conversion of P5 to P6 in wild-type cells is marked by the recruitment of Vps1p from the cytosol to the outer face of mature peroxisomes.

Importantly, Vps1p was bound to the division-competent mature peroxisomes of wild-type or *aox1KO*, *aox2KO* and *aox3KO* mutant strains (Figure 6.2 E). In the membranes of mature peroxisomes of all these strains, LPA was converted to PA and

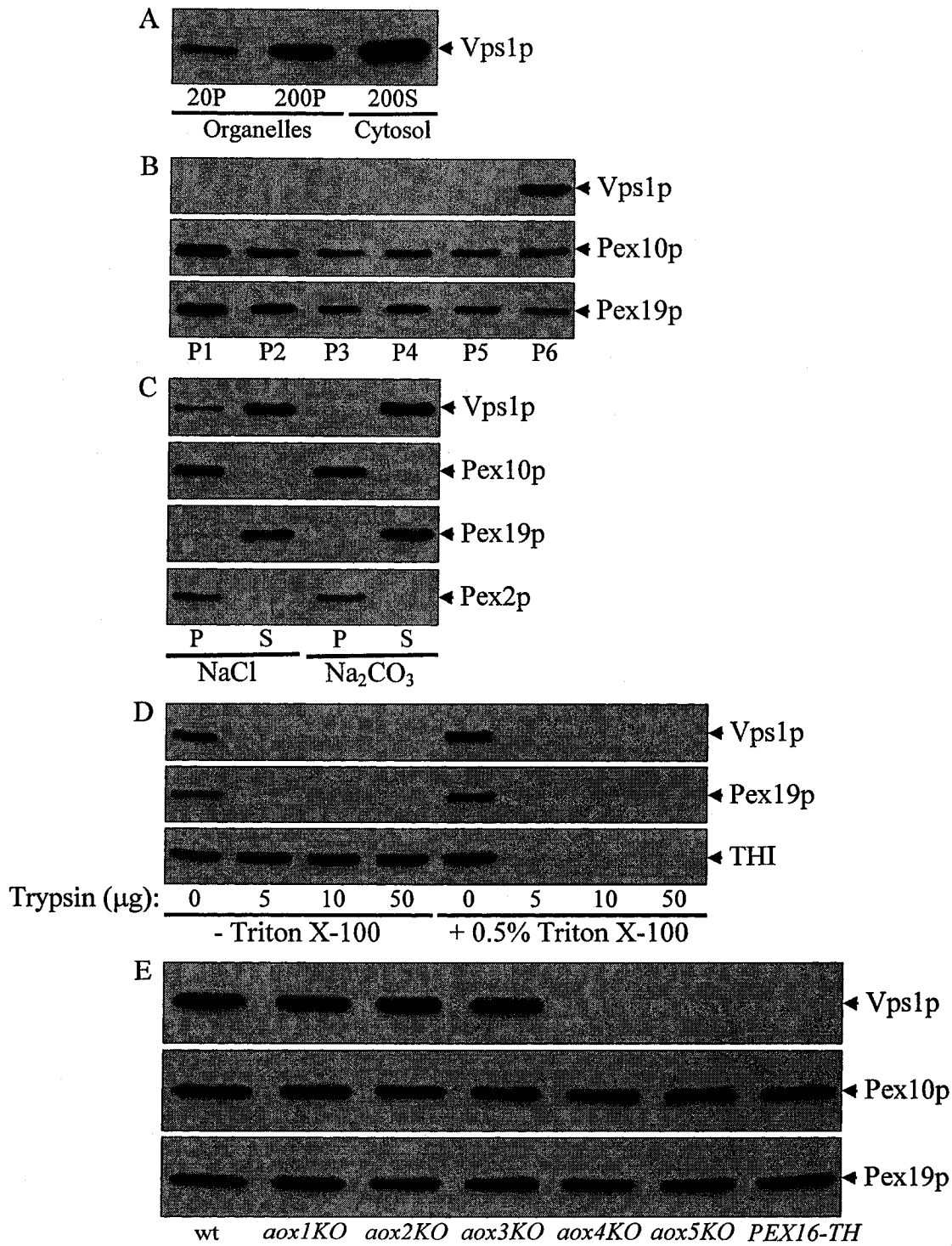

Figure 6.2. Only division-competent mature peroxisomes recruit Vps1p from the cytosol to the outer face of their membrane. (A) Wild-type cells were subjected to subcellular fractionation to yield low-speed (20,000 x *g*) and high-speed (200,000 x *g*) pelletable organellar fractions (20P and 200P, respectively). Cytosol was recovered as a supernatant fraction (200S) following centrifugation at 200,000 x *g*. Equal

portions of organellar and cytosolic fractions were separated by SDS-PAGE and analyzed by immunoblotting with anti-Vps1p antibodies. (B) Peroxisomal subforms P1 to P6 were purified from wild-type cells. Equal quantities (20 μg) of protein from these peroxisomes were analyzed by immunoblotting with antibodies to Vps1p, Pex10p and Pex19p. (C) Mature peroxisomes were purified from wild-type cells. Equal aliquots (20 μg of total protein) of these peroxisomes were treated with either 1 M NaCl or 0.1 M Na_2CO_3, pH 11.0. After incubation on ice for 30 min, samples were separated into supernatant (S) and pellet (P) fractions by centrifugation and then immunoblotted with antibodies to Vps1p, Pex10p, Pex19p and Pex2p. (D) Mature peroxisomes were purified from wild-type cells. Equal aliquots (20 μg of total protein) of these peroxisomes were treated with the indicated amounts of trypsin in the absence (-) or presence (+) of 0.5% (vol/vol) Triton X-100 for 30 min on ice. Samples were subjected to SDS-PAGE and immunoblotting with antibodies to Vps1p, Pex19p and thiolase (THI). (E) Mature peroxisomes were purified from wild-type and mutant cells. Equal quantities (20 μg) of protein from these peroxisomes were analyzed by immunoblotting with the indicated antibodies.

DAG (Figure 5.5). In contrast, Vps1p was not attached to mature peroxisomes of *aox4KO*, *aox5KO* or *PEX16-TH* mutant strains (Figure 6.2 E). All these strains are deficient in the division of mature peroxisomes (see Chapters 2, 3 and 4), being unable to convert LPA to PA and DAG in the peroxisomal membrane (Figure 5.1 and Figure 5.5). These findings strongly suggest that the recruitment of Vps1p from the cytosol to the outer face of mature peroxisomes relies on the Pex16p/Aox-dependent biosynthesis of PA and/or DAG in their membranes.

6.5 Discussion

Data presented in Figure 6.1 provide evidence that the *Y. lipolytica* dynamin-like protein Vps1p is essential for the division of mature peroxisomes. In fact, lack of this protein impairs the ability of completely assembled peroxisomes to divide, resulting in fewer, but greatly enlarged, mature peroxisomes. Thus, similar to the process of peroxisome division in the yeast *S. cerevisiae* [25, 99, 208, 209], the division of mature peroxisomes in *Y. lipolytica* depends on Vps1p. I found that, similar to its *S. cerevisiae* counterpart [219], the *Y. lipolytica* Vps1p is mainly a cytosolic protein (Figure 6.2). Furthermore, as findings reported in Figures 6.2 imply, the formation of the Aox/Pex16p complex at the

inner (lumenal) face of the mature peroxisome and the resulting biosynthesis of PA and/or DAG in the inner (lumenal) leaflet of its membrane trigger the recruitment of Vps1p from the cytosol to the surface of mature peroxisomes. Such promoted from inside of an organelle recruitment of Vps1p from the cytosol to the organelle surface has not been reported before. This novel mechanism for the docking of Vps1p to the outer face of the division-competent mature peroxisome in response to a signal emanated from its lumen provides further support for the notion that the process of peroxisome division is highly organized in space and time.

6.6 Conclusions

Taken together, the data presented in Chapter 6 strongly suggest that the biosynthesis of PA and/or DAG in the inner (lumenal) leaflet of the peroxisomal membrane at the final step of the peroxisome assembly pathway promotes the recruitment of Vps1p, a member of the dynamin protein superfamily of large GTPases, from the cytosol to the surface of the mature peroxisome. The attachment of Vps1p to the outer face of the mature peroxisome is mandatory for executing the membrane scission event that results in peroxisome division.

7 The recruitment of Vps1p to the peroxisomal membrane results in the formation of a multiprotein complex that includes proteins regulating actin cytoskeleton dynamics

7.1 Abstract

Immunoaffinity purification of Vps1p from the membrane of mature peroxisomes pre-treated with a thiol-cleavable cross-linker revealed the existence of a Vps1p-containing

complex on the outer face of this membrane. The following 6 components of this complex were identified by mass spectrometry: 1) Vps1p, a dynamin-like GTPase that is required for the division of mature peroxisomes; 2) Sla1p, a protein that regulates actin cytoskeleton organization and dynamics; 3) Abp1p, a protein that promotes F-actin assembly; 4) Act1p, a structural constituent of actin cytoskeleton in yeast; 5) the peroxin Pex19p, a protein required for the import and/or membrane assembly of numerous PMPs; and 6) the peroxin Pex10p, an integral PMP required for peroxisomal matrix protein import. I found that that the Vps1p-containing complex on the outer face of mature peroxisomes is formed in a series of spatially and temporally distinct steps. The initial step involves the recruitment of Pex19p from the cytosol to the peroxisomal membrane during the early steps of the peroxisome assembly pathway. The attachment of Pex19p to the peroxisomal membrane requires its docking factor, Pex10p. The membrane-bound form of Pex19p, but not its cytosolic form, is mandatory for the attachment of the Vps1p-Sla1p-Abp1p complex, which is pre-formed in the cytosol, to the outer face of mature peroxisomes. Only after it has been attached to the membrane of mature peroxisomes, the Vps1p-Sla1p-Abp1p complex is able to interact with Act1p, thereby promoting the recruitment of actin to the outer face of division-competent mature peroxisomes.

7.2 Introduction

Data presented in Chapter 6 provided evidence that the dynamin-like protein Vps1p is essential for the division of mature peroxisomes. I also found that the conversion of P5 to P6 in wild-type cells is marked by the recruitment of Vps1p from the cytosol to the surface of mature peroxisomes. I thought that it would be interesting to see whether

Vps1p is attached to the outer face of the mature peroxisome alone or whether it forms a complex with any of the protein constituents of the peroxisomal membrane. I decided to address this question by first exposing the membrane of mature peroxisomes to a thiol-cleavable cross-linker that could covalently link Vps1p to any of its interacting protein partner(s). I was planning to immunoprecipitate then these membrane proteins with anti-Vps1p antibodies under denaturing, nonreducing conditions. The cross-linker could then be cleaved with a reducing agent and the immunoprecipitated proteins could be resolved electrophoretically under reducing conditions. Any proteins other than Vps1p detected in the gel by silver staining could be identified using mass spectrometry.

7.3 Materials and methods

The *Y. lipolytica* wild-type strain *P01d* (*MatA ura3-302 leu2-270 xpr2-302*) [176], the mutant strains *vps1KO* (*MatA ura3-302 leu2-270 xpr2-3 vps1::URA3*), [177], *pex10KO* (*MatA ura3-302 leu2-270 xpr2-3 pex10::URA3*) [123], *pex16-TH* (*MatA ura3-302::PEX16TH-URA3 leu2-270 xpr2-3 pex16-1*) [123] and *pex19KO* (*MatA ura3-302 leu2-270 xpr2-3 pex19::LEU2*) [180], and the single *AOX* gene knock-out strains *aox1KO* (*MatA ura3-302 leu2-270 xpr2-3 aox1::URA3*), *aox2KO* (*MatA ura3-302 leu2-270 xpr2-3 aox2::URA3*), *aox3KO* (*MatA ura3-302 leu2-270 xpr2-3 aox3::URA3*), *aox4KO* (*MatA ura3-302 leu2-270 xpr2-3 aox4::URA3*) and *aox5KO* (*MatA ura3-302 leu2-270 xpr2-3 aox5::URA3*) [176] were used. Targeted integrative disruption of the *PEX10* and *VPS1* genes was performed with the *URA3* gene of *Y. lipolytica*, using a previously described modification of the sticky-end polymerase chain reaction procedure [176]. Growth was at 30°C. Yeast strains were initially grown in YPD (1% yeast extract,

2% peptone, 2% glucose) medium to an OD_{600} of ~1.5 and then shifted to YPBO (0.3% yeast extract, 0.5% peptone, 0.5% K_2HPO_4, 0.5% KH_2PO_4, 1% Brij-35, 1% [wt/ vol] oleic acid) medium to proliferate peroxisomes.

Rabbit polyclonal antibodies to the Aox1p, -3p and –5p subunits of the Aox complex [175], Pex2p [177], Pex5p [178], Pex16p [123], Pex19p [180], isocitrate lyase (ICL) [48], thiolase (THI) [178] and malate synthase (MLS) [48] have been described. Monospecific antibodies to Vps1p and Pex10p were raised in rabbit against their amino- and carboxyl-terminal peptides MDKELISTVNKLQDALA and CRQGVREQNLLPIR, respectively. Anti-Vps1p and anti-Pex10p antibodies were made at the "Open Biosystems" Company.

The initial step in the subcellular fractionation of YPBO-grown cells included the differential centrifugation of lysed and homogenized spheroplasts at 1,000 x *g* for 8 min at 4°C in a rotor (model JS13.1; Beckman Instrs., Inc., Palo Alto, CA) to yield a postnuclear supernatant (PNS) fraction. The PNS fraction was further subjected to differential centrifugation at 20,000 x *g* for 30 min at 4°C in a rotor (model JS13.1; Beckman Instrs.) to yield pellet (20KgP) and supernatant (20KgS) fractions. The 20KgS fraction was further subfractionated by differential centrifugation at 200,000 x *g* for 1 h at 4°C in a rotor (model TLA120.2; Beckman Instrs., Inc.) to yield pellet (200KgP) and supernatant (200KgS) fractions.

To purify mature peroxisomes P6, the 20 KgP was further fractionated by flotation on a three-step sucrose gradient. Specifically, the 20 KgP was resuspended in 400 µl of 60% (wt/wt) sucrose in buffer H (5 mM MES, pH 5.5, 1 mM KCl, 0.5 mM EDTA, 0.1%

[vol/vol] ethanol), overlaid with 2.3 ml of 50% (wt/wt) sucrose and 2.3 ml of 20% (wt/wt) sucrose (both in buffer H), and subjected to centrifugation in a rotor (model SW50.1; Beckman Instrs.) at 200,000 x *g* for 18 h at 4°C. Gradients were fractionated from the bottom, and 18 fractions of ~270 µl each were collected. To further purify mature peroxisomes P6, 4 vol of 0.5 M sucrose in buffer H were added to the peak peroxisomal fraction 4 recovered after isopycnic centrifugation on a discontinuous sucrose gradient. Peroxisomes were sedimented through a 150-µl cushion of 2 M sucrose in buffer H by centrifugation at 200,000 x *g* for 20 min at 4°C in a TLA120.2 rotor. The resultant pellet was resuspended in buffer H containing 1 M sorbitol and was subjected to further centrifugation on a linear 20-60% (wt/wt) sucrose gradient (in buffer H) at 197,000 x *g* for 18 h at 4°C in a rotor (model SW41Ti; Beckman Instrs., Inc.). Peak peroxisomal fraction 5 equilibrating at a density of 1.21 g/cm^3 was recovered, and purified mature peroxisomes were pelleted at 200,000 x *g* for 20 min at 4°C in a TLA120.2 rotor, as described above. Pelleted peroxisomes were resuspended in 400 µl of 60% (wt/wt) sucrose in buffer H and subjected to flotation on a three-step sucrose gradient as described above. Peak peroxisomal fraction 4 was recovered and used for biochemical analyses. Peroxisomes isolated by this multistep method were greater than 97% pure, as judged by the presence of marker proteins of other organelles.

To purify immature peroxisomes P1 to P5, a 200,000-*g* pellet fraction (200KgP) was subjected to centrifugation on a discontinuous sucrose (18, 25, 30, 35, 40, and 53%, wt/wt) gradient at 120,000 x *g* for 18 h at 4°C in a Beckman SW28 rotor. 36 fractions of 1 ml each were collected. Fractions containing different subforms of immature

peroxisomes were recovered, and 4 vol of 0.5 M sucrose in buffer H (5 mM MES, pH 5.5, 1 mM KCl, 0.5 mM EDTA, 0.1% ethanol, and a mixture of protease inhibitors) were added. Immature peroxisomes were pelleted onto a 150-µl cushion of 2 M sucrose in buffer H by centrifugation at 200,000 x *g* for 20 min at 4°C in a Beckman TLA120.2 rotor. Individual pellets of different subforms of immature peroxisomes were resuspended in 3 ml of 50% (wt/wt) sucrose in buffer H.

For purification of immature peroxisomes P1 and P2, pellets of P1 and P2 resuspended in 50% (wt/wt) sucrose in buffer H were overlaid with 30, 28, 26, 24, 22, and 10% sucrose (all wt/wt in buffer H). After centrifugation at 120,000 x *g* for 18 h at 4°C in a SW28 rotor, 18 fractions of 2 ml each were collected. P1 and P2 were pelleted, resuspended and subjected to a second flotation on the same multistep sucrose gradient. Gradients were fractionated into 2-ml fractions as above, and P1 and P2 were recovered and pelleted.

For purification of immature peroxisomes P3 and P4, pellets of P3 and P4 resuspended in 50% (wt/wt) sucrose in buffer H were overlaid with 38%, 35%, 33% and 20% sucrose (all wt/wt in buffer H). After centrifugation at 120,000 x *g* for 18 h at 4°C in a SW28 rotor, 18 fractions of 2 ml each were collected. P3 and P4 were pelleted, resuspended in 3 ml of 50% (wt/wt) sucrose in buffer HE (20 mM MES, pH 5.5, 20 mM EDTA, 0.1% ethanol), overlaid with 39, 37, 35, 33, and 20% sucrose (all wt/wt in buffer HE), and subjected to centrifugation as above. Gradients were fractionated into 2-ml fractions, and P3 and P4 were recovered and pelleted. After resuspension in 3 ml of 50% (wt/wt) sucrose in buffer H, P3 and P4 were again subjected to flotation on the second

multistep sucrose gradient described above. Gradients were fractionated into 2-ml fractions, and P3 and P4 were recovered and pelleted.

Chemical cross-linking of peroxisome-bound proteins was performed using dithiobis(succinimidylpropionate) (DSP) (Pierce Chemical Co., Rockford, IL). Highly purified mature peroxisomes were lysed in 20 mM sodium phosphate buffer, pH 7.5, containing 150 mM NaCl. Lysates were clarified by centrifugation at 200,000 *g* for 20 min at 4°C in a rotor (model TLA120.2; Beckman Instrs., Inc.), and the resultant supernatants were used for chemical cross-linking. Sodium phosphate buffer, pH 7.5, and NaCl were added to the supernatants to final concentrations of 20 and 150 mM, respectively. Cross-linking with DSP was initiated by the addition of cross-linker (50 mM stock in DMSO) and continued for 1 h at 4°C. Cross-linking was quenched by addition of 0.1 vol of 1 M Tris-HCl, pH 7.5, and incubation for 30 min at 4°C. SDS was added to 1.25%, and samples were warmed at 65°C for 20 min and then cooled to room temperature. 4 vol of 60 mM Tris-HCl, pH 7.4, 1.25% (vol/vol) Triton X-100, 190 mM NaCl, and 6 mM EDTA were added to the cooled samples, which were then cleared of any nonspecifically binding proteins by incubation for 20 min at 4°C with protein A-Sepharose washed five times with 10 mM Tris-HCl, pH 7.5. The cleared samples were then subjected to immunoaffinity chromatography under denaturing conditions and in the absence of a reducing agent. Covalent coupling of the affinity-purified anti-Vps1p antibodies to protein A-Sepharose for immunoaffinity chromatography was performed as described previously [175]. Proteins bound to the covalently linked anti-Vps1p antibodies were washed five times with 50 mM Tris-HCl, pH 7.5, 150 mM NaCl, 1% (v/v) Triton

X-100, and eluted with 2% SDS at 95°C for 5 min. Eluted proteins were subjected to a second immunoprecipitation (recapture) step, resolved by SDS-PAGE, and visualized by silver staining [221]. Protein bands were excised from the gel, reduced, alkylated and in-gel-digested with trypsin [221]. The proteins were identified by matrix-assisted laser desorption/ionization mass spectrometric peptide mapping [222], using a Micromass M@LDI time-of-flight mass spectrometer (Waters). Database searching using peptide masses was performed with the Mascot web-based search engine. 14 peptides of a 138-kD protein that were used for the identification of Sla1p covered 17% of the protein sequence with mass accuracy better than 100 ppm over the mass to charge ratio range of 1000 to 2400. 11 peptides of a 81-kD protein that were used for the identification of Vps1p covered 23% of the protein sequence with mass accuracy better than 100 ppm over the mass to charge ratio range of 700 to 2200. 9 peptides of a 53-kD protein that were used for the identification of Abp1p covered 27% of the protein sequence with mass accuracy better than 100 ppm over the mass to charge ratio range of 800 to 2100. 10 peptides of a 47-kD protein that were used for the identification of Pex19p covered 32% of the protein sequence with mass accuracy better than 100 ppm over the mass to charge ratio range of 900 to 2300. 8 peptides of a 41-kD protein that were used for the identification of Act1p covered 29% of the protein sequence with mass accuracy better than 100 ppm over the mass to charge ratio range of 1000 to 2100. 10 peptides of a 37-kD protein that were used for the identification of Pex10p covered 38% of the protein sequence with mass accuracy better than 100 ppm over the mass to charge ratio range of 800 to 2300.

7.4 Results

To test whether Vps1p is physically associated with other components of the peroxisomal membrane, membrane proteins recovered after centrifugation of osmotically lysed mature peroxisomes of wild-type cells were treated with the thiol-cleavable cross-linker dithio-*bis*-(succinimidylpropionate) (DSP). These membrane proteins were immunoprecipitated with anti-Vps1p antibodies under denaturing, nonreducing conditions. The cross-linker was then cleaved with DTT and the immunoprecipitated proteins were resolved by SDS-PAGE under reducing conditions, followed by silver staining. A cohort of proteins was specifically co-immunoprecipitated with Vps1p under these conditions (Figure 7.1 A, lane 1), suggesting the existence of a Vps1p-containing complex on the outer face of the peroxisomal membrane. The following 6 components of this complex were identified by mass spectrometry: 1) Vps1p, a dynamin-like GTPase that is required for the division of mature peroxisomes (see Chapter 6); 2) Sla1p, a protein that regulates actin cytoskeleton organization and dynamics [223-226]; 3) Abp1p, a protein that promotes F-actin assembly [223-225, 227]; 4) Act1p, a structural constituent of actin cytoskeleton in yeast [228, 229]; 5) the peroxin Pex19p, a protein required for the import and/or membrane assembly of numerous PMPs [3, 12, 21, 180]; and 6) the peroxin Pex10p, an integral PMP required for peroxisomal matrix protein import [3, 12, 20, 21, 34, 180]. Importantly, antibodies specific to Pex10p and Pex19p, the two components of the Vps1p-containing complex, immunoprecipitated the same set of DSP-treated PMPs as anti-Vps1p antibodies did (Figure 7.1 A, compare lanes 1, 3 and 7). Thus, all Vps1p, Sla1p, Abp1p, Act1p, Pex19p and Pex10p form a single multicomponent complex, and do not compose

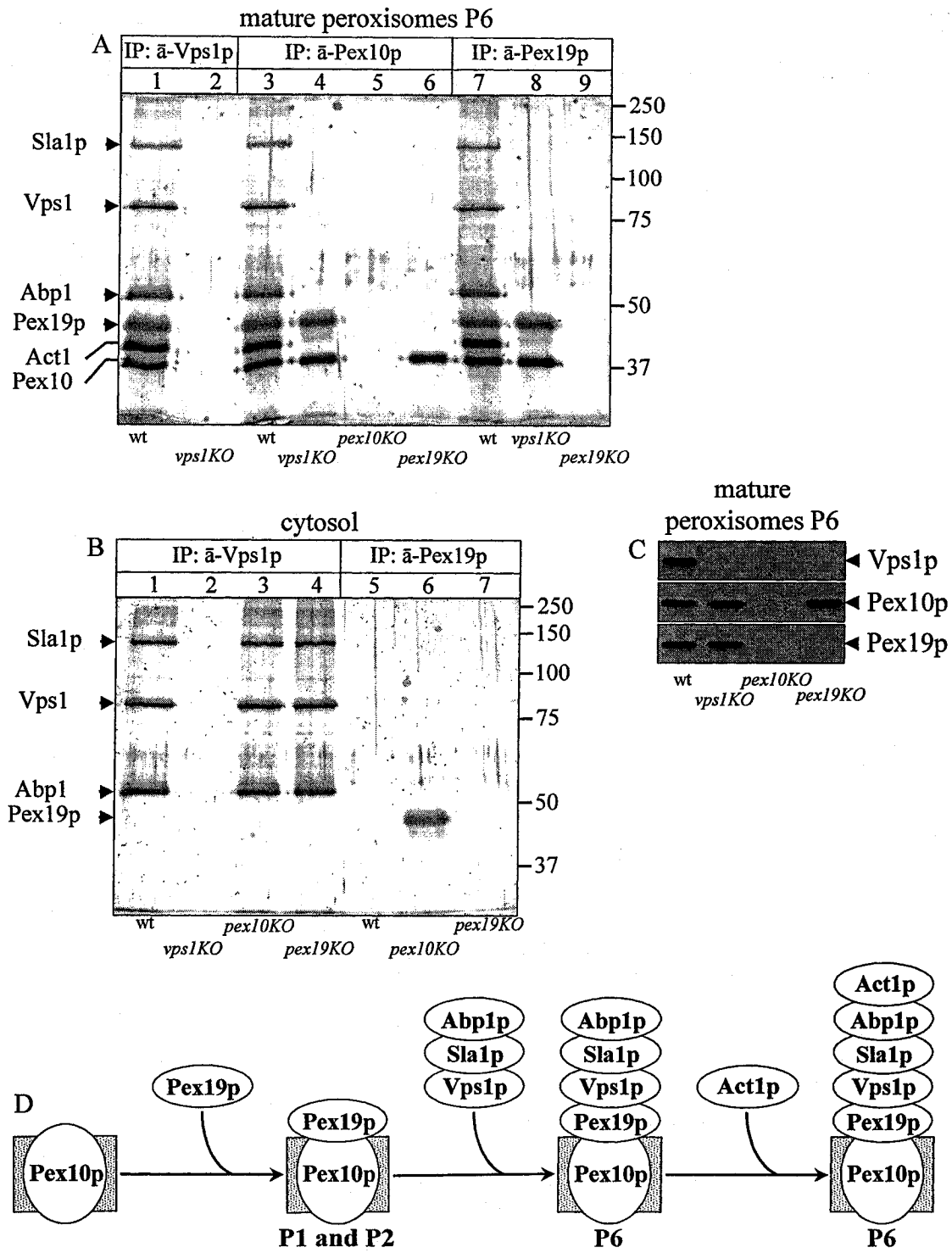

Figure 7.1. A multiprotein complex that comprises a dynamin-like GTPase, three components of actin cytoskeleton, and two peroxins is assembled only on the outer face of the division-competent mature peroxisome. (A) Highly purified mature peroxisomes of wild-type and mutant strains were osmotically

lysed and subjected to centrifugation to yield supernatant (matrix proteins) and pellet (membrane proteins) fractions. Recovered membrane proteins were treated with the thiol-cleavable cross-linker DSP. These DSP-treated membrane proteins were immunoprecipitated with anti-Vps1p, anti-Pex10p and anti-Pex19p antibodies under denaturing, nonreducing conditions. The cross-linker was then cleaved with DTT and the immunoprecipitated proteins were resolved by SDS-PAGE under reducing conditions, followed by silver staining. Arrows indicate the positions of Sla1p, Vps1p, Abp1p, Pex19p, Act1p and Pex10p, which were identified by mass spectrometry. (B) Wild-type and mutant cells were subjected to subcellular fractionation to yield the 200S (cytosolic) fraction. Cytosolic proteins were treated with the thiol-cleavable cross-linker DSP. These DSP-treated cytosolic proteins were subjected to immunoprecipitation with anti-Vps1p and anti-Pex19p antibodies under denaturing, nonreducing conditions. The cross-linker was then cleaved with DTT and the immunoprecipitated proteins were resolved by SDS-PAGE under reducing conditions, followed by silver staining. Arrows indicate the positions of Sla1p, Vps1p, Abp1p and Pex19p, which were identified by mass spectrometry. (C) Equal quantities (20 μg) of protein from highly purified mature peroxisomes of wild-type and mutant strains were analyzed by immunoblotting with antibodies to Vps1p, Pex10p and Pex19p. (D) A model for the multistep assembly of the Act1p-Abp1p-Sla1p-Vps1p-Pex19p-Pex10p complex on the cytosolic face of mature peroxisomes.

several subcomplexes formed by the association of a bait protein (Vps1p, Pex10p or Pex19p) with different subsets of interacting protein partners. It seems that not the entire pools of membrane-bound Pex10p and Pex19p are engaged in the Vps1p-containing complex. In fact, each of these two peroxins was present at a higher level among co-immunoprecipitated polypeptides when it was used as a bait protein for the immunoprecipitation, as compared to its level among co-immunoprecipitated polypeptides when Vps1p served as a bait protein (Figure 7.1 A, compare lanes 1, 3 and 7).

My findings suggest that the Vps1p-containing complex on the outer face of mature peroxisomes is formed in a series of spatially and temporally distinct steps. In fact, Vps1p was only present in mature peroxisomes P6, whereas both Pex10p and Pex19p were associated with all six peroxisomal subforms (Figure 6.2 B). Furthermore, lack of either Pex10p or Pex19p abolished the recruitment of Vps1p from the cytosol to the membrane of mature peroxisomes (Figure 7.1 C). Moreover, in the absence of Vps1p, none of the actin cytoskeleton-related components of the Vps1p-containing complex,

including Sla1p, Abp1p and Act1p, was attached to membrane-bound Pex10p and Pex19p (Figure 7.1 A, lanes 4 and 8). Taken together, these data imply that the Pex10p- and Pex19p-dependent recruitment of Vps1p from the cytosol to the outer face of the mature peroxisome is mandatory for the attachment of Sla1p, Abp1p and Act1p to this division-competent peroxisomal subform.

It seems that Vps1p, Sla1p and Abp1p initially form a complex in the cytosol. This complex is then targeted from the cytosol to the outer face of mature peroxisomes. Only after its binding to mature peroxisomes, the Vps1p-Sla1p-Abp1p complex is able to interact with Act1p, thereby promoting the attachment of actin to the peroxisomal membrane. In fact, both Sla1p and Abp1p, but not Act1p, co-immunoprecipitated with Vps1p from the DSP-treated cytosolic fractions of wild-type, *pex10Δ* and *pex19Δ* cells (Figure 7.1 B, lanes 1, 3 and 4). In contrast, the membrane-bound form of Act1p could be co-immunoprecipitated with all three components of the Vps1p-Sla1p-Abp1p complex only if these components are attached to the outer face of mature peroxisomes (Figure 7.1 A, lanes 1, 3 and 7).

Both Pex10p and Pex19p are required for the recruitment of Vps1p from the cytosol to the membrane of mature peroxisomes (Figure 7.1 C) and, therefore, for the docking of the cytosolic Vps1p-Sla1p-Abp1p complex to the outer face of these peroxisomes (Figure 7.1 A, lanes 4 and 8, and Figure 7.1 B, lanes 3 and 4). Pex10p is an integral PMP that could not be stripped off the peroxisomal membrane by either 1 M NaCl or 0.1 M Na_2CO_3 (pH 11.0) (Figure 6.2 C). On the contrary, Pex19p is a peripheral membrane protein on the outer face of peroxisomes that could be solubilized by either 1

M NaCl or 0.1 M Na_2CO_3 (pH 11.0) and was sensitive to digestion by external protease added to intact peroxisomes (Figure 6.2, panels C and D). Pex10p and Pex19p form a complex in the membrane of mature peroxisomes (Figure 7.1 A, lanes 4 and 8) and immature peroxisomal vesicles P1 to P5 (C. Gregg and V. Titorenko, unpublished data). Thus, the Pex10p-Pex19p complex assembles in the peroxisomal membrane during the initial steps of the peroxisome assembly pathway. The attachment of Pex19p to the peroxisomal membrane requires Pex10p. In fact, lack of Pex10p abolished the recruitment of Pex19p from the cytosol to the peroxisome (Figure 7.1 C). Of note, Pex19p that was accumulated in the cytosol of *pex10KO* cells did not co-immunoprecipitate with Vps1p, Sla1p, Abp1p or Act1p (Figure 7.1 B, lane 6). Furthermore, the Vps1p-Sla1p-Abp1p complex could be formed even in the cytosol of *pex19KO* cells (Figure 7.1 B, lane 4). These findings support the notion that, while cytosolic Pex19p is not required for the assembly of the Vps1p-Sla1p-Abp1p complex prior to its recruitment to the membrane, the membrane-bound form of Pex19p is mandatory for the attachment of the pre-formed Vps1p-Sla1p-Abp1p complex to the outer face of mature peroxisomes.

7.5 Discussion

Data presented in Figure 7.1 provide evidence that the dynamin-like GTPase Vps1p on the outer face of the mature peroxisome form a complex with 5 other proteins. I identify the following 5 interacting partners of Vps1p: 1) the Sla1p protein regulating actin cytoskeleton organization and dynamics; 2) the Abp1p protein promoting F-actin assembly; 3) the Act1p component (actin 1) of actin cytoskeleton in yeast; 4) the Pex19p

protein required for the import and/or membrane assembly of numerous PMPs; and 5) the Pex10p protein acting in peroxisomal matrix protein import. Furthermore, as findings reported in Figures 7.1 imply, the assembly of the Pex10p-Pex19p-Vps1p-Sla1p-Abp1p-Act1p complex is a dynamic process that includes several consecutive steps. It seems that during the first step of this process, Pex19p docks to the outer face of one of the earliest intermediates in the peroxisome assembly pathway by interacting with the peroxin Pex10p. In addition, my data show that only after being recruited to the outer face of the peroxisomal membrane Pex19p can interact with the Vps1p-Sla1p-Abp1p complex, which is pre-formed in the cytosol. Finally, my findings provide evidence that the formation of the Pex10p-Pex19p-Vps1p-Sla1p-Abp1p complex on the outer face of the mature peroxisome is a prerequisite for the recruitment of the structural component Act1p of actin cytoskeleton.

7.6 Conclusions

In summary, my data suggest that the assembly of the Vps1p-Sla1p-Abp1p complex in the cytosol precedes its attachment to the outer face of division-competent mature peroxisomes (Figure 7.1 D). The Vps1p-Sla1p-Abp1p complex binds to mature peroxisomes by interacting with Pex19p, a component of the Pex10p-Pex19p complex that is formed in the peroxisomal membrane during the earliest steps of peroxisome assembly and maturation (Figure 7.1 D). Only after it has been attached to the membrane of mature peroxisomes, the Vps1p-Sla1p-Abp1p complex is able to interact with Act1p, thereby promoting the recruitment of actin to the outer face of division-competent peroxisomes.

8 Conclusions and suggestions for future work

8.1 General conclusions

8.1.1 Mechanism of peroxisome division

Taken together, my findings presented in Chapters 2 to 7 suggest the following model for peroxisome division (Figure 8.1). In immature peroxisomal vesicles P1 to P5, Pex16p binds LPA in the inner (lumenal) leaflet of the peroxisomal membrane. The binding of Pex16p to LPA prevents the biosynthesis of PA and DAG in a two-step pathway, which includes two consecutive enzymatic reactions catalyzed by an LPAAT and a PAP (Figure 5.1 D). The stepwise import of distinct subsets of matrix proteins into immature peroxisomal vesicles P1 to P5 provides them with an increasing fraction of the matrix proteins present in mature peroxisomes. This increase in the total mass of matrix proteins above a critical level causes the redistribution of Aox from the matrix to the membrane. A significant redistribution of Aox occurs only in mature peroxisomes. Overloading these peroxisomes with matrix proteins other than Aox, thereby creating the effect of "molecular crowding" [230], is a major factor in the observed redistribution of Aox from the matrix to the membrane. Inside mature peroxisomes, Aox interacts with Pex16p. This interaction between Aox and Pex16p greatly decreases the affinity between Pex16p and LPA, thereby allowing LPA to enter the two-step biosynthetic pathway leading to the formation of PA and DAG. The glycerophospholipid PC, which is transferred to the peroxisomal membrane from the P3- and P4-associated subcompartment of the ER, activates both the LPAAT and PAP reactions in this pathway. The resulting accumulation of PA and DAG in the lumenal leaflet of the membrane of mature peroxisomes triggers a

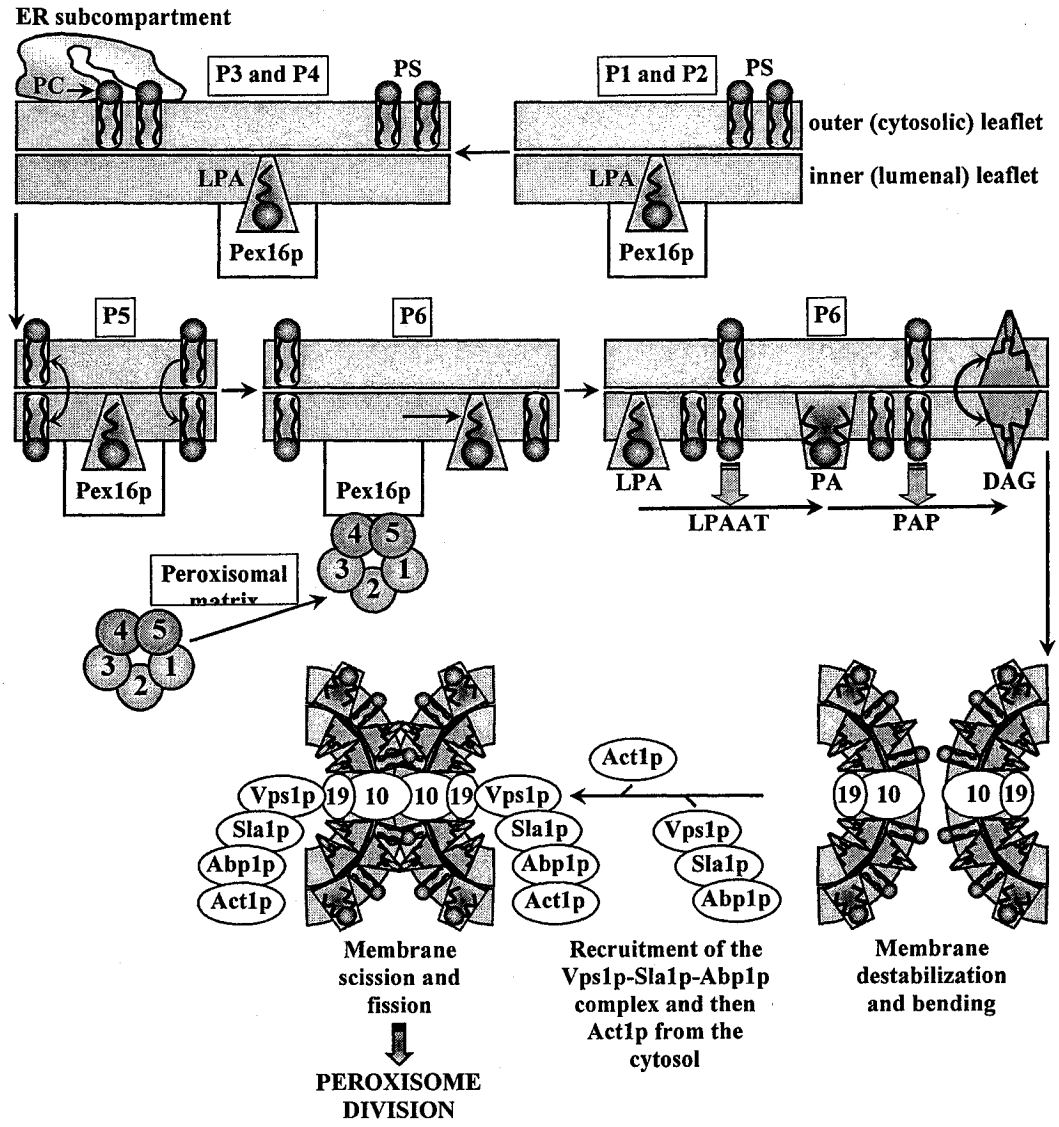

Figure 8.1. The Pex16p- and Aox-dependent intraperoxisomal signaling cascade drives the division of mature peroxisomes P6 by promoting the stepwise remodeling of lipid and protein composition of the peroxisomal membrane.

cascade of events ultimately leading to peroxisome division. This cascade of events is initiated by the spontaneous flipping of DAG, which is known for its very fast transbilayer translocation [136, 148, 172-174], between the two membrane leaflets. The movement of DAG, a particularly potent cone-shaped inducer of negative monolayer

curvature and membrane bending [154, 155, 172-174], from the lumenal to the cytosolic leaflet of the membrane bilayer coincides with the translocation of the glycerophospholipid PS in the opposite direction. This bi-directional movement of DAG and PS generates a lipid imbalance across the bilayer, thereby promoting the destabilization and bending of the membrane. The biosynthesis of PA and DAG in the membrane of mature peroxisomes and, perhaps, the bending of the membrane due to the bi-directional transbilayer movement of DAG and PS promote the docking of the Vps1p-Sla1p-Abp1p complex to the outer face of mature peroxisomes. This pre-assembled in the cytosol protein complex binds to mature peroxisomes by interacting with the peroxin Pex19p. Pex19p is a component of the Pex10p-Pex19p complex that is formed in the peroxisomal membrane during the earliest steps of peroxisome assembly (Figure 7.1 D). After its attachment to the peroxisomal membrane, the Vps1p-Sla1p-Abp1p complex interacts with Act1p, thereby recruiting this structural constituent of actin cytoskeleton to the cytosolic face of mature peroxisomes. The subsequent scission and fission of the peroxisomal membrane lead to peroxisome division.

It remains to be established how exactly Vps1p promotes peroxisome division. It seems unlikely that this dynamin-like GTPase acts only as a mechanochemical enzyme [217, 231] whose GTPase activity provides the mechanical force required for the scission of the peroxisomal membrane in the constricted neck. In fact, prior to its binding to the peroxisomal membrane, Vps1p interacts in the cytosol with Sla1p and Abp1p, two proteins that regulate actin cytoskeleton organization and dynamics (Figure 7.1). Furthermore, Vps1p is needed for the targeting of the Vps1p-Sla1p-Abp1p protein

complex from the cytosol to the outer face of mature peroxisomes, were it binds to Pex19p. Moreover, the Vps1p- and Pex19p-dependent docking of the Vps1p-Sla1p-Abp1p complex to mature peroxisomes is mandatory for the subsequent attachment of actin (Act1p) to the surface of these peroxisomes. Therefore, I believe that Vps1p may function as a regulatory GTPase [216, 232, 233] whose GTP-bound form promotes the multistep assembly of the membrane fission machinery, initially in the cytosol and then on the surface of division-competent mature peroxisomes. This machinery includes the Sla1p, Abp1p and Act1p components of actin cytoskeleton. It remains to be seen whether actin binds to mature peroxisomes in the monomeric G form or in its filamentous F form.

8.1.2 Organelle division machineries can be turned on in response to signals transmitted from inside or outside the organelle

My findings described in Chapters 2 to 7 define an unusual mechanism that turns on the multicomponent machinery serving peroxisome division. This mechanism acts through the Pex16p- and Aox-dependent intraperoxisomal signaling cascade. The cascade is turned off inside immature peroxisomal vesicles (Figure 8.1). Lack of membrane-bound Aox in these vesicles allows Pex16p to sequester LPA in the peroxisomal membrane, thereby preventing its conversion to PA and DAG. In the absence of these two potent lipid inducers of membrane fission, the entire peroxisome division machinery remains inactive in the membranes of immature peroxisomal vesicles. The Pex16p- and Aox-dependent signaling cascade is activated only inside mature peroxisomes, due to the redistribution of Aox from the matrix to the membrane and its specific binding to Pex16p. The resulting release of LPA from Pex16p makes this lipid available for the

conversion to PA and DAG, the two cone-shaped lipids that initiate the stepwise assembly of the multicomponent peroxisome division machinery on the cytosolic face of the membrane. This ultimately leads to the division of mature, metabolically active peroxisomes. Thus, the Pex16p- and Aox-dependent cascade for fine-tuning the fission of peroxisomal membrane is an intrinsic feature of the multistep peroxisome biogenesis program. It is tempting to speculate that this program has been evolved in order to separate the dramatic changes in the composition and architectural design of the membrane bilayer, all of which occur during peroxisome division (Figure 8.1), from the highly organized process of protein translocation across this bilayer, which takes place during peroxisome assembly. One of the benefits of employing such strategy for the temporal separation of the processes of peroxisome assembly and division is that some of the membrane components can efficiently function in both processes. In fact, the peroxins Pex10p and Pex19p known for their essential role in peroxisomal import of numerous matrix proteins and PMPs [3, 12, 20, 21, 34, 180] are also required for the assembly of the peroxisome division machinery on the cytosolic face of mature peroxisomes (see Chapter 7).

A different mechanism for activating the organelle division machinery is used for the fission of Golgi membranes during mitosis. This mechanism initiates Golgi membrane fission in response to a signal transmitted from outside the organelle. During interphase, the Golgi matrix proteins on the cytosolic face of the membrane cross-link Golgi cisternae into stacks [234-236]. Phosphorylation of the matrix proteins GRASP55, GRASP65 and GM130 during mitosis promotes the disassembly of these stacks into a

tubular network [237-240]. This, in turn, greatly increases the accessibility of Golgi membranes to the protein CtBP3/BARS [94, 96]. After being recruited from the cytosol to the outer face of Golgi tubules, CtBP3/BARS drives fission of Golgi membranes, thereby fragmenting Golgi tubular networks into clusters of small vesicles and tubules [94, 96, 171]. Importantly, akin to the LPAAT that promotes peroxisome division (Figure 8.1), CtBP3/BARS catalyzes the conversion of LPA to PA [171]. Furthermore, this enzymatic activity of CtBP3/BARS is essential for the fission of Golgi membranes during mitosis [94, 96, 171], just like the acyltransferase activity of peroxisomal LPAAT is required for peroxisome division (see Chapters 5, 6 and 7). It remains to be established whether, similar to peroxisomal LPAAT, CtBP3/BARS can facilitate the assembly of other components of the membrane fission machinery on the cytosolic face of the membrane. Of note, a version of CtBP3/BARS that lacks the acyltransferase activity can still promote the fission of Golgi membranes, although much less efficiently [96]. Thus, even enzymatically inactive CtBP3/BARS may function in facilitating the recruitment and/or proper assembly of other proteins required for mitotic Golgi fragmentation [96]. Altogether, these findings suggest that, even though the mechanisms responsible for initiating the fission of the peroxisomal membrane during interphase and of the Golgi membrane during mitosis are quite different, these mechanisms can employ the peroxisomal- and cytosolic/Golgi-specific forms of LPAAT, respectively, as their direct downstream effectors. Thus, the peroxisome and the Golgi apparatus, the two organelles that derive from the endoplasmic reticulum (ER) as distinct branches of the secretory pathway [47-54], may employ at least one functionally similar component, an LPAAT,

during the early stage of their division.

The release of Ca^{2+} from the ER and concurrent uptake of Ca^{2+} into mitochondria trigger the multistep assembly of the mitochondrial division machinery during apoptosis [241-243]. The earliest recognizable event in this assembly pathway, which is induced in response to an extramitochondrial signal, is the recruitment of the dynamin-related protein Drp1p from the cytosol to the surface of the outer mitochondrial membrane [241, 244, 245]. The temporally and spatially regulated interactions between Drp1p and several other proteins on the cytosolic face of the outer mitochondrial membrane, including Fis1p and Mdv1p, result in the assembly of the functional mitochondrial division machinery [88, 91, 92, 245]. One of the essential components of this machinery is endophilin B1, whose recruitment from the cytosol to the mitochondrial surface is greatly promoted during apoptosis [245, 246]. Importantly, similar to the LPAAT promoting peroxisome division and to the Golgi-bound CtBP3/BARS, endophilin B1 catalyzes the conversion of LPA to PA [157, 247-249]. However, in contrast to peroxisomal LPAAT, whose enzymatic activity is required for the recruitment of the dynamin-related GTPase Vps1p (Figure 8.1), endophilin B1 functions downstream of the dynamin-family member Drp1p in the multistep process of membrane fission [245, 246]. The coordinated action of the Drp1p-Fis1p-Mdv1p complex, endophilin B1 and pro-apoptotic factors BAX and BAK drives synchronous mitochondrial fission in apoptotic cells, thereby promoting dramatic fragmentation of the mitochondrial network [69, 92, 244-246, 250]. The resulting efflux of intermembrane space proteins, including cytochrome c, initiates a series of events ultimately leading to apoptosis.

8.1.3 Lipid metabolism and movement in the membrane bilayer drive organelle division

My findings reported in Chapters 5, 6 and 7 support the notion that a distinct set of lipid metabolic pathways operating in organellar membranes and specific changes in the distribution of some lipids across the membrane bilayers provide a driving force for organelle division [94, 96, 155, 158, 170, 171, 174]. The temporally and spatially regulated reorganization of membrane lipids may orchestrate organelle division by facilitating the formation of highly curved fission intermediates, promoting the coordinated changes in local membrane curvature, and recruiting and/or assembling the protein team that operates in membrane fission [94, 170, 171, 174]. In fact, we found that the biosynthesis of PA from LPA in the peroxisomal membrane and the subsequent conversion of PA to DAG are mandatory for the division of mature peroxisomes. Furthermore, the glycerophospholipid PC, which is transferred to the peroxisomal membrane from the P3- and P4-associated ER subcompartment, activates both enzymatic reactions in the pathway for DAG biosynthesis. Moreover, the movement of DAG from the lumenal to the cytosolic leaflet of the membrane bilayer coincides with the translocation of PS in the opposite direction, perhaps generating a lipid imbalance across the bilayer and thereby driving the process of membrane fission. I believe that, after its spontaneous flipping between the two membrane leaflets, DAG undergoes the selective enrichment in distinct lipid domains that facilitate membrane scission through coordinated changes in local membrane curvature. The formation of such DAG-enriched domains in the cytosolic leaflet of the membrane bilayer may also initiate the assembly of

the Act1p-Abp1p-Sla1p-Vps1p-Pex19p-Pex10p complexes on the surface of peroxisomes and/or promote the clustering of these protein complexes at the membrane scission site. Such clustering may, in turn, lead to the formation of a peroxisomal dividing ring similar to the dividing rings of dynamin-related proteins that promote the division of mitochondria and chloroplasts [88, 91, 92, 245].

8.2 Suggestions for future work

My model for peroxisome division predicts that the activities of LPA acyltransferase and PA phosphatase are essential for the division of mature peroxisomes. Both enzymatic activities are present in all six peroxisomal subforms. It would be important to purify LPA acyltransferase and PA phosphatase. In order to do that, detergent-solubilized PMPs of mature peroxisomes could be fractionated by ion exchange chromatography. Aliquots of chromatographic fractions could be analyzed for LPA acyltransferase and PA phosphatase activities in order to identify proteins that have these enzymatic activities and to guide further purification efforts, using hydrophobic interaction chromatography and subsequent gel filtration chromatography. LPA acyltransferase could also be purified by a complementary affinity chromatographic approach, using commercial palmitoyl-CoA agarose ("Sigma"). Membrane proteins that exhibit LPA acyltransferase and PA phosphatase activities could be analyzed by mass spectrometry and identified by database searching. The data on mass spectrometric identification of these proteins could be then used to disrupt the encoding genes. The effects of knocking out these genes on the levels of LPA, PA and DAG in the membrane of mature peroxisomes and on peroxisome

division in living cells could be determined.

In my model for peroxisome division (Figure 8.1), the movement of DAG, which is synthesized in the inner leaflet of the membrane, into the outer leaflet of the membrane in mature peroxisomes promotes their division. It is tempting to speculate that, after its spontaneous flipping between the two membrane leaflets, DAG undergoes the selective enrichment in distinct lipid domains that facilitate membrane scission through coordinated changes in local membrane curvature. To test this hypothesis, fluorescence microscopy and immunoelectron microscopy could be used to monitor DAG in the outer leaflet of the membranes of different peroxisomal forms. The DAG-binding C1b domain of protein kinase C has recently been used to examine DAG localization in vacuolar membrane by fluorescence microscopy [251, 252]. C1b could be produced, purified and labeled with the fluorophore Alexa Fluor 488 as described [251, 252]. In addition, antibodies specific for C1b could be raised in order to use them for monitoring DAG in the membrane by immunoelectron microscopy. Fluorescence microscopy and electron microscopy could be also used to visualize membrane lipids other than DAG. The following lipid-specific probes could be used for microscopy: 1) a tandem FYVE domain that specifically binds PI(3)P [252, 253]; 2) MED [254] and ENTH [255] domains specific for $PI(4,5)P_2$ [256]; 3) the intrinsically fluorescent ergosterol ligand fillipin [257] and a biotinylated derivative of the sterol-binding ligand perfringolysin O[257, 258]; 4) the PS-specific antibodies [133] and fluorescent sensor PSS-380 [259]; and 5) antibodies to ceramide [133]. The presence and spatial distribution of DAG and other lipid species in the outer leaflet of the peroxisomal membrane could be microscopically monitored in

intact immature peroxisomal vesicles and mature peroxisomes. These organelles could be purified from wild-type cells and from *aox1KO* to *aox5KO* and *PEX16-TH* mutant cells. Furthermore, using lipid-specific fluorescent probes, one could also evaluate the arrangement of DAG and other lipid species between the two leaflets of the membrane bilayers in different peroxisomal subforms. In the membranes of osmotically lysed peroxisomes, both leaflets of the bilayer are accessible to these fluorescent probes. In contract, in the membranes of intact peroxisomes, these lipid-specific fluorescent probes can detect only lipid molecules that reside in the outer leaflet. For each lipid-specific fluorescent probe, one could calculate the ratio "fluorescence for intact peroxisomes/fluorescence for osmotically lysed peroxisomes", which is equal to the fraction of the total pool of a monitored lipid that is located in the outer leaflet of the membrane [133].

My data imply that the Pex2p-dependent transfer of PC from the P3- and P4-associated ER subcompartment to the acceptor membranes of P3 and P4 provides these peroxisomal membranes with the bulk quantities of PC and is essential for the conversion of P4 to P5 (Chapter 5). A distinct set of proteins associated only with the P3- and P4-bound ER subcompartment but not with the free form of the ER (Figure 5.7) may operate in the transfer of PC from the ER subcompartment to the membranes of P3 and P4 peroxisomes via membrane contact sites. These proteins could be analyzed by mass spectrometry and identified by database searching. These data on mass spectrometric identification of proteins associated only with the P3- and P4-bound ER subcompartment could be used to disrupt the encoding genes. The effects of knocking out these genes on

the efficiency of delivery of PC to the membranes of different peroxisomal subforms *in vivo* could be determined.

My findings provided evidence that the targeting of the *S. cerevisiae* dynamin-like protein Vps1p, which is essential for peroxisome division in this yeast, to the cytosolic face of mature peroxisomes from *Y. lipolytica* relies on the Pex16p/Aox-dependent biosynthesis of PA and/or DAG in their membranes. The available antibodies to *Y. lipolytica* Vps1p could be used to establish the mechanism governing the recruitment of Vps1p from the cytosol to the surface of the mature peroxisome, as specified below. For instance, the binding of Vps1p to individual lipid species in vitro could be examined. One could also monitor the efficiency of the binding of Vps1p to the outer face of liposomes reconstituted with different quantities of DAG and other lipid species, including PA and PC, that, similar to DAG, regulate peroxisome division. To test whether Vps1p co-localizes with DAG and/or any other "regulatory lipid" in the outer leaflet of the membrane of mature peroxisomes, the wild-type strain and mutant strains deficient in peroxisome division, as well as P6 peroxisomes purified from these strains, could be analyzed by fluorescence microscopy, immunofluorescence microscopy and immunoelectron microscopy. Samples could be processed for double labeling with anti-Vps1p antibodies and with lipid-specific probes for monitoring the distribution of DAG, PI(3)P, PI(4,5)P_2, ergosterol, PS and ceramide. The following lipid-specific probes could be used for microscopical monitoring of the above lipid species: 1) a tandem FYVE domain that specifically binds PI(3)P [252, 253]; 2) MED [254] and ENTH [255] domains specific for PI(4,5)P_2 [256]; 3) the intrinsically fluorescent ergosterol ligand

fillipin [257] and a biotinylated derivative of the sterol-binding ligand perfringolysin O[257, 258]; 4) the PS-specific antibodies [133] and fluorescent sensor PSS-380 [259]; and 5) antibodies to ceramide [133].

9 References

1. Lazarow, P.B., and Fujiki, Y. (1985). Biogenesis of peroxisomes. *Annu. Rev. Cell Biol.* 1:489-530.
2. Subramani, S. (1993). Protein import into peroxisomes and biogenesis of the organelle. *Annu. Rev. Cell Biol.* 9:445-478.
3. Purdue, P.E., and Lazarow, P.E. (2001). Peroxisome biogenesis. *Annu. Rev. Cell Dev. Biol.* 17:701-52.
4. Bodnar, A.G., and Rachubinski, R.A. (1991). Characterization of the integral membrane polypeptides of rat liver peroxisomes isolated from untreated and clofibrate-treated rats. *Biochem. Cell Biol.* 69:499-508.
5. Kim, P.K., Mullen, R.T., Schumann, W., and Lippincott-Schwartz, J. (2006). The origin and maintenance of mammalian peroxisomes involves a *de novo* PEX16-dependent pathway from the ER. *J. Cell Biol.* 173:521-532.
6. van den Bosch, H., Schutgens, R.B., Wanders, R.J., and Tager, J.M. (1992). Biochemistry of peroxisomes. *Annu. Rev. Biochem.* 61:157-197.
7. Wanders, R.J., and Tager, J.M. (1998). Lipid metabolism in peroxisomes in relation to human disease. *Mol. Aspects Med.* 19:69-154.

8. Wanders, R.J., Vreken, P., Ferdinandusse, S., Jansen, G.A., Waterham, H.R., van Roermund, C.W., and Van Grunsven, E.G. (2001). Peroxisomal fatty acid alpha- and beta-oxidation in humans: enzymology, peroxisomal metabolite transporters and peroxisomal diseases. *Biochem. Soc. Trans.* 29:250-267.

9. Fujiki, Y. (2000). Peroxisome biogenesis and peroxisome biogenesis disorders. *FEBS Lett.* 476:42-46.

10. Gould, S.J., and Valle, D. (2000). Peroxisome biogenesis disorders: genetics and cell biology. *Trends Genet.* 16:340-345.

11. Subramani, S. (1997). PEX genes on the rise. *Nature Genet.* 15:331-333.

12. Subramani, S., Koller, A., and Snyder, W.B. (2000). Import of peroxisomal matrix and membrane proteins. *Annu. Rev. Biochem.* 69:399-418.

13. Wanders, R.J. (1999). Peroxisomal disorders: clinical, biochemical, and molecular aspects. *Neurochem. Res.* 24:565-580.

14. Sacksteder, K.A., and Gould, S.J. (2000). The genetics of peroxisome biogenesis. *Annu. Rev. Genet.* 34:623-652.

15. Gould, S.G., Valle, D., and Raymond, G.V. (2001). The peroxisome biogenesis disorders. *In* The Metabolic and Molecular Bases of Inherited Disease. C.R. Scriver, A.L. Beaudet, W.S. Sly, and D. Valle, editors. McGraw-Hill, New York, pp. 3181-3217.

16. Matsumoto, N., Tamura, S., and Fujiki, Y. (2003). The pathogenic peroxin Pex26p recruits the Pex1p-Pex6p AAA ATPase complexes to peroxisomes. *Nature Cell Biol.* 5:454-460.

17. Powers, J.M., and Moser, H.W. (1998). Peroxisomal disorders: genotype, phenotype, major neuropathologic lesions, and pathogenesis. *Brain Pathol.* 8:101-120.

18. Moser, H.W. (1999). Genotype–phenotype correlations in disorders of peroxisome biogenesis. *Mol. Genet. Metab.* 68:316-327.

19. Purdue, P.E., Skoneczny, M., Yang, X., Zhang, J.W., and Lazarow, P.B. (1999). Rhizomelic chondrodysplasia puncatata, a peroxisomal biogenesis disorder caused by defects in Pex7p, a peroxisomal protein import receptor: a minireview. *Neurochem. Res.* 24:581-586.

20. Titorenko, V.I., and Rachubinski, R.A. (2001). The life cycle of the peroxisome. *Nature Rev. Mol. Cell Biol.* 2:57-68.

21. Eckert, J.H., and Erdmann, R. (2003). Peroxisome biogenesis. *Rev. Physiol. Biochem. Pharmacol.* 147:75-121.

22. Smith, J.J., Marelli, M., Christmas, R.H., Vizeacoumar, F.J., Dilworth, D.J., Ideker, T., Galitski, T., Dimitrov, K., Rachubinski, R.A., and Aitchison, J.D. (2002). Transcriptome profiling to identify genes involved in peroxisome assembly and function. *J. Cell Biol.* 158:259-271.

23. Tam, Y.Y., and Rachubinski, R.A. (2002). *Yarrowia lipolytica* cells mutant for the *PEX24* gene encoding a peroxisomal membrane peroxin mislocalize peroxisomal proteins and accumulate membrane structures containing both peroxisomal matrix and membrane Proteins. *Mol. Biol. Cell* 13:2681-2691.

24. Tam, Y.Y.C., Torres-Guzman, J.C., Vizeacoumar, F.J., Smith, J.J., Marelli, M., Aitchison, J.D., and Rachubinski, R.A. (2003). Pex11-related proteins in peroxisome dynamics: a role for the novel peroxin Pex27p in controlling peroxisome size and number in *Saccharomyces Cerevisiae. Mol. Biol. Cell.* 14:4089-4102.

25. Vizeacoumar, F.J., Torres-Guzman, J.C., Tam, Y.Y.C., Aitchison, J.D., and Rachubinski, R.A. (2003). YHR150w and YDR479c encode peroxisomal integral membrane proteins involved in the regulation of peroxisome number, size, and distribution in *Saccharomyces cerevisiae J. Cell Biol.* 161:321-332.

26. Vizeacoumar, F.J., Torres-Guzman, J.C., Bouard, D., Aitchison, J.D., and Rachubinski, R.A. (2004). Pex30p, Pex31p, and Pex32p form a family of peroxisomal integral membrane proteins regulating peroxisome size and number in *Saccharomyces cerevisiae. Mol. Biol. Cell.* 15:665-677.

27. Titorenko, V.I., Ogrydziak, D.M., and Rachubinski, R.A. (1997). Four distinct secretory pathways serve protein secretion, cell surface growth, and peroxisome biogenesis in the yeast *Yarrowia lipolytica. Mol. Cell. Biol.* 17:5210-5226.

28. Lin, Y., Sun, L., Nguyen, L.V., Rachubinski, R.A., and Goodman, H.M. (1999). The Pex16p homolog SSE1 and storage organelle formation in Arabidopsis seeds. *Science* 284:328-330.

29. Cohen, G.B., Rangan, V.S., Chen, B.K., Smith, S., and Baltimore, D. (2000). The human thioesterase II protein binds to a site on HIV-1 Nef critical for CD4 down-regulation. *J. Biol. Chem.* 275:23097-23105.

30. Jedd, G., and Chua, N.-H. (2000). A new self-assembled peroxisomal vesicle required for efficient resealing of the plasma membrane. *Nature Cell Biol.* 2:226-231.

31. Kersten, S., Desvergne, B., and Wahli, W. (2000). Roles of PPARs in health and disease. *Nature* 405:421-424.

32. Motley, A.M., Hettema, E.H., Ketting, R., Plasterk, R., and Tabak, H.F. (2000). *Caenorhabditis elegans* has a single pathway to target matrix proteins to peroxisomes. *EMBO Rep.* 1:40-46.

33. Kimura, A., Takano, Y., Furusawa, I., and Okuno, T. (2001). Peroxisomal metabolic function is required for appressorium-mediated plant infection by *Colletotrichum lagenarium*. *Plant Cell* 13:1945-1957.

34. Titorenko, V.I., and Rachubinski, R.A. (2001). Dynamics of peroxisome assembly and function. *Trends Cell Biol.* 11:22-29.

35. Di-Poi, N., Tan, N.S., Michalik, L., Wahli, W., and Desvergne, B. (2002). Antiapoptotic role of PPARbeta in keratinocytes via transcriptional control of the Akt1 signaling pathway. *Mol. Cell* 10:721-733.

36. Footitt, S., Slocombe, S.P., Larner, V., Kurup, S., Wu, Y., Larson, T., Graham, I., Baker, A., and Holdsworth, M. (2002). Control of germination and lipid mobilization by COMATOSE, the Arabidopsis homologue of human ALDP. *EMBO J.* 21:2912-2922.

37. Gavva, N.R., Wen, S.C., Daftari, P., Moniwa, M., Yang, W.M., Yang-Feng, L.P., Seto, E., Davie, J.R., and Shen, C.K. (2002). NAPP2, a peroxisomal membrane

protein, is also a transcriptional corepressor. *Genomics* 79:423-431.

38. Hu, J., Aguirre, M., Peto, C., Alonso, J., Ecker, J., and Chory, J. (2002). A role for peroxisomes in photomorphogenesis and development of Arabidopsis. *Science* 297:405-409.

39. Ma, L., Gao, Y., Qu, L., Chen, Z., Li, J., Zhao, H., and Deng, X.W. (2002). Genomic evidence for COP1 as a repressor of light-regulated gene expression and development in Arabidopsis. *Plant Cell* 14:2383-2398.

40. Michalik, L., Desvergne, B., Dreyer, C., Gavillet, M., Laurini, R.N., and Wahli, W. (2002). PPAR expression and function during vertebrate development. *Int. J. Dev. Biol.* 46:105-114.

41. Mohan, K.V., Som, I., and Atreya, C.D. (2002). Identification of a type 1 peroxisomal targeting signal in a viral protein and demonstration of its targeting to the organelle. *J. Virol.* 76:2543-2547.

42. Petriv, O.I., Pilgrim, D.B., Rachubinski, R.A., and Titorenko, V.I. (2002). RNA interference of peroxisome-related genes in C. elegans: a new model for human peroxisomal disorders. *Physiol. Genomics* 10:79-91.

43. Titorenko, V.I., and Rachubinski, R.A. (2004). The peroxisome: orchestrating important developmental decisions from inside the cell. *J. Cell Biol.* 164:641-645.

44. Alberts, B., Bray, D., Johnson, A., Lewis, J., Raff, M., Roberts, K., and Walter, P. (1998). *Essential Cell Biology*. Garland Publishing, Inc., New York.

45. Cooper, G. (2000). *The Cell: A Molecular Approach*, 2nd edition. ASM Press., Washington, D.C./ Sinauer Associates, Inc., Sunderland, MA.

46. Lodish, H., Berk, A., Zipursky, S.L., Matsudaira, P., Baltimore, D., and Darnell, J. (2000). *Molecular Cell Biology*, 4th edition. W.H. Freeman and Co., New York.

47. Titorenko, V.I., Ogrydziak, D.M., and Rachubinski, R.A. (1997). Four distinct secretory pathways serve protein secretion, cell surface growth, and peroxisome biogenesis in the yeast *Yarrowia lipolytica*. *Mol. Cell. Biol.* 17:5210-5226.

48. Titorenko, V.I., and Rachubinski, R.A. (1998). Mutants of the yeast *Yarrowia lipolytica* defective in protein exit from the endoplasmic reticulum are also defective in peroxisome biogenesis. *Mol. Cell. Biol.* 18:2789-2803.

49. Mullen, R.T., Lisenbee, C.S., Miernyk, J.A., and Trelease, R.N. (1999). Peroxisomal membrane ascorbate peroxidase is sorted to a membranous network that resembles a subdomain of the endoplasmic reticulum. *Plant Cell.* 11:2167-2185.

50. Hoepfner, D., Schildknegt, D., Braakman, I, Philippsen, P., and Tabak, H.F. (2005). Contribution of the endoplasmic reticulum to peroxisome formation. *Cell.* 122:85-95.

51. Kragt, A., Voorn-Brouwer, T., van den Berg, M., and B. Distel, B. (2005). Endoplasmic reticulum-directed Pex3p routes to peroxisomes and restores peroxisome formation in a *Saccharomyces cerevisiae pex3*Δ strain. *J. Biol. Chem.* 280:34350-34357.

52. Tam, Y.Y.C., Fagarasanu, A., Fagarasanu, M., and Rachubinski, R.A. (2005). Pex3p initiates the formation of a preperoxisomal compartment from a subdomain of the endoplasmic reticulum in *Saccharomyces cerevisiae*. *J. Biol. Chem.*

280:34933-34939.

53. Haan, G.-J., Baerends, R.J.S., Krikken, A.M., Otzen, M., Veenhuis, M., and van der Klei, I.J. (2006). Reassembly of peroxisomes in *Hansenula polymorpha pex3* cells on reintroduction of Pex3p involves the nuclear envelope. *FEMS Yeast Res.* 6:186-194.

54. Kim, P.K., Mullen, R.T., Schumann, W., and Lippincott-Schwartz, J. (2006). The origin and maintenance of mammalian peroxisomes involves a *de novo* PEX16-dependent pathway from the ER. *J. Cell Biol.* 173:521-532.

55. Titorenko, V.I., Chan, H. and Rachubinski, R.A. (2000). Fusion of small peroxisomal vesicles in vitro reconstructs an early step in the *in vivo* multistep peroxisome assembly pathway of *Yarrowia lipolytica. J. Cell Biol.* 148:29-43.

56. Titorenko, V.I., and Rachubinski, R.A. (2000). Peroxisomal membrane fusion requires two AAA family ATPases, Pex1p and Pex6p. *J. Cell Biol.* 150:881-886.

57. Geuze, H.J., Murk, J.L., Stroobants, A.K., Griffith, J.M., Kleijmeer, M.J., Koster, A.J., Verkleij, A.J., Distel, B, and Tabak, H.F. (2003). Involvement of the endoplasmic reticulum in peroxisome formation. *Mol. Biol. Cell.* 14:2900-2907.

58. Guo, T., Kit, Y.Y., Nicaud, J.-M, Le Dall, M. –T., Sears, S.K., Vali, H., Chan, H., Rachubinski, R.A., and Titorenko, V.I. (2003). Peroxisome division is regulated by a signal from inside the peroxisome. *J. Cell Biol.* 162:1255-1266.

59. Lazarow, P.B. (2003). Peroxisome biogenesis: advances and conundrums. *Curr. Opin. Cell Biol.* 15:489-497.

60. Beevers, H. (1979). Microbodies in higher plants. *Annu. Rev. Plant Physiol.*

30:159-193.

61. South, S.T., Baumgart, E., and Gould, S.J. (2001). Inactivation of the endoplasmic reticulum protein translocation factor, Sec61p, or its homolog, Ssh1p, does not affect peroxisome biogenesis. *Proc. Natl. Acad. Sci. USA.* 98:12027-12031.

62. Mullen, R.T., Flynn, C.R., and Trelease, R.N. (2001). How are peroxisomes formed? The role of the endoplasmic reticulum and peroxins. *Trends Plant Sci.* 6:256-261.

63. Tabak, H.F., Murk, J.L., Braakman, I., and Geuze, H.J. (2003). Peroxisomes start their life in the endoplasmic reticulum. *Traffic.* 4:512-518.

64. Lisenbee, C.S., Heinze, M., and Trelease, R.N. (2003). Peroxisomal ascorbate peroxidase resides within a subdomain of rough endoplasmic reticulum in wild-type Arabidopsis cells. *Plant Physiol.* 132:870-882.

65. Titorenko, V.I., and Mullen, R.T. (2006). Peroxisome biogenesis: The peroxisomal endomembrane system and the role of the ER, J. Cell Biol. In Press.

66. Baerends, R.J.S., Rasmussen, S.W., Hilbrands, R.E., van der Heide, M., K.N. Faber, K.N., Reuvekamp, P.T.W., Kiel, J.A.K.W., Cregg, J.M., van der Klei, I, J., and Veenhuis, M. (1996). The *Hansenula polymorpha PER9* gene encodes a peroxisomal membrane protein essential for peroxisome assembly and integrity. *J. Biol. Chem.* 271:8887-8894.

67. Elgersma, Y., Kwast, L., van den Berg, M., Snyder, W.B., Distel, B., Subramani, S., and Tabak, H.F. (1997). Overexpression of Pex15p, a phosphorylated peroxisomal integral membrane protein required for peroxisome assembly in *S.*

cerevisiae, causes proliferation of the endoplasmic reticulum membrane. *EMBO J.* 16:7326-7341.

68. Mullen, R.T., and Trelease, R.N. (2000). The sorting signals for peroxisomal membrane-bound ascorbate peroxidase are within its C-terminal tail. *J. Biol. Chem.* 275:16337-16344.

69. Lee, M.C., Miller, E.A., Goldberg, J., Orci, L., and Schekman, R. (2004). Bi-directional protein transport between the ER and Golgi. *Annu. Rev. Cell Dev. Biol.* 20:87-123.

70. Watson, P., and Stephens, D.J. (2005). ER-to-Golgi transport: form and formation of vesicular and tubular carriers. *Biochim. Biophys. Acta.* 1744:304-315.

71. Rossanese, O.W., Soderholm, J., Bevis, B.J., Sears, I.B., O'Connor, J., Williamson, E.K., and Glick, B.S. (1999). Golgi structure correlates with transitional endoplasmic reticulum organization in *Pichia pastoris* and *Saccharomyces cerevisiae*. *J. Cell Biol.* 145:69-81.

72. Hammond, A.T., and Glick, B.S. (2000). Dynamics of transitional endoplasmic reticulum sites in vertebrate cells. *Mol. Biol. Cell.* 11:3013-3030.

73. Hanton, S.L., Bortolotti, L.E., Renna, L., Stefano, G., and F. Brandizzi, F. (2005). Crossing the divide – transport between the endoplasmic reticulum and Golgi apparatus in plants. *Traffic.* 6:267-277.

74. Titorenko, V.I., and Rachubinski, R.A. (1998). The endoplasmic reticulum plays an essential role in peroxisome biogenesis. *Trends Biochem. Sci.* 23:231-233.

75. Titorenko, V.I., Eitzen, G.A., and Rachubinski, R.A. (1996). Mutations in the *PAY5* gene of the yeast *Yarrowia lipolytica* cause the accumulation of multiple subpopulations of peroxisomes. *J. Biol. Chem.* 271:20307-20314.

76. Wang, X., M.A. McMahon, S.N. Shelton, M. Nampaisansuk, J.L. Ballard, and J.M. Goodman. (2004). Multiple targeting modules on peroxisomal proteins are not redundant: discrete functions of targeting signals within Pmp47 and Pex8p. *Mol. Biol. Cell.* 15:1702-1710.

77. Veenhuis, M., and Goodman, J.M. (1990). Peroxisomal assembly: membrane proliferation precedes the induction of the abundant matrix proteins in the methylotrophic yeast *Candida boidinii. J. Cell Sci.* 96:583-590.

78. Salomons, F.A., van der Klei, I.J., Kram, A.M., Harder, W., and Veenhuis, M. (1997). Brefeldin A interferes with peroxisomal protein sorting in the yeast *Hansenula polymorpha. FEBS Lett.* 411:133-139.

79. South, S.T., K.A. Sacksteder, K.A., Li, X., Liu, Y., and Gould, S.J. (2000). Inhibitors of COPI and COPII do not block PEX3-mediated peroxisome synthesis. *J. Cell Biol.* 149:1345-1360.

80. Voorn-Brouwer, T., A. Kragt, A., Tabak, H.F., and B. Distel, B. (2001). Peroxisomal membrane proteins are properly targeted to peroxisomes in the absence of COPI- and COPII-mediated vesicular transport. *J. Cell Sci.* 114:2199-2204.

81. Mullen, R.T., McCartney, A.W., Flynn, C.R., and Smith, G.S.T. (2006). Peroxisome biogenesis and the formation of multivesicular peroxisomes during

tombusvirus Infection: A role for ESCRT? *Can. J. Bot.* In Press.

82. McCartney, A.W., Greenwood, J.S., Fabian, M.R., White, K.A., and Mullen, R.T. 2005. Localization of the tomato bushy stunt virus replication protein p33 reveals a peroxisome-to-endoplasmic reticulum sorting pathway. *Plant Cell.* 17:3513-3531.

83. Aniento, F., Helms, J.B., and Memon, A.R. (2003). How to make a vesicle: Coat protein-membrane interactions. *In* The Golgi Apparatus and the Plant Secretory Pathway. D.G. Robinson, editor. Blackwell Publishing, Oxford, UK. pp36–62.

84. Serviene, E., Jiang, Y., Cheng, C.P., Baker, J., and Nagy, P.D. (2006). Screening of the yeast yTHC collection identifies essential host factors affecting tombusvirus RNA recombination. *J. Virol.* 80:1231-1241.

85. Martelli, G.P., Gallitelli, D., and Russo, M. (1988). Tombusviruses. *In* The Plant Viruses: Vol 3. Polyhedral virions with monpartite RNA genomes. R. Koenig editor. Plenum Press, New York and London. pp 13-72.

86. Scholthof, K.B., Scholthof, H.B., and Jackson, A.O. (1995). The tomato bushy stunt virus replicase proteins are coordinately expressed and membrane associated. *Viology*. 208:365-369.

87. Shorter, J., and Warren, G. (2002). Golgi architecture and inheritance. *Annu. Rev. Cell Biol.Dev* 18:379-420.

88. Osteryoung, K.W., and Nunnari, J. (2003). The division of endosymbiotic organelles. *Science* 302:1698-1704.

89. Du, Y., Ferro-Novick, S., and Novick, P. (2004). Dynamics and inheritance of the endoplasmic reticulum. *J. Cell Sci.* 117:2871-2878.

90. Yan, M., Rayapuram, N., and Subramani, S. (2005). The control of peroxisome number and size during division and proliferation. *Curr. Opin. Cell Biol.* 17:376-383.

91. Shaw, J.M., and Nunnari, J. (2002). Mitochondrial dynamics and division in budding yeast. *Trends Cell Biol.* 12:178-184.

92. Bossy-Wetzel, E., Barsoum, M.J., Godzik, A., Schwarzenbacher, R., and Lipton, S.A. (2003). Mitochondrial fission in apoptosis, neurodegeneration and aging. *Curr. Opin. Cell Biol.* 15:706-716.

93. Youle, R.J., and Karbowski, M. (2005). Mitochondrial fission in apoptosis. *Nature Rev. Mol. Cell Biol.* 6:657-663.

94. Corda, D., Hidalgo Carcedo, C., Bonazzi, M., Luini, A., and Spano, S. (2002). Molecular aspects of membrane fission in the secretory pathway. *Cell. Mol. Life Sci.* 59:1819-1832.

95. Colanzi, A., Suetterlin, C., and Malhotra, V. (2003). Cell-cycle-specific Golgi fragmentation: how and why? *Curr. Opin. Cell Biol.* 15:462-467.

96. Hidalgo Carcedo, C., Bonazzi, M., Spanò, S., Turacchio, G., Colanzi, A., Luini, A., and Corda, D. (2004). Mitotic Golgi partitioning is driven by the membrane-fissioning protein CtBP3/BARS. *Science* 305:93-96.

97. Schekman, R. (2005). Peroxisomes: another branch of the secretory pathway? *Cell.* 122:1-2.

98. Kunau, W.-H. (2005). Peroxisome biogenesis: end of the debate. *Curr. Biol.* 15:R774-R776.

99. Hoepfner, D., van den Berg, M., Philippsen, P., Tabak, H.F., and Hettema, E.H. (2001). A role for Vps1p, actin, and the Myo2p motor in peroxisome abundance and inheritance in *Saccharomyces cerevisiae*. *J. Cell Biol.* 155:979–990.

100. Koch, A., Thiemann, M., Grabenbauer, M., Yoon, Y., McNiven, M.A., and Schrader, M. (2003). Dynamin-like protein 1 is involved in peroxisomal fission. *J. Biol. Chem.* 278:8597-8605.

101. Li, X., and Gould, S.J. (2003). The dynamin-like GTPase DLP1 is essential for peroxisome division and is recruited to peroxisomes in part by PEX11. *J. Biol. Chem.* 278:17012-17020.

102. Koch, A., Schneider, G., Luers, G.H., and Schrader, M. (2004). Peroxisome elongation and constriction but not fission can occur independently of dynamin-like protein 1. *J. Cell Sci.* 117:3995-4006.

103. Thoms, S., and R. Erdmann. (2005). Dynamin-related proteins and Pex11 proteins in peroxisome division and proliferation. *FEBS J.* 272:5169-5181.

104. Schrader, M. (2006). Shared components of mitochondrial and peroxisomal division. *Biochim. Biophys. Acta*, doi: 10.1016/j.bbamcr.2006.01.004.

105. Nebenfuhr, A., Frohlick, J.A., and Staehelin, L.A. (2000). Redistribution of Golgi stacks and other organelles during mitosis and cytokinesis in plant cells. *Plant*

Physiol. 124:135-151.

106. Bevis, B.J., Hammond, A.T., Reinke, C.A., and Glick, B.S. (2002). De novo formation of transitional ER sites and Golgi structures in *Pichia pastoris*. *Nature Cell Biol.* 4:750-756.

107. Munro, S. (2002). More than one way to replicate the Golgi apparatus. *Nature Cell Biol.* 4:E223-E224.

108. Pelletier, L., Stern, C.A., Pypaert, M., Sheff, D., Ngo, H.M., Roper, N., He, C.Y., Hu, K., Toomre, D., Coppens, I. Roos, D.S., Joiner, K.A., and Warren, G. (2002). Golgi biogenesis in *Toxoplasma gondii*. *Nature* 418:548-552.

109. Passreiter, M., Anton, M., Lay, D., Frank, R., Harter, C., Wieland, F.T., Gorgas, K., and Just, W.W. (1998). Peroxisome biogenesis: involvement of ARF and coatomer. *J. Cell Biol.* 141:373-383.

110. Lay, D., Grosshans, B.L., Heid, H., Gorgas, K., and Just, W.W. (2005). Binding and functions of ADP-ribosylation factor on mammalian and yeast peroxisomes. *J. Biol. Chem.* 280:34489-34499.

111. Anton, Passreiter, M., Lay, D., Thai, T.P., Gorgas, K., and Just, W.W. (2000). ARF- and coatomer-mediated peroxisomal vesiculation. *Cell Biochem. Biophys.* 32:27-36.

112. Erdmann, R., and Blobel, G. (1995). Giant peroxisomes in oleic acid-induced *Saccharomyces cerevisiae* lacking the peroxisomal membrane protein Pmp27p. *J. Cell Biol.* 128:509-523.

113. Marshall, P. A., Dyer, J. M., Quick, M. E., and Goodman, J. M. (1996). Redox-

sensitive homodimerization of Pex11p: a proposed mechanism to regulate peroxisomal division. *J. Cell Biol.* 135:123-137.

114. Marshall, P.A, Krimkevich, Y.I., Lark, R.H., Dyer, J.M., Veenhuis, M., Goodman, J.M. (1995). Pmp27 promotes peroxisomal proliferation. *J. Cell Biol.* 129:345-355

115. van Roermund, C.W.T., Tabak, H.F., van den Berg, M., Wanders, R.J.A., and Hettema, E.H. (2000). Pex11p plays a primary role in medium-chain fatty acid oxidation, a process that affects peroxisome number and size in *Saccharomyces cerevisiae*. *J. Cell Biol.* 150:489-497.

116. Lorenz, P., Maier, A.G., Baumgart, E., Erdmann, R., and Clayton, C. (1998). Elongation and clustering of glycosomes in *Trypanosoma brucei* overexpressing the glycosomal Pex11p. *EMBO J.* 17:3542-3555.

117. Chang, C.C., South, S., Warren, D., Jones, J., Moser, A.B., Moser, H.W., and S.J. Gould, S.J. (1999). Metabolic control of peroxisome abundance. *J. Cell Sci.* 112:1579-1590.

118. Poll-Thé, B.T., Poll-Thé, B.T., Roels, F., Ogier, H., Scotto, J., Vamecq, J., Schutgens, R.B., Wanders, R.J., van Roermund, C.W., van Wijland, M.J., Schram, A.W., J.M. Tager, J.M., and Saudubray, J.-M. (1998). A new peroxisomal disorder with enlarged peroxisomes and a specific deficiency of acyl-CoA oxidase (pseudo-neonatal adrenoleukodystrophy). *Am. J. Hum. Genet.* 42:422-434.

119. Nakagawa, T., Imanaka, T., Morita, M., Ishiguro, K., Yurimoto, H., Yamashita, A., Kato, N. and Sakai, Y. (2000). Peroxisomal membrane protein Pmp47 is essential in the metabolism of middle-chain fatty acid in yeast peroxisomes and is associated with peroxisome proliferation. *J. Biol. Chem.* 275:3455-3461.

120. Fan, C.Y., Pan, J., Usuda, N., Yeldandi, A.V., Rao, M.S., and Reddy, J.K. (1998). Steatohepatitis, spontaneous peroxisome proliferation and liver tumors in mice lacking peroxisomal fatty acyl-CoA oxidase. Implications for peroxisome proliferator-activated receptor α natural ligand metabolism. *J. Biol. Chem.* 273:15639-15645.

121. Smith, J.J., Brown, T.W., Eitzen, G.A., and Rachubinski, R.A. (2000). Regulation of peroxisome size and number by fatty acid β-oxidation in the yeast *Yarrowia lipolytica*. *J. Biol. Chem.* 275:20168-20178.

122. Baerends, R.J.S., Salomons, F.A., Kiel, J.A.K.W., van der Klei, I.J., and Veenhuis, M. (1997). Deviant Pex3p levels affect normal peroxisome formation in *Hansenula polymorpha*: a sharp increase of the protein level induces the proliferation of numerous, small protein-import competent peroxisomes. *Yeast* 13:1449-1463.

123. Eitzen, G.A., Szilard, R.K., and Rachubinski, R.A. (1997). Enlarged peroxisomes are present in oleic acid-grown *Yarrowia lipolytica* overexpressing the *PEX16* gene encoding an intraperoxisomal peripheral membrane peroxin. *J. Cell Biol.* 137:1265-1278.

124. South, S.T., and Gould, S.J. (1999). Peroxisome synthesis in the absence of preexisting peroxisomes. *J. Cell Biol.* 144:255-266.

125. Muñiz, M., Morsomme, P., and Riezman, H. (2001). Protein sorting upon exit from the endoplasmic reticulum, *Cell* 104:313-320.

126. Glick, B.S. (2001). ER export: More than one way out. *Current Biology* 11:R361-R363.

127. Morsomme, P., and Riezman, H. (2002). The Rab GTPase Ypt1p and tethering factors couple protein sorting at the ER to vesicle targeting to the Golgi apparatus. *Dev. Cell.* 2:307-317.

128. Watanabe, R., Funato, K., Venkataraman, K., Futerman, A.H., and Riezman, H. (2002). Sphingolipids are required for the stable membrane association of glycosylphosphatidylinositol-anchored proteins in yeast. *J. Biol. Chem.* 277:49538-49544.

129. Morsomme, P., Prescianotto-Baschong, C., and Riezman, H. (2003). The ER v-SNAREs are required for GPI-anchored protein sorting from other secretory proteins upon exit from the ER. *J. Cell Biol.* 162:403-412.

130. Mayor, S., and Riezman, H. (2004). Sorting GPI-anchored proteins. *Nature Rev. Mol. Cell Biol.* 5:110-120.

131. Watanabe, R., and Riezman, H. (2004). Differential ER exit in yeast and mammalian cells. *Curr. Opin. Cell Biol.* 16:350-355.

132. Bagnat, M., Keranen, S., Shevchenko, A., Shevchenko, A., and Simons, K. (2000). Lipid rafts function in biosynthetic delivery of proteins to the cell surface

in yeast. *Proc. Natl. Acad. Sci. USA* 97:3254-3259.

133. Boukh-Viner, T., Guo, T., Alexandrian, A., Cerracchio, A., Gregg, C., Haile, S., Kyskan, R., Milijevic, S., Oren, D., Solomon, J., Wong, V., Nicaud, J.-M., Rachubinski, R.A., English, A.M., and Titorenko, V.I. (2005). Dynamic ergosterol- and ceramide-rich domains in the peroxisomal membrane serve as an organizing platform for peroxisome fusion. *J. Cell Biol.* 168 761-773.

134. Pierini, L.M., and Maxfield, F.R. (2001). Flotillas of lipid rafts fore and aft. *Proc. Natl. Acad. Sci. USA* 98:9471-9473.

135. Kenworthy, A.K., Nichols, B.J., Remmert, C.L., Hendrix, G.M., Kumar, M., Zimmerberg, J., and Lippincott-Schwartz, J. (2004). Dynamics of putative raft-associated proteins at the cell surface. *J. Cell Biol.* 165:735-746.

136. Sprong, H., van der Sluijs, P., and van Meer, G. (2001). How proteins move lipids and lipids move proteins. *Nature Rev. Mol. Cell Biol.* 2:504-513.

137. Xu, X., Bittman, R., Duportail, G., Heissler, D., Vilcheze, C., and London, E. (2001). Effect of the structure of natural sterols and sphingolipids on the formation of ordered sphingolipid/sterol domains (rafts). Comparison of cholesterol to plant, fungal, and disease-associated sterols and comparison of sphingomyelin, cerebrosides, and ceramide. *J. Biol. Chem.* 276:33540-33546.

138. Munro, S. (2003). Lipid rafts: elusive or illusive? *Cell* 115:377-388.

139. Pomorski, T., Holthuis, J.C., Herrmann, A., and van Meer, G. (2004). Tracking down lipid flippases and their biological functions. *J. Cell Sci.* 117:805-813.

140. Bishop, W.R., and Bell, R.M. (1988). Assembly of phospholipids into cellular

membranes: biosynthesis, transmembrane movement and intracellular translocation. *Annu. Rev. Cell Biol.* 4:579-610.

141. Chapman, K.D., and Trelease, R.N. (1991). Acquisition of membrane lipids by differentiating glyoxysomes: role of lipid bodies. *J. Cell Biol.* 115:995-1007.

142. Zinser, E., Sperka-Gottlieb, C.D., Fasch, E.V., Kohlwein, S.D., Paltauf, F., and Daum, G. (1991). Phospholipid synthesis and lipid composition of subcellular membranes in the unicellular eukaryote *Saccharomyces cerevisiae*. *J. Bacteriol.* 173:2026-2034.

143. Martin, S., and Parton, R.G. (2005). Caveolin, cholesterol, and lipid bodies. *Semin. Cell Dev. Biol.* 16:163-174.

144. Voelker, D.R. (1991). Organelle biogenesis and intracellular lipid transport in eukaryotes. *Microbiol. Rev.* 55:543-560.

145. Blanchette-Mackie, E.J., Dwyer, N.K., Barber, T., Coxey, R.A., Takeda, T., Rondinone, C.M., Theodorakis, J.L., Greenberg, A.S., and C. Londos, C. (1995). Perilipin is located on the surface layer of intracellular lipid droplets in adipocytes. *J. Lipid Res.* 36:1211-1226.

146. Bascom, R.A., Chan, H., and Rachubinski, R.A. (2003). Peroxisome biogenesis occurs in an unsynchronized manner in close association with the endoplasmic reticulum in temperature-sensitive *Yarrowia lipolytica* Pex3p mutants. *Mol. Biol. Cell* 14:939-957.

147. Schneiter, R., Brugger, B., Sandhoff, R., Zellnig, G., Leber, A., Lampl, M., Athenstaedt, K., Hrastnik, C., Eder, S., Daum, G., Paltauf, F., Wieland, F.T., and

Kohlwein, S.D. (1999). Electrospray ionization tandem mass spectrometry (ESI-MS/MS) analysis of the lipid molecular species composition of yeast subcellular membranes reveals acyl chain-based sorting/remodeling of distinct molecular species en route to the plasma membrane. *J. Cell Biol.* 146:741-754.

148. Holthuis, J.C., and Levine, T.P. (2005). Lipid traffic: floppy drives and a superhighway. *Nature Rev. Mol. Cell Biol.*, 6:209-220.
149. Voelker, D.R. (2003). New perspectives on the regulation of intermembrane glycerophospholipid traffic. *J. Lipid Res.* 44:441-449.
150. Levine, T. (2004). Short-range intracellular trafficking of small molecules across endoplasmic reticulum junctions. *Trends Cell Biol.* 14:483-490.
151. Voelker, D.R. (2004). Genetic analysis of intracellular aminoglycerophospholipid traffic. *Biochem. Cell Biol.* 82:156-169.
152. Voelker, D.R. (2005). Bridging gaps in phospholipid transport. *Trends Biochem. Sci.* 30:396-404.
153. Huttner, W.B., and Zimmerberg, J. (2001). Implications of lipid microdomains for membrane curvature, budding and fission. *Curr. Opin. Cell Biol.* 13:478-484.
154. Chernomordik, L.V., and Kozlov, M.M. (2003). Protein-lipid interplay in fusion and fission of biological membranes. *Annu. Rev. Biochem.* 72:175-207.
155. Kooijman, E.E., Chupin, V., de Kruijff, B., and Burger, K.N.J. (2003). Modulation of membrane curvature by phosphatidic acid and lysophosphatidic acid. *Traffic* 4:162-174.
156. Zimmerberg, J., and Kozlov, M.M. (2006). How proteins produce cellular

membrane curvature. Nature Rev. *Mol. Cell Biol.* 7:9-19.

157. Farsad, K., Ringstad, N., Takei, K., Floyd, S.R., K. Rose, K., and De Camilli, P. (2001). Generation of high curvature membranes mediated by direct endophilin bilayer interactions. *J. Cell Biol.* 155:193-200.

158. Baron, C.L., and Malhotra, V. (2002). Role of diacylglycerol in PKD recruitment to the TGN and protein transport to the plasma membrane. *Science* 295:325-328.

159. Corda, D., Hidalgo Carcedo, C., Bonazzi, M., Luini, A., Spano, S. (2002). Molecular aspects of membrane fission in the secretory pathway. *Cell. Mol. Life Sci.* 59:1819-1832.

160. Ford, M.G.J., Mills, L.G., Peter, B.J., Vallis, Y., Praefcke, G.J., Evans, P.R., and McMahon, H.T. (2002). Curvature of clathrin-coated pits driven by epsin. *Nature* 419:361-366.

161. Bigay, J., Gounon, P., Robineau, S., and Antonny, B. (2003). Lipid packing sensed by ArfGAP1 couples COPI coat disassembly to membrane bilayer curvature. *Nature* 426:563-566.

162. Bossy-Wetzel, E., Barsoum, M.J., Godzik, A., Schwarzenbacher, R., and Lipton, S.A. (2003). Mitochondrial fission in apoptosis, neurodegeneration and aging. *Curr. Opin. Cell Biol.* 15:706-716.

163. Freyberg, Z., Siddhanta, A., and Shields, D. (2003). "Slip, sliding away": phospholipase D and the Golgi apparatus. *Trends Cell Biol.* 13:540-546.

164. Hidalgo Carcedo, C., Bonazzi, M., Spanò, S., Turacchio, G., Colanzi, A., A. Luini, A., and Corda, D. (2004). Mitotic Golgi partitioning is driven by the

membrane-fissioning protein CtBP3/BARS. *Science* 305:93-96.

165. Peter, B.J., Kent, H.M., Mills, I.G., Vallis, Y., Butler, P.J., Evans, P.R., and McMahon, H.T. (2004).BAR domains as sensors of membrane curvature: the amphiphysin BAR structure. *Science* 303:495-499.

166. Yoshida, Y., Kinuta, M., Abe, T., Liang, S., Araki, K., Cremona, O., Di Paolo, G., Moriyama, Y., Yasuda, T., De Camilli, P. and Takei, K. (2004). The stimulatory action of amphiphysin on dynamin function is dependent on lipid bilayer curvature. *EMBO J.* 23:3483-3491.

167. Bonazzi, M., Spano, S., Turacchio, G., Cericola, C., Valente, C., Colanzi, A., Kweon, H.S., Hsu, V.W., Polishchuck, E.V., Polishchuck, R.S., Sallese, M., Pulvirenti, T., Corda, D., and Luini, A. (2005). CtBP3/BARS drives membrane fission in dynamin-independent transport pathways. *Nature Cell Biol.* 7:570-580.

168. McMahon, H.T., and Gallop, J.L. (2005). Membrane curvature and mechanisms of dynamic cell membrane remodeling. *Nature* 438:590-596.

169. Cremona, O., and De Camilli, P. (2001). Phosphoinositides in membrane traffic at the synapse. *J. Cell Sci.* 114:1041-1052.

170. Bankaitis, V.A. (2002). Slick recruitment to the Golgi. *Science* 295:290-291.

171. Weigert, R., Silletta, M.G., Spano, S., Turacchio, G., Cericola, C., A. Colanzi, A., Senatore, S., Mancini, R., Polishchuk, E.V., Salmona, M., Facchiano, F., Burger, K.N., A. Mironov, Luini, A., and Corda, D. (1999). CtBP/BARS induces fission of Golgi membranes by acylating lysophosphatidic acid. *Nature* 402:429-433.

172. Goni, F.M., and Alonso, A. (1999). Structure and functional properties of

diacylglycerols in membranes. *Prog. Lipid Res.* 38:1-48.

173. Szule, J.A., Fuller, N.L., and Rand, R.P. (2002). The effects of acyl chain length and saturation of diacylglycerols and phosphatidylcholines on membrane monolayer curvature, *Biophys. J.* 83:977-984.

174. Shemesh, T., Luini, A., Malhotra, V., Burger, K.N., and Kozlov, M.M. (2003). Prefission constriction of Golgi tubular carriers driven by local lipid metabolism: a theoretical model. *Biophys. J.* 85:3813-3827.

175. Titorenko, V.I., Nicaud, J.-M., Wang, H., Chan, H., and Rachubinski. R.A. (2002). Acyl-CoA oxidase is imported as a heteropentameric, cofactor-containing complex into peroxisomes of *Yarrowia lipolytica*. *J. Cell Biol.* 156:481-494.

176. Wang, H.J., Le Dall, M.T., Wach Y., Laroche C., Belin, J.M., Gaillardin C., and Nicaud, J.M. (1999). Evaluation of acyl coenzyme A oxidase (Aox) isozyme function in the *n*-alkane-assimilating yeast *Yarrowia lipolytica*. *Journal of Bacteriology* 181:5140-5148.

177. Eitzen, G.A., Titorenko, V.I., Smith, J.J., Veenhuis, M., Szilard, R.K., and Rachubinski, R.A. (1996). The *Yarrowia lipolytica* gene *PAY5* encodes a peroxisomal integral membrane protein homologous to the mammalian peroxisome assembly factor PAF-1. *J. Biol. Chem.* 271:20300-20306.

178. Szilard, R.K., Titorenko, V.I., Veenhuis, M., and R.A. Rachubinski, R.A. (1995). Pay32p of the yeast *Yarrowia lipolytica* is an intraperoxisomal component of the matrix protein translocation machinery. *J. Cell Biol.* 131:1453–1469.

179. Smith, J.J., Szilard, R.K., Marelli, M., and Rachubinski, R.A. (1997). The peroxin

Pex17p of the yeast *Yarrowia lipolytica* is associated peripherally with the peroxisomal membrane and is required for the import of a subset of matrix proteins. *Mol. Cell. Biol.* 17:2511-2520.

180. Lambkin, G.R., and Rachubinski, R.A. (2001). *Yarrowia lipolytica* cells mutant for the peroxisomal peroxin Pex19p contain structures resembling wild-type peroxisomes. *Mol. Biol. Cell* 12:3353-3364.

181. Fang, M., Rivas, M.P., and Bankaitis, V.A. (1998). The contribution of lipids and lipid metabolism to cellular functions of the Golgi complex. *Biochim. Biophys. Acta* 1404:85-100.

182. De Matteis, M., Godi, A., and Corda, D. (2002). Phosphoinositides and the Golgi complex. *Curr. Opin. Cell Biol.* 14:434-447.

183. Jose Lopez-Andreo, M., Gomez-Fernandez, J.C., and Corbalan-Garcia, S. (2003). The simultaneous production of phosphatidic acid and diacylglycerol is essential for the translocation of protein kinase Cε to the plasma membrane in RBL-2H3 cells. *Mol. Biol. Cell* 14:4885-4895.

184. Dickson, R.C., Nagiec, E.E., Wells, G.B., Nagiec, M.M., and Lester, R.L. (1997). Synthesis of mannose-(inositol-P)2-ceramide, the major sphingolipid in Saccharomyces cerevisiae, requires the IPT1 (YDR072c) gene. *J. Biol. Chem.* 272:29620-29625.

185. Nagiec, M.M., Nagiec, E.E., Baltisberger, J.A., Wells, G.B., Lester, R.L., and Dickson, R.C. (1997). Sphingolipid synthesis as a target for antifungal drugs. Complementation of the inositol phosphorylceramide synthase defect in a mutant

strain of *Saccharomyces cerevisiae* by the *AUR1* gene. *J. Biol. Chem.* 272:9809-9817.

186. Zou, J., Katavic, V., Giblin, E.M., Barton, D.L., MacKenzie, S.L., Keller, W.A., Hu, X., and Taylor, D.C. (1997). Modification of seed oil content and acyl composition in the brassicaceae by expression of a yeast sn-2 acyltransferase gene. *Plant Cell* 9:909-923.

187. Hannun, Y.A., Luberto, C., and Argraves, K.M. (2001). Enzymes of sphingolipid metabolism: from modular to integrative signaling. *Biochemistry* 40:4893-4903.

188. Johnson, J.E., Giorgione, J., and Newton, A.C. (2000). The C1 and C2 domains of protein kinase C are independent membrane targeting modules, with specificity for phosphatidylserine conferred by the C1 domain. *Biochemistry* 39:11360-11369.

189. McGee, T.P., Skinner, H.B., Whitters, E.A., Henry, S.A., and Bankaitis, V.A. (1994). A phosphatidylinositol transfer protein controls the phosphatidylcholine content of yeast Golgi membranes. *J. Cell Biol.* 124:273-287.

190. Kearns, B.G., Alb, J.G., and Bankaitis, V.A. (1998). Phosphatidylinositol transfer proteins: the long and winding road to physiological function. *Trends Cell Biol.* 8:276-282.

191. Li, X, Xie, Z., and Bankaitis, V.A. (2000). Phosphatidylinositol/ phosphatidylcholine transfer proteins in yeast. *Biochim. Biophys. Acta* 1486:55-71.

192. Hanada, K., Kumagai, K., Yasuda, S., Miura, Y., Kawano, M., Fukasawa, M., and

Nishijima, M. (2003). Molecular machinery for non-vesicular trafficking of ceramide. *Nature* 426:803-809.

193. Munro, S. (2003). Earthworms and lipid couriers. *Nature* 426:775-776.

194. Riezman, H., and van Meer, G. (2004). Lipid pickup and delivery. *Nature Cell Biol.* 6:15-16.

195. van Meer, G. (1998). Lipids of the Golgi membrane. *Trends Cell Biol.* 8:29-33.

196. Liscum, L., and Munn, N.J. (1999). Intracellular cholesterol transport. *Biochim. Biophys. Acta* 1438:19-37.

197. Hoekstra, D., and van Ijzendoorn, S.C. (2000). Lipid trafficking and sorting: how cholesterol is filling gaps. *Curr. Opin. Cell Biol.* 12:496-502.

198. Simons, K., and Ikonen, E. (2000). How cells handle cholesterol. *Science* 290:1721-1726.

199. Funato, K., and Riezman, H. (2001). Vesicular and nonvesicular transport of ceramide from ER to the Golgi apparatus in yeast. *J. Cell Biol.* 155:949-959.

200. Sillence, D.J., and Platt, F.M. (2003). Storage diseases: new insights into sphingolipid functions. *Trends Cell Biol.* 13:195-203.

201. Sillence, D.J., and Platt, F.M. (2004). Glycosphingolipids in endocytic membrane transport. *Semin. Cell Dev. Biol.* 15:409-416.

202. van Meer, G., and Sprong, H. (2004). Membrane lipids and vesicular traffic. *Curr. Opin. Cell Biol.* 16:373-378.

203. Ladinsky, M.S., Mastronarde, D.N., McIntosh, J.R., Howell, K.E., and Staehelin, L.A. (1999). Golgi structure in three dimensions: functional insights from the

normal rat kidney cell. *J. Cell Biol.* 144:1135-1149.

204. Wu, W.I., and Voelker, D.R. (2004). Reconstitution of phosphatidylserine transport from chemically defined donor membranes to phosphatidylserine decarboxylase 2 implicates specific lipid domains in the process. *J. Biol. Chem.* 279:6635-6642.

205. Daum, G., and Vance, J.E. (1997). Import of lipids into mitochondria. *Prog. Lipid Res.* 36:103-130.

206. Achleitner, G., Gaigg, B., Krasser, A., Kainersdorfer, E., Kohlwein, S.D., Perktold, A., Zellnig, G., and Daum, G. (1999). Association between the endoplasmic reticulum and mitochondria of yeast facilitates interorganelle transport of phospholipids through membrane contact. *Eur. J. Biochem.* 264:545-553.

207. de Kroon, A.I., Koorengevel, M.C., Vromans, T.A., and de Kruijff, B. (2003). Continuous equilibration of phosphatidylcholine and its precursors between endoplasmic reticulum and mitochondria in yeast. *Mol. Biol. Cell* 14:2142-2150.

208. Marelli, M., Smith, J.J., Jung, S., Yi, E., Nesvizhskii, A.I., Christmas, R.H., Saleem, R.A., Tam, Y.Y., Fagarasanu, A., Goodlett, D.R., Aebersold, R., Rachubinski, R.A., and Aitchison, J.D. (2004). Quantitative mass spectrometry reveals a role for the GTPase Rho1p in actin organization on the peroxisome membrane. *J. Cell Biol.* 167:1099-1112.

209. Fagarasanu, M., Fagarasanu, A., Tam, Y.Y.C., Aitchison, J.D., and Rachubinski, R.A. (2005). Inp1p is a peroxisomal membrane protein required for peroxisome

inheritance in *Saccharomyces cerevisiae*. *J. Cell Biol.* 169:765-775.

210. Hinshaw, J.E. (2000). Dynamin and its role in membrane fission. *Annu. Rev. Cell Dev. Biol.* 16:483-519.

211. McNiven, M.A., Cao, H., Pitts, K.R., and Yoon, Y. (2000). The dynamin family of mechanoenzymes: pinching in new places. *Trends Biochem. Sci.* 25:115-120.

212. Griparic, L., and van der Bliek, A.M. (2001). The many shapes of mitochondrial membranes. *Traffic* 2:235-244.

213. Zhang, P., and Hinshaw, J.E. (2001). Three-dimensional reconstruction of dynamin in the constricted state. *Nature Cell Biol.* 3:922-926.

214. Allan, V.J., Thompson, H.M., and McNiven, M.A. (2002). Motoring around the Golgi. *Nature Cell Biol.* 4:E236-E242.

215. Sever, S. (2002). Dynamin and endocytosis. *Curr. Opin. Cell Biol.* 14:463-467.

216. Newmyer, S.L., Christensen, A., and Sever, S. (2003). Auxilin-dynamin interactions link the uncoating ATPase chaperone machinery with vesicle formation. *Dev. Cell* 4:929-940.

217. Praefcke, G.J., and McMahon, H.T. (2004). The dynamin superfamily: universal membrane tubulation and fission molecules? *Nature Rev. Mol. Cell Biol.* 5:133-147.

218. Schafer, D.A. (2004). Regulating actin dynamics at membranes: a focus on dynamin. *Traffic* 5:463-469.

219. Peters, C., Baars, T.L., Bühler, S., and Mayer, A. (2004). Mutual control of membrane fission and fusion proteins. *Cell* 119:667-678.

220. Rothman, J.H., Raymond, C.K., Gilbert, T., O'Hara, P.J., and Stevens, T.H. (1990). A putative GTP binding protein homologous to interferon-inducible Mx proteins performs an essential function in yeast protein sorting. *Cell* 61:1063–1074.

221. Shevchenko, A., Jensen, O.N., Podtelejnikov, A.V., Sagliocco, F., Wilm, M., Vorm, O., Mortensen, P., Shevchenko, A., Boucherie, H., and Mann, M. (1996). Linking genome and proteome by mass spectrometry: large-scale identification of yeast proteins from two dimensional gels. *Proc. Natl. Acad. Sci. USA.* 93:14440-14445.

222. Jiménez, C.R., Huang, L., Qiu, Y., and Burlingame, A.L. (1998). Searching sequence databases over the Internet: protein identification using MS-Fit. *In* Current Protocols in Protein Science, J.E. Coligan, B.M. Dunn, H.L. Ploegh, D.W. Speicher, and P.T. Wigfield, editors. John Wiley and Sons, New York, pp. 16.5.1-16.5.6.

223. Warren, D.T., Andrews, P.D., Gourlay, C.W., and Ayscough, K.R. (2002). Sla1p couples the yeast endocytic machinery to proteins regulating actin dynamics. *J. Cell Sci.* 115:1703-1715.

224. Gourlay, C.W., Dewar, H., Warren, D.T., Costa, R., Satish, N., and Ayscough, K.R. (2003). An interaction between Sla1p and Sla2p plays a role in regulating actin dynamics and endocytosis in budding yeast. *J. Cell Sci.* 116:2551-2564.

225. Kaksonen, M., Sun, Y., and Drubin, D.G. (2003). A pathway for association of receptors, adaptors, and actin during endocytic internalization. *Cell* 115:475-487.

226. Yu, X., and Cai, M. (2004). The yeast dynamin-related GTPase Vps1p functions in the organization of the actin cytoskeleton via interaction with Sla1p. *J. Cell Sci.* 117:3839-3853.

227. Olazabal, I.M., and Machesky, L.M. (2001). Abp1p and cortactin, new "hand-holds" for actin. *J. Cell Biol.* 154:679-682.

228. Botstein, D., Amberg, D., Molholland, J., Huffaker, T., Adams, A., Drubin, D., and Stearns, T. (1997). The yeast cytoskeleton. *In* The Molecular and Cellular Biology of the Yeast Saccharomyces: Cell Cycle and Cell Biology, J.R. Pringle, J.R. Broach and E.W. Jones, editors. Cold Spring Harbor, NY: Cold Spring Harbor Laboratory Press, pp. 1-90.

229. Pruyne, D., and Bretscher, A. (2000). Polarization of cell growth in yeast. I. Establishment and maintenance of polarity states. *J. Cell Sci.* 113:365-375.

230. Elcock, A.H. (2003). Atomic-level observation of macromolecular crowding effects: Escape of a protein from the GroEL cage. *Proc. Natl. Acad. Sci. USA* 100:2340–2344.

231. Danino, D., Moon, K.H., and Hinshaw, J.E. (2004). Rapid constriction of lipid bilayers by the mechanochemical enzyme dynamin. *J. Struct. Biol.* 147:259-267.

232. Sever, S., Muhlberg, A.B., and Schmid, S.L. (1999). Impairment of dynamin's GAP domain stimulates receptor-mediated endocytosis. *Nature* 398:481-486.

233. Sever, S., Damke, H., and Schmid, S.L. (2000). Garrotes, springs, ratchets, and whips: putting dynamin models to the test. *Traffic* 1:385-392.

234. Seemann, J., Jokitalo, E., Pypaert, M., and Warren, G. (2000). Matrix proteins can

generate the higher order architecture of the Golgi apparatus. *Nature* 407:1022-1026.

235. Pfeffer, S.R. (2001). Constructing a Golgi complex. *J. Cell Biol.* 155:873-876.

236. Seemann, J., Pypaert, M., Taguchi, T., Malsam, J., and Warren, G. (2002). Partitioning of the matrix fraction of the Golgi apparatus during mitosis in animal cells. *Science* 295:848-851.

237. Seemann, J., Jokitalo, E.J., and Warren, G. (2000). The role of the tethering proteins p115 and GM130 in transport through the Golgi apparatus in vivo. *Mol. Biol. Cell* 11:635–645.

238. Sütterlin, C., Lin, C.-Y., Feng, Y., Ferris, D.K., Erikson, R.L., and Malhotra, V. (2001). Polo-like kinase is required for the fragmentation of pericentriolar Golgi stacks during mitosis. *Proc. Natl. Acad. Sci. USA* 98:9128–9132.

239. Lowe, M., Rabouille, C., Nakamura, N., Watson, R., Jackman, M., Jämsä, E., Rahman, D., Pappin, D.J.C., and Warren, G. (2002). Cdc2 kinase directly phosphorylates the *cis*-Golgi matrix protein GM130 and is required for Golgi fragmentation in mitosis. *Cell* 94:783-793.

240. Wang, Y., Seemann, J., Pypaert, M., Shorter, J., and Warren, G. (2003). A direct role for GRASP65 as a mitotically regulated Golgi stacking factor. *EMBO J.* 22:3279–3290.

241. Breckenridge, D.G., Germain, M., Mathai, J.P., Nguyen, M., and Shore, G.C. (2003). Regulation of apoptosis by endoplasmic reticulum pathways. *Oncogene* 22:8608-8618.

242. Breckenridge, D.G., Stojanovic, M., Marcellus, R.C., and Shore, G.C. (2003). Caspase cleavage product of BAP31 induces mitochondrial fission through endoplasmic reticulum calcium signals, enhancing cytochrome c release to the cytosol. *J. Cell Biol.* 160:1115-1127.

243. Mathai, J.P., Germain, M., and Shore, G.C. (2005). BH3-only BIK regulates BAX, BAK-dependent release of Ca^{2+} from endoplasmic reticulum stores and mitochondrial apoptosis during stress-induced cell death. *J. Biol. Chem.* 280:23829-23836.

244. Frank, S., Gaume, B., Bergmann-Leitner, E.S., Leitner, W.W., Robert, E.G., Catez, F., Smith, C.L., and Youle, R.J. (2001). The role of dynamin-related protein 1, a mediator of mitochondrial fission, in apoptosis. *Dev. Cell* 1:515-525.

245. Youle, R.J., and Karbowski, M. (2005). Mitochondrial fission in apoptosis. *Nature Rev. Mol. Cell Biol.* 6:657-663.

246. Karbowski, M., Jeong, S.Y., and Youle, R.J. (2004). Endophilin B1 is required for the maintenance of mitochondrial morphology. *J. Cell Biol.* 166:1027-1039.

247. Schmidt, A., Wolde, M., Thiele, C., Fest, W., Kratzin, H., Podtelejnikov, A.V., Witke, W., Huttner, W.B., and Söling, H.-D. (1999). Endophilin I mediates synaptic vesicle formation by transfer of arachidonate to lysophosphatidic acid. *Nature* 401:133-141.

248. Huttner, W.B., and Schmidt, A.A. (2002). Membrane curvature: a case of endofelin' … *Trends Cell Biol.* 12:155-158.

249. Modregger, J., Schmidt, A.A., Ritter, B., Huttner, W.B., and Plomann, M. (2003).

Characterization of Endophilin B1b, a brain-specific membrane-associated lysophosphatidic acid acyl transferase with properties distinct from endophilin A1. *J. Biol. Chem.* 278:4160-4167.

250. Karbowski, M., Lee, Y.J., Gaume, B., Jeong, S.Y., Frank, S., Nechushtan, A., Santel, A., Fuller, M., Smith, C.L., and Youle, R.J. (2002). Spatial and temporal association of Bax with mitochondrial fission sites, Drp1, and Mfn2 during apoptosis. *J. Cell Biol.* 159:931-938.

251. Jun, Y., Fratti, R.A., and Wickner, W. (2004). Diacylglycerol and its formation by phospholipase C regulate Rab- and SNARE-dependent yeast vacuole fusion. *J. Biol. Chem.* 279:53186-53195.

252. Fratti, R.A., Jun, Y., Merz, A.J., Margolis, N., and Wickner, W. (2004). Interdependent assembly of specific regulatory lipids and membrane fusion proteins into the vertex ring domain of docked vacuoles. *J. Cell Biol.* 167:1087-1098.

253. Gillooly, D.J., Morrow, I.C., Lindsay, M., Gould, R., Bryant, N.J., Gaullier, J.M., Parton, R.G., and Stenmark, H. (2000). Localization of phosphatidylinositol 3-phosphate in yeast and mammalian cells. *EMBO J.* 19:4577-4588.

254. Wang, J., Arbuzova, A., Hangyas-Mihalyne, G., and McLaughlin, S. (2001). The effector domain of myristoylated alanine-rich C kinase substrate binds strongly to phosphatidylinositol 4,5-bisphosphate. *J. Biol. Chem.* 276:5012-5019.

255. Rosenthal, J.A., Chen, H., Slepnev, V.I., Pellegrini, L., Salcini, A.E., Di Fiore, P.P., and De Camilli, P. (1999). The epsins define a family of proteins that

interact with components of the clathrin coat and contain a new protein module. *J. Biol. Chem.* 274:33959-33965.

256. DiNitto, J.P., Cronin, T.C., and Lambright, D.G. (2003). Membrane recognition and targeting by lipid-binding domains. *Sci. STKE* 213:re16.

257. Möbius, W., Ohno-Iwashita, Y., van Donselaar, E.G., Oorschot, V.M., Shimada, Y., Fujimoto, T., Heijnen, H.F., Geuze, H.J., and Slot, J.W. (2002). Immunoelectron microscopic localization of cholesterol using biotinylated and non-cytolytic perfringolysin O. *J. Histochem. Cytochem.* 50:43-55.

258. Möbius, W., van Donselaar, E., Ohno-Iwashita, Y., Shimada, Y., Heijnen, H.F., Slot, J.W., and Geuze, H.J. (2003). Recycling compartments and the internal vesicles of multivesicular bodies harbor most of the cholesterol found in the endocytic. *Traffic* 4:222-231.

259. Koulov, A.V., Stucker, K.A., Lakshmi, C., Robinson, J.P., and Smith, B.D. (2003). Detection of apoptotic cells using a synthetic fluorescent sensor for membrane surfaces that contain phosphatidylserine. *Cell Death Differ.* 10:1357-1359.